
Electronic Thesis and Dissertation Repository

8-17-2018 12:30 PM

Plant stimuli-responsive biodegradable polymers for the use in timed release fertilizer coatings

Spencer Heuchan

The University of Western Ontario

Supervisor

Henry, Hugh A.L

The University of Western Ontario Joint Supervisor

Gillies, Elizabeth R.

The University of Western Ontario

Graduate Program in Biology

A thesis submitted in partial fulfillment of the requirements for the degree in Master of Science

© Spencer Heuchan 2018

Follow this and additional works at: <https://ir.lib.uwo.ca/etd>



Part of the [Agricultural Science Commons](#), [Agronomy and Crop Sciences Commons](#), [Environmental Chemistry Commons](#), [Integrative Biology Commons](#), [Polymer Chemistry Commons](#), [Polymer Science Commons](#), and the [Terrestrial and Aquatic Ecology Commons](#)

Recommended Citation

Heuchan, Spencer, "Plant stimuli-responsive biodegradable polymers for the use in timed release fertilizer coatings" (2018). *Electronic Thesis and Dissertation Repository*. 5696.

<https://ir.lib.uwo.ca/etd/5696>

This Dissertation/Thesis is brought to you for free and open access by Scholarship@Western. It has been accepted for inclusion in Electronic Thesis and Dissertation Repository by an authorized administrator of Scholarship@Western. For more information, please contact wlsadmin@uwo.ca.

Abstract

The use of nitrogen-based fertilizers continues to accelerate with human population growth and increases in global food requirements. Enhanced efficiency fertilizers (EEFs) have been developed to improve the synchronization between nutrient supply and crop nutrient demand. However, many of the current controlled release fertilizers are coated with non-degradable polymers that contribute to accumulation of microplastics within ecosystems. This thesis describes research towards the development of a new class of fertilizer coatings using a self-immolative polymer known as poly (ethyl glyoxylate) (PEtG). PEtG itself does not have suitable properties to produce a viable coating but once blended with another degradable polyester such as polycaprolactone its overall properties improve. I demonstrated that PEtG with a pH-sensitive carbamate end-cap degraded in response to the presence of plant roots, which suggests that fertilizer coatings could be developed with PEtG that may release nutrients more efficiently while degrading into innocuous by products.

Keywords

Coating, polymer, self-immolative, polyglyoxylates, fertilizer, controlled-release, biodegradable, stimuli-responsive, agriculture, urea

Co-Authorship Statement

The research described in this thesis is a result of contributions from the author as well as coworkers from Western University and supervisors Dr. Elizabeth Gillies and Dr. Hugh Henry. The detailed contributions for each chapter are as follows:

Chapter 1 was written by the author and edited by both supervisors Dr. Gillies and Dr. Henry.

Chapter 2 describes a project proposed by Dr. Gillies. Dr. Bo Fan synthesized the PEtG material. Dr. Jarret McDonald prepared and chemically characterized co-polymers PCL-*b*-PEtG-*b*-low/high. Blend characterization was carried out by author with assistance from Lukas Bauman for AFM. The manuscript was prepared by the author and was revised with the assistance of Dr. Gillies, Dr. McDonald, and Dr. Henry.

Chapter 3 describes a project proposed by Dr. Henry and Dr. Gillies. Dr. Bo Fan synthesized the PEtG with the carbamate end-cap. The author conducted all the experiments under the supervision of Dr. Henry and Dr. Gillies. The manuscript was written by the author and edited by both Dr. Henry and Dr. Gillies.

Chapter 4 was written by the author and edited by both supervisors Dr. Gillies and Dr. Henry.

Acknowledgements

I would like to give my sincere thanks to my supervisors Dr. Hugh Henry and Dr. Beth Gillies. Their continue guidance, and assistance motived me throughout this project. This project was unique and created a great narrative with each step creating more questions with awaiting answers. This project was very interdisciplinary intensive exposing me to disciplines of chemistry, biology, ecology, and engineering. I am thankful for the experienced gained in the different fields of study and friends I made along the way.

I would also like to thank my lab mates across both Chemistry and Biology for their assistance in this process as well. I want to personally thank Dr. Bo Fan for helping me along the way. Bo showed me the ropes of the lab; assisting with protocols and counselling with research questions. He also synthesized the material that made my project possible. Dr. Jarret McDonald also provided continual guidance and assisted in many of the unfamiliar chemical aspects of my project.

I would also like to thank my friends and family for the constant support. It was a fast two years, and I am proud with the outcomes.

Table of Contents

Abstract.....	i
Co-Authorship Statement.....	ii
Acknowledgements.....	iii
Table of Contents.....	iv
List of Tables.....	viii
List of Figures.....	ix
List of Appendices.....	xi
List of Schemes.....	xiv
List of Abbreviations.....	xv
Chapter 1.....	1
1 Introduction.....	1
1.1 Plant mineral nutrition.....	1
1.2 Plant nutrient availability.....	2
1.3 Nutrients and agriculture.....	3
1.4 Improvement of fertilizer efficiency.....	7
1.5 Controlled release fertilizer.....	8
1.6 Polymers.....	9
1.7 Stimuli-responsive polymers.....	11
1.8 Self-immolative polymers (SIPs).....	12
1.9 Overall thesis objective.....	14
1.10 Specific objectives.....	18
1.11 References.....	19
Chapter 2.....	24
2 Triggerable degradation of polymer coatings using polyglyoxylate-polyester blends and copolymers.....	24

2.1	Introduction.....	24
2.2	Experimental.....	28
2.2.1	General materials and procedures.....	28
2.2.2	Preparation of the polyester:PEtG blends.....	29
2.2.3	Synthesis of Br-PCL-low.....	29
2.2.4	Synthesis of Br-PCL-high.....	30
2.2.5	Synthesis of N ₃ -PCL-low.....	30
2.2.6	Synthesis of N ₃ -PCL-high.....	31
2.2.7	Synthesis of PCL- <i>b</i> -PETG- <i>b</i> -PCL-low.....	31
2.2.8	Synthesis of PCL- <i>b</i> -PEtG- <i>b</i> -PCL-high.....	32
2.2.9	Thermal analyses.....	32
2.2.10	Atomic force microscopy (AFM).....	32
2.2.11	Tensile testing.....	33
2.2.12	Coating Degradation studies.....	33
2.2.13	Scanning electron microscopy.....	34
2.2.14	Data Analyses.....	34
2.3	Results and Discussion.....	35
2.3.1	Preparation of PEtG-polyester Blends.....	35
2.3.2	Synthesis of a PEtG-PCL block copolymer.....	36
2.3.3	Thermal Properties.....	39
2.3.4	Atomic force microscopy (AFM).....	43
2.3.5	Mechanical testing.....	45
2.3.6	Coating Degradation.....	48
2.4	Conclusions.....	54
2.5	References.....	56
	Chapter 3.....	59

3	Plant root responsive slow-release fertilizer coatings using polyglyoxylate-polyester blends for improved nutrient delivery.....	59
3.1	Introduction.....	59
3.2	Experimental section.....	63
3.2.1	General materials and procedures.....	63
3.2.2	Visualization of plant root-zone acidification.....	63
3.2.3	Blend coating preparation.....	64
3.2.4	Degradation of PEtG blended films in aqueous buffer solutions	64
3.2.5	Degradation of PEtG blended films in clay-loam agricultural soil.....	65
3.2.6	Degradation of PEtG blended films exposed to plant roots.....	66
3.2.7	Fourier transform infrared spectra - attenuated total reflectance (FTIR-ATR)	67
3.2.8	Surface Morphology	67
3.2.9	Preparation of spray coated urea.....	67
3.2.10	Preparation of hand coated urea.....	68
3.2.11	Determination of urea release rates in solution.....	68
3.2.12	Data analyses	69
3.3	Results and Discussion	70
3.3.1	Root zone acidification	70
3.3.2	Mass loss profiles of the coating exposed to buffer solutions	72
3.3.3	Mass loss profiles of coatings exposed to buffered agricultural soil	74
3.3.4	Mass loss profiles of coatings exposed to plant roots.....	77
3.3.5	Preparation and analysis of coated fertilizer pellets	79
3.3.6	Urea release study.....	83
3.4	Conclusions.....	85
3.5	References.....	86
4	Summary, outlooks, and conclusions.....	88

4.1 Summary and outcomes	88
4.2 Future outlooks	91
4.3 Conclusions.....	93
4.4 References.....	94
Appendix.....	95
Chapter 2 Appendix A Supporting Information	95
Chapter 3 Appendix B Supporting Information.....	128
Curriculum Vitae	129

List of Tables

Table 2-1 . Thermal transitions from DSC for polymer blends and copolymers	42
Table 2-2 Summary of results for PEtG blends and PCL Co-polymer for mechanical property testing.....	47

List of Figures

Figure 1-1 Nitrogen use efficiency (NUE) and common nitrogen losses to the surrounding environment.	6
Figure 1-2 Enhanced efficiency fertilizers.....	7
Figure 1-3 Schematic of a coated fertilizer pellet.	9
Figure 1-4 Schematic of a stimulus-responsive polymer and a self-immolative polymer.	12
Figure 1-5 Schematic illustrating the end-cap cleavage and depolymerization mechanism for poly(ethyl glyoxylate) (PEtG).....	14
Figure 1-6 Schematic of coated PEtG pellets with a phenyl carbamate end-cap in the presence of plant roots.	17
Figure 2-1 Chemical structures of A) PEtG and its depolymerization products; b) PCL; c) PLA; d) PHB.....	26
Figure 2-2 Analysis of PEtG:PCL blends by A) TGA and B) DSC.....	41
Figure 2-3 Phase contrast AFM images of PEtG blends and copolymer with PCL.....	44
Figure 2-4 Phase contrast AFM images of PEtG blends with PLA and PHB..	45
Figure 2-5 Mass loss profiles for UV light irradiated (IR; A, C, E), and non-irradiated (B, D, F) coatings immersed in 0.1 M pH 7.4 buffer at 22 °C	50
Figure 2-6 SEM images of polyester:PEtG 25:75 coatings after UV exposure and 0, 15, and 30 d of immersion in 0.1 M, pH 7.4 buffer at 22 °C.....	52
Figure 2-7 SEM images of polyester:PEtG 25:75 coatings without UV irradiation after 15 d and 45 d of immersion in 0.1 M, pH 7.4 buffer at 22 °C.....	53
Figure 3-1 Synthesis and degradation of PEtG when in the presence of acidic conditions....	61
Figure 3-2 Visualization of rhizosphere acidification of creeping bentgrass roots.	71

Figure 3-3 Mass loss profiles for coatings immersed in buffers at pH 5 or 7 and either 22 °C or 30 °C	73
Figure 3-4 Mass loss profiles for coatings immersed in agricultural clay-loam soil with pH adjusted to either pH 5 (0.1 M citrate acid) or pH 7 (0.1 M phosphate) at 22 °C or 30 °C....	76
Figure 3-5 Mass loss profiles for coatings imbedded in pots with either creeping bentgrass roots, gravel substrate alone, or weekly dosages of pH 5 0.1M citrate buffer at 22 °C or 30°C.	78
Figure 3-6 . SEM images of PEtG:PCL coatings	80
Figure 3-7 SEM image of surface morphology of PEtG:PCL manually-coated pellets from melted polymer blend.	82
Figure 3-8 IR spectra of A) PEtG-PCL 50 wt%, and B) PEtG-PLA 50 wt%.....	82
Figure 3-9 Urea release from PEtG:PCL coated pellets exposed to citrate buffer (pH 5) or phosphate buffer (pH 7) at either 22 °C or 30 °C for 21 d.	84

List of Appendices

Appendix A 1. ¹ H NMR spectrum of UV-responsive PEtG (600 MHz, CDCl ₃).....	95
Appendix A 2. ¹ H NMR spectrum of alkyne-PEtG-65k (600 MHz, CDCl ₃).....	96
Appendix A 3. ¹ H NMR spectrum of alkyne-PEtG-58k (600 MHz, CDCl ₃).....	97
Appendix A 4. ¹ H NMR spectrum of Br-PCL-low (600 MHz, CDCl ₃).....	98
Appendix A 5. ¹ H NMR spectrum of Br-PCL-high (600 MHz, CDCl ₃).....	99
Appendix A 6. ¹ H NMR spectrum of N ₃ -PCL-low (600 MHz, CDCl ₃).....	100
Appendix A 7. ¹ H NMR spectrum of N ₃ -PCL-high (600 MHz, CDCl ₃).....	101
Appendix A 8. ¹ H NMR spectrum of PCL- <i>b</i> -PEtG- <i>b</i> -PCL-low (400 MHz, CDCl ₃).....	102
Appendix A 9. ¹ H NMR spectrum of PCL- <i>b</i> -PEtG- <i>b</i> -PCL-high (400 MHz, CDCl ₃).....	103
Appendix A 10. FTIR spectrum of alkyne-PEtG-65k.....	104
Appendix A 11. FTIR spectrum of alkyne-PEtG-58k.....	105
Appendix A 12. FTIR spectrum of Br-PCL-low.....	106
Appendix A 13. FTIR spectrum of Br-PCL-high.....	107
Appendix A 14. FTIR spectrum of N ₃ -PCL-low.....	108
Appendix A 15. IR spectrum of N ₃ -PCL-high.....	109
Appendix A 16. IR spectrum of PCL- <i>b</i> -PEtG- <i>b</i> -PCL-low.....	110
Appendix A 17. IR spectrum of PCL- <i>b</i> -PEtG- <i>b</i> -PCL-high.....	111
Appendix A 18. SEC trace for UV-responsive PEtG.....	112
Appendix A 19. SEC trace for alkyne-PEtG-58k.....	113

Appendix A 20. SEC trace for alkyne-PEtG-65k	114
Appendix A 21. SEC trace for Br-PCL-low.	115
Appendix A 22. SEC trace for Br-PCL-high.	116
Appendix A 23. SEC traces for PCL- <i>b</i> -PEtG- <i>b</i> -PCL-low (solid line) and mixture of alkyne-PEtG-65k/N ₃ -PCL-low before CuAAC reaction (dashed line)	117
Appendix A 24. SEC traces for PCL- <i>b</i> -PEtG- <i>b</i> -PCL-high (solid line) and mixture of alkyne-PEtG-58k/N ₃ -PCL-high before CuAAC reaction (dashed line)..	118
Appendix A 25. A) TGA and B) DSC thermograms for pure PEtG.	119
Appendix A 26. A) TGA and B) DSC thermograms for PCL- <i>b</i> -PEtG- <i>b</i> -PCL-low and PCL- <i>b</i> -PEtG- <i>b</i> -PCL-high.	120
Appendix A 27. A) TGA and B) DSC thermograms of PLA:PEtG blends.....	121
Appendix A 28. A) TGA and B) DSC thermograms for PLA:PHB:PEtG blends.	122
Appendix A 29. Phase contrast AFM images of the pure polymers.....	123
Appendix A 30. Representative stress-strain curves for the pure polymers and 50:50 polyester:PEtG blends acquired by tensile testing at a strain of 5 mm/min.	124
Appendix A 31. SEM images of polyester:PEtG 50:50 coatings after UV exposure and 0, 15 or 30 d of immersion in 0.1 M, pH 7.4 buffer at 22 °C..	125
Appendix A 32. SEM images of polyester:PEtG 50:50 coatings without UV irradiation and 15 or 45 d of immersion in 0.1 M, pH 7.4 buffer at 22 °C.	126
Appendix A 33. SEM images of pure polyester or PEtG coatings after UV exposure and 5 or 45 d of immersion in 0.1 M, pH 7.4 buffer at 22 °C.....	127

Appendix B 1. SEM image of a commercially available controlled release coated urea pellet from Osmocote.....	128
Appendix B 2. SEM images of PCL:PEtG spray-coated films.	128

List of Schemes

Scheme 1. A) Synthesis of PCL-PEtG triblock copolymers and B) Synthesis of azide-terminated PCL.	38
---	----

List of Abbreviations

AFM	Atomic force microscopy
ANOVA	Analysis of variance
CRF	Controlled release fertilizer
DMF	Dimethylformamide
DSC	Differential scanning calorimetry
Đ	Dispersity
EEF	Enhanced efficiency fertilizers
FT-IR	Fourier transform infrared spectroscopy
M_n	Number average molecular weight
M_w	Weight average molecular weight
MPa	Megapascal
N	Nitrogen
NI	Nitrification inhibitors
NUE	Nitrogen use efficiency
NMR	Nuclear magnetic resonance
NVOC	6-Nitroveratryloxycarbonyl
IR	Irradiated
PE	Polyethylene
PEtG	Poly(ethyl glyoxylate)
PEG	Poly(ethylene glycol)
PCL	Polycaprolactone
PHB	Poly(<i>R</i> -3-hydroxybutyrate)
PPHA	Polyphthalaldehyde
PLA	Poly(L-lactic acid)
PS	Polystyrene
PU	Polyurethane
ROP	Ring-opening polymerization
SEC	Size exclusion chromatography
TGA	Thermalgravimetric analysis
SEM	Scanning electron microscope
SRP	Stimuli-responsive polymer
SIP	Self-immolative polymer
T_g	Glass transition temperature
THF	Tetrahydrofuran
T_m	Melting point temperature
Ui	Urease inhibitors
UV	Ultraviolet

Chapter 1

1 Introduction

1.1 Plant mineral nutrition

Plant growth, development, and reproduction are often limited by the availability of mineral nutrients in the soil (Chapin et al. 1986). Macronutrients, which are required in relatively large quantities, include nitrogen, phosphorus and potassium (NPK) (Maathuis 2009). Nitrogen is required in particularly large quantities as a component of amino acids and proteins, and it is also present in chlorophyll (Zhao et al. 2005). Micronutrients are those which are required in much smaller quantities to maintain proper physiological function (White and Brown 2010).

Plant nutrient uptake from soil is achieved within root hair tips either through simple and facilitated diffusion or from active transport systems (Barber et al. 1963). Simple diffusion allows very few ions (O_2 , CO_2 , and NH_3) to move freely through plant lipid bilayers membranes as they follow a concentration gradient (Reid and Hayes 2003). Facilitated diffusion is the rapid movement of solutes or ions following a concentration gradient, using transport proteins (Reid and Hayes 2003). Active transport requires ions to move against a concentration which require high levels of energy in the form of ATP to power the pumps that move out H^+ ions out into the root hair tips in an area called the rhizosphere (Marschner et al. 1987). Nutrient uptake occurs in the rhizosphere, which is the narrow region of soil that is directly influenced by root secretions and associated soil microorganisms (Gonzalez et al. 2015). It is characterized by chemical, biological, and physical concentration gradients that spread and change longitudinally along the root

(Bais et al. 2004). The rhizosphere also contains bacteria that form symbiotic relationships with plants; the plants provide microbes with a source of carbon, and the microbes provide the plants with mineral nutrients in exchange (Bais et al. 2004). Many interactions that occur between plant roots, their associated soil microorganisms and nutrients are influenced by root exudates in the rhizosphere (Morrissey et al. 2004). These exudates include organic acids, sugars, amino acids, inorganic molecules, and enzymes, some of which play an important role in plant nutrient acquisition (Dakora and Phillips, 2000).

Nutrient absorption from active transport typically begins when hydrogen ions are used to displace cations attached to negatively charged soil particles, thus allowing the cations to be readily taken up by the roots (Marschner et al. 1987). When entering root tips, ions are transported to the center of the root (also known as the stele) until they reach conducting tissues (xylem and phloem) (Haynes 1990). The xylem is responsible for the movement of water and inorganic molecules within the plant using the water potential gradient present from the roots tips to the leaves (White and Brown 2010).

1.2 Plant nutrient availability

In many ecosystems NPK availability often limits plant growth because the high macronutrient demand of plants is matched by a relatively low supply (Masclaux-Daubresse et al. 2010). Nitrogen is often limited despite the atmosphere consisting of 78% N₂, as the triple bond of this nitrogen gas must be broken via nitrogen fixation before the nitrogen can become available to plants (Galloway et al. 2004). Soils commonly contain around 0.1 – 0.6% nitrogen by mass within the upper 15 cm (Cameron

et al. 2013). Mineral nitrogen is present within soil as ammonium (NH_4^+), nitrite (NO_2^-), nitrate (NO_3^-), and nitrogen gas (N_2) (Cameron et al. 2013). Soil nitrogen also is present in organic matter and soil microorganisms. However, to obtain nitrogen from many of these organic sources, plants must rely on the biogeochemical cycling of nitrogen into mineral forms or simple organic forms such as amino acids (Galloway et al. 2004). Nitrogen for plant use is converted through chemical and biological processes including fixation, ammonification, nitrification, and denitrification, which only be performed by a limited number of bacterial, fungal and archaea genera (van der Heijden et al. 2008). For example, bacteria such as *Azotobacter* fix atmospheric N_2 into ammonia (NH_3) (Raymond et al. 2004). Meanwhile, bacteria such as the *Nitrobacter* genus perform nitrification to produce nitrate (the preferred form for many plants, because they have different affinities for nitrates and ammonium) by oxidizing ammonia (Prosser 1989, Xu et al. 2012). Nitrogen availability in soil is directly influenced by these transformations as many forms of nitrogen are highly mobile in soil (van der Heijden et al. 2008). Many soils types are negatively charged and because of this they cannot sustain forms of nitrate and are often lost through leaching. When soils are saturated with high levels of nitrates denitrification may occur also contributing to nitrogen losses through N_2 and N_2O production (Galloway et al. 2004). Nitrogen availability may be diminished from volatilization of ammonia (Cameron et al. 2013).

1.3 Nutrients and agriculture

Within the last 100 000 years, the cultivation of land for agriculture has allowed humans to shift from a nomadic hunter lifestyle to building civilizations around the world (Thrall et al. 2010, Paoletti et al. 2011). Cultivation of plants has given rise to

agroecosystems and to the study of agronomy (science of agriculture). Agricultural practices have been crucial for the evolution of modern humans by increasing food production and security (Thrall et al. 2010). Prior to the 1900's, crop rotation, tilling of land and manure addition were the main practices used to improve crop yield (Thrall et al. 2010). Since then, greater agricultural efficiencies increasing crop productivity have been achieved through plant breeding, agrochemicals and synthetic fertilizers (Moyle and Muir 2010, Gomiero et al. 2011) . Plant breeding focuses on changing the traits of plants by propagating lineages through selection of desirable attributes, while agrochemicals use chemical products to protect crops from pathogens, and to enhance plant growth (Burdon and Thrall 2008, Van Tassel et al. 2010). Fertilizers (including organic and inorganic sources) supplement the delivery of essential nutrients for plant growth and development, which is required over time given that many agroecosystems become limited by the amount of naturally occurring nutrients, and the mineral nutrient demands of most annual crops are relatively high (e.g. 20-50 g of N is needed to produce around 1 kg of dry biomass for nonlegume plants) (Maathuis 2009, Xu et al. 2012).

After World War II, a “Green Revolution” began, which focused on the large-scale commercialization of N based fertilizers (Tilman et al. 2001). This was achieved through development of the Haber-Bosch process, which produces ammonia for use in N-based fertilizers (Xu et al. 2012). Common anthropogenic fertilizers are synthesized into forms of either ammonium nitrate (34 wt% N) or urea (46 wt% N). Many soil bacteria possess the enzyme urease, which is responsible for catalyzing the conversion of urea to ammonium salts (a form that can be taken up readily by plant roots) (Dave et al. 1999).

Ammonium salts also can be oxidized to form nitrite, which subsequently is converted by *Nitrobacter* species into nitrate (Raymond et al. 2004).

Although increased productivity and crop yields have been achieved with the increased use of commercial synthetic fertilizer, only a minor fraction of the added fertilizer is typically taken up by plants; nitrogen use efficiency (NUE) – defined here as the amount of nitrogen taken up by plants in relation to the amount added to the soil – is 30-50% in many agricultural systems (Figure 1-1 A) (Zhao et al. 2013, Abalos et al. 2014). Low NUE in agricultural fields is caused by poor soil nutrient retention caused in part by asynchronies between the timing of fertilizer application and plant growth (Morgan et al. 2009). N fertilizer that is not taken up by plant roots can be lost from the soil through denitrification, (leading to volatile losses), immobilization and leaching (Figure 1-1 B) (Cameron et al. 2013). The escape of excess N from agricultural systems into the surrounding environment pollutes the air, water and soil (Timilsena et al. 2015). Nitrate entering rivers, lakes and basins contribute to eutrophication, resulting in loss of biodiversity (Tilman et al. 2001). N inputs also increase greenhouse gas emissions in the form of N_2O and increased wet and dry deposition from the atmosphere (originating in part from agricultural sources), which increases soil acidification and eutrophication of terrestrial systems (Stuart et al. 2014). In addition, nitrate in drinking water has been linked to an increased risk of methaemoglobinaemia in newborns, and heart disease (Cameron et al. 2013).

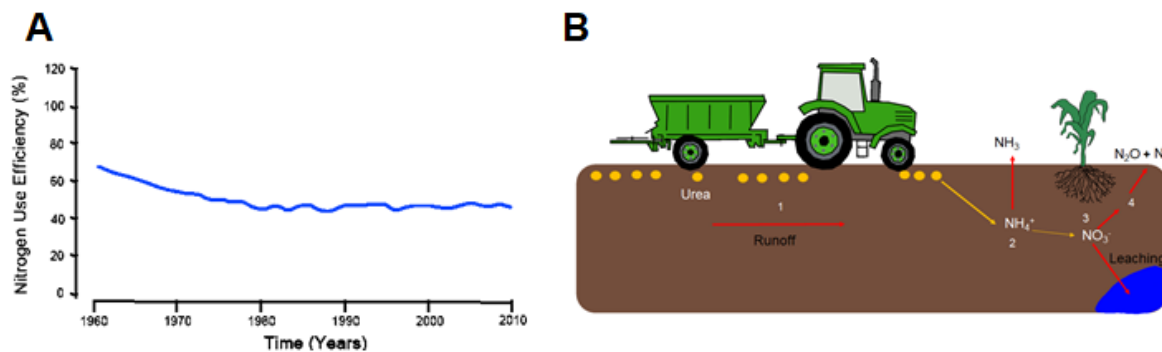


Figure 1-1 Nitrogen use efficiency (NUE) and common nitrogen losses to the surrounding environment. (A) NUE has not improved over the past 50 years (Modified from Timilsena et al., 2015). (B) Common losses of nitrogen depicted for urea-based fertilizers: (1) Urea lost via runoff; (2) Ammonia volatilization; (3) Leaching of nitrates; (4) nitrous oxide emissions.

Over the past 5 decades, the world consumption of nitrogen has increased at a rate of approximately 2% per annum, which is driven by global food requirements and human population increase (Timilsena et al. 2015). The World Summit on Food Security reported that by 2050, overall food production must increase to 44 million metric tons to feed the estimated 9 billion people (Paoletti et al. 2011). To achieve this demand, there are several options: 1) increasing N-fertilizer doses by 3-fold 2) applying fertilizer more frequently 3) a drastic improvement in NUE (Xu et al. 2012). The first option would intensify the undesirable side effects on the surrounding environment. The second option is constrained by logistics, because it is typically difficult and costly to apply fertilizer to an agricultural field with an established crop. The third option, however, could be achieved through the development of techniques that improve nutrient delivery, the improvement of management practices, and from the use of enhanced efficiency fertilizers (EEFs) (Timilsena et al. 2015).

1.4 Improvement of fertilizer efficiency

Enhanced efficiency fertilizers (EEFs) have been developed to increase the synchronization between nutrient supply and crop nutrient demand, and to ultimately reduce nutrient loss (i.e. increased NUE), thereby decreasing the economic cost of reapplying fertilizers, as well as decreasing adverse environmental outcomes (Timilsena et al. 2015). EEFs include those containing nitrification inhibitors (NIs) and urease inhibitors (UIs), as well as controlled release fertilizers (CRF) (Abalos et al. 2014). The respective aims of using NIs and UIs are to delay the oxidation of ammonium (Figure 1-2 A) and the hydrolysis of urea by reducing microbial activity (Figure 1-2 B), thereby avoiding the rapid transformation of N into forms that are less stable (Halvorson et al. 2014). The aim of using CRFs is to delay nutrient release (Akiyama et al. 2010).

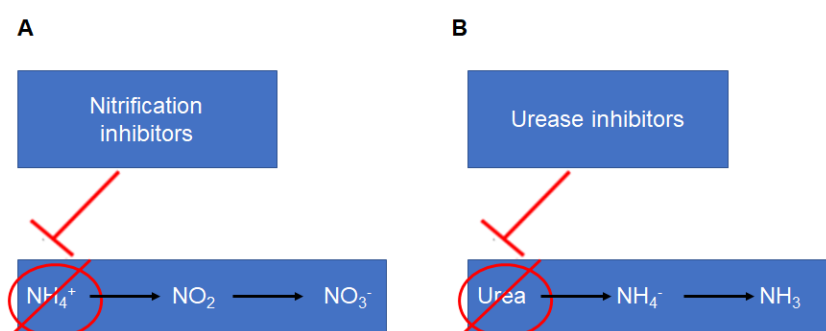


Figure 1-2 Enhanced efficiency fertilizers: (A) Nitrification inhibitors delay the oxidation of ammonium; (B) Urease inhibitors delay the hydrolysis of urea, reducing nitrification, volatilization and microbial activity.

1.5 Controlled release fertilizer

Controlled release fertilizer pellets contain conventional soluble nutrients that are encapsulated by a protective coating that acts as a physical barrier to extend the timing of nutrient release (Chagas et al. 2016). CRF coatings were designed to selectively release nitrogen in synchronization with plant needs during the growing season to minimize nutrient losses (Xia et al. 2017). Protective coatings can be classified into two categories, which are made up of either inorganic (sulphur) materials or synthetic polymeric materials (Figure 1-3) (Lu et al. 2013). Inorganic sulphur coatings are commonly referred to as slow-release fertilizer, and the main method of release is from microbial decomposition (Morgan et al. 2009). The rate of release is highly dependent on the thickness of the coating material, with the average mass of the coating being around 20 wt% of the urea pellet (Shaviv et al. 2003). In contrast, for synthetic polymeric coatings, which consist of either thermoplastic or resin materials (including polyethylene (PE) and polyurethane (PU)), the coating weights are 5-15 wt% of the pellet (Liang and Liu 2006) (Yang et al. 2011). The nutrient release mediated by these polymers is highly dependent on environmental conditions (primarily temperature), soil type, and coating thickness (Shaviv et al. 2003, Adams et al. 2013, Wei et al. 2017).

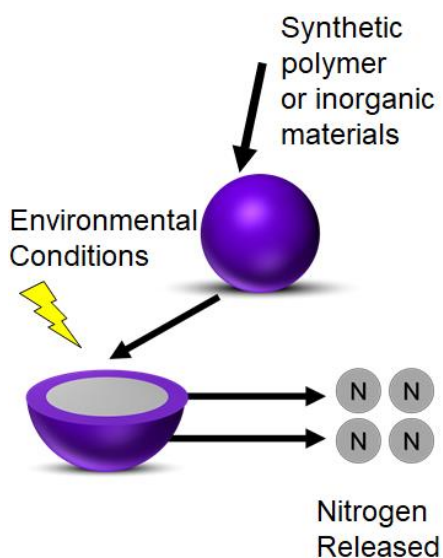


Figure 1-3 Schematic of a coated fertilizer pellet. The protective coating delays the release of nitrogen (or other nutrients), and the coating consists of either synthetic polymers or inorganic materials that release fertilizer in response to environmental conditions (mainly temperature).

1.6 Polymers

Polymers are defined as macromolecules composed of many repeating units linked together by covalent bonds (Gao et al. 2017). There are many different types of macromolecules, ranging from naturally occurring DNA, carbohydrates and protein, to synthetic polymers such as polyethylene (PE), polyurethane (PU) and polystyrene (PS) (Gao et al. 2017). The large molecular mass of polymers makes them very unique in their physical properties, and it allows them to have variable toughness, elasticity and crystallinities (Stein and Tobolsky 1948). Synthetic polymeric materials have become integral to our everyday lives, fulfilling a range of functions, including packaging, building materials and coatings. Polymers are used often because their physical properties can be tuned to achieve specific functions, depending on the molecular weight, polymer

backbone, and degree of branching. For example, polystyrene (PS) (also known as Styrofoam) is commonly used in packings for protection against mechanical load when it is in its low-density form (expanded polystyrene), whereas PS also is used as a disposable plastic such as petri dishes in its high density form (Aubert and Clough 1985, Kannan et al. 2007).

Despite their uses, many of these commonly used plastics are non-biodegradable and around 40% of them are non-reusable (Nair and Laurencin 2007). Annually, 322 million metric tons are used, and much of this ends up in landfills or contaminating ecosystems (Weithmann et al. 2018). Because many traditional polymers have undesirable environmental outcomes, there has been steady research into developing biodegradable polymers (Lubkowski et al. 2015). Biodegradable polymers are broken down after their intended uses into natural byproducts, such as simple, benign carbon compounds and water (Amass et al. 1998). The predominant mechanism for biodegradation over time is from enzymatic activity of microorganisms (Majeed et al. 2015). These biodegradable polymers commonly consist of esters and amides, with degradation dependent on chemical structure (Amass et al. 1998). Polyesters such as poly(lactic acid) (PLA) and polycaprolactone (PCL) are commonly used for both 3D printing, packaging and biomedical applications (Amass et al. 1998). Although they degrade into non-toxic byproducts, they do have limitations, because they typically break down in a highly unpredictable manner (Tokiwa and Jarerat 2004). However, a family of biodegradable polyesters known as stimuli-responsive polymers (SRPs) has been being targeted for a wide range of applications, because the degradation can be controlled and triggered (Stuart et al. 2010).

1.7 Stimuli-responsive polymers

Stimuli-responsive polymers are of interest, because their properties can be controlled and changed by specific stimuli, unlike other traditional biodegradable polyesters, which generally degrade slowly through an uncontrolled pathway that relies heavily on random hydrolysis backbone scission (Stuart et al. 2010). SRPs can respond to intrinsic biological stimuli, such as enzymes, redox events, pH changes and even temperature changes (Qiu and Park 2001, Bajpai et al. 2008). Stimuli can trigger changes in the state or solubility of the polymer backbone. However, SRPs can require a large number of the mediated stimuli-mediated events to achieve cleavage of the polymer backbone (Figure 1-4 A) (Sagi et al. 2008a). Because of this limitation, further research has gone into developing polymeric materials that are stimulus-responsive and exhibit an amplified response (Roth et al. 2016). These polymers are categorized into a new class called self-immolative polymers (SIPs) (Sagi et al. 2008a).

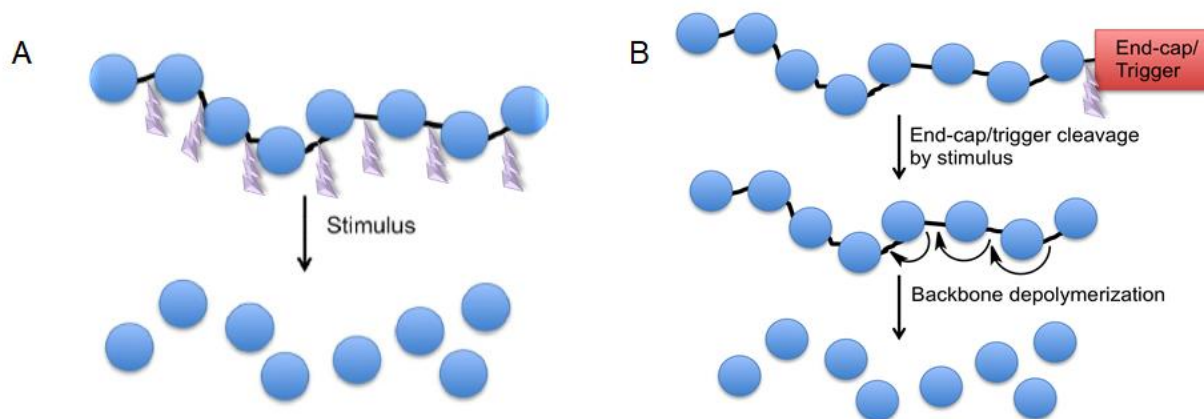


Figure 1-4. Schematic of a stimulus-responsive polymer and a self-immolative polymer. (A) Typical stimulus-responsive polymer, which requires many stimulus-mediated events (one to break each individual bond) (B) Self-immolative polymer requires one stimulus event to cleave the end-cap and initiate backbone depolymerization.

1.8 Self-immolative polymers (SIPs)

SIPs undergo end-to-end backbone depolymerization in a highly predictable manner upon removal of a stabilizing end-caps via stimulus-induced cleavage (Figure 1-4 B) (Sagi et al. 2008a). Once the stable functional group is removed, the polymers self-depolymerize into monomers and small molecule by-products (Sagi et al. 2008a). End-cap removal has been achieved through a number of pathways, such as in response to heat, pH changes, light, enzymes and changes in redox potential (Fan et al. 2016, Fan and Gillies 2017). The response to the stimulus is amplified by a single detection event leading to the release of many depolymerization products, and it can be tuned in these systems by control of the monomer to end-cap ratio as well as the polymer composition and length (McBride and Gillies 2013). This allows for there to be a high degree of control over the conditions and time over which degradation occurs.

Poly(glyoxylates) are a recently developed class of SIPs which can respond rapidly to stimuli, and which produce innocuous degradation by-products (Figure 1-5 A) (Fan et al. 2014). Poly(ethyl glyoxylate) (PEtG) in particular has been a research focus, because it degrades rapidly upon removal of its stabilizing end-cap, and it can be coupled with end-caps that respond to a wide range of stimuli (e.g. pH, redox, H₂O₂, heat and UV-light) (Fan et al. 2016, Fan et al. 2017). It degrades into glyoxylic acid hydrate and ethanol (Belloncle et al. 2012). Glyoxylic acid hydrate is a metabolic intermediate in the glyoxylic acid cycle. This cycle commonly occurs in plants, bacteria and protists, which convert glyoxylic acid to carbon dioxide. The by-products also have been demonstrated to be non-toxic in ecotoxicity models with invertebrates, and they even have the potential to improve plant growth (Belloncle et al. 2012). However, PEtG lacks suitable physical properties for many applications due to its low glass transition (T_g) and its amorphous structure, which cause it to become extremely adhesive and soft under ambient conditions (Figure 1-5 B) (Fan and Gillies 2002, Fan et al. 2014, Kaitz and Moore 2014). Exploratory research to improve these properties never has been conducted.

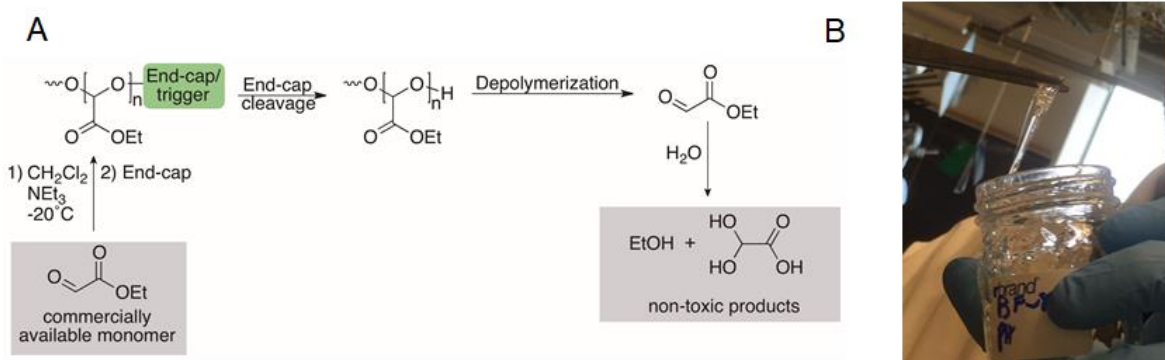


Figure 1-5 Schematic illustrating the end-cap cleavage and depolymerization mechanism for poly(ethyl glyoxylate) (PEtG). (A) PEtG is synthesized from monomers of glyoxylate into polymer chains, and capped with an end-cap trigger. Once the end cap trigger is removed from stimuli mediated event end-to-end depolymerization occurs, producing glyoxylate, which can go through hydrolysis to produce the non-toxic products ethanol and glyoxylic acid hydrate (a metabolic intermediate in glyoxylic acid cycle that occurs in plants and bacteria). (B) Raw PEtG is extremely sticky in its natural state

1.9 Overall thesis objective

Although current CRFs increase NUE compared to conventional fertilizer, given that the release is proportional mainly to temperature, it is not directly synchronized with plant root growth (Lubkowski et al. 2015). Plant growth often increases with increasing temperature in the late spring and early summer, which provides a certain degree of synchronization of nutrient release with plant growth. However, the plant rooting zone continues to expand at this time, and conventional CRFs may release nutrients in soil patches that have not yet been explored by plant roots. Many companies claim that they have designed "smart coatings," but these coatings simply enable release through water penetration (micro holes on coating surface) and release rates increase with higher temperatures. As suggested above, this merely gives the impression that release is

synchronized with increasing plant nutrient demand over the growing season, but there is not a high degree of control over nutrient release, and it does not respond directly to the presence of plant roots.

A further drawback is many of the current CRF products such as Osmocote, Nutricote, ESN, and Polyon are comprised of polymers that are not environmentally-friendly (alkyd resins, polyurethane, and polyolefins), because they do not degrade, and they thus contribute to the accumulation of microplastics in soil (Shaviv 2001, Lubkowski et al. 2015). A considerable amount of these non-functional and undesired microplastics are being left in soil at rate of 50 kg/ha a year (Lubkowski et al. 2015). Small fragments of plastics that become part of the soil deteriorate overall soil quality (Majeed et al. 2015). Microplastics are becoming a major concern in both aquatic and terrestrial ecosystems, although most studies of effects to date have focused on aquatic environments. Weithmann et al. (2018) reported that the potential effects of many of the plastics used for fertilizer applications are currently being ignored, and they will become problematic in the future (Weithmann et al. 2018). This concern suggests that there needs to be a shift to coatings that do not persist and accumulate in agroecosystems and their surrounding environment.

Although current CRF's increase nitrogen use efficiency to some degree by prolonging nutrient release, the residual coating materials nevertheless have negative environmental impacts (i.e. decreasing soil quality and contributing to microplastic accumulation). A possible solution that has not yet been implemented on a large scale is the development of CRFs using biodegradable materials. Some biodegradable materials that have been explored contain either starch or cellulose derivatives, and poly (lactic) acid (Han et al. 2009). Although these products are biodegradable, they are not stimu-

responsive, and degradation occurs in a manner that is not synchronized with plant growth and nutrient demand (Azeem et al. 2014).

An ideal fertilizer coating would enable the release of nutrients in a controlled and delayed manner and in synchrony with the needs of plants. It should also incorporate an inexpensive, non-toxic and biodegradable polymer that can easily be applied to fertilizer in industrial scale production, and which does not exhibit negative downstream effects on non-target soil organisms (Tomaszewska et al. 2002). As of today, none of the currently available polymer-based products meet these requirements. I propose that the unique stimuli-responsive properties of polyglyoxylates make them ideal for use as fertilizer coatings. The ability to engineer SIP backbones to respond to different stimuli, by changing only the end-cap, offers a significant advantage over conventional slow release fertilizers. However, the scope of functional end-caps remains unexplored, and the effects of different environmental conditions (e.g., pH, and temperature) on the depolymerization process and rate have not been studied. In addition, poly(ethyl glyoxylate) has a very low glass transition temperature (the point in which polymeric material goes from a soft to a rigid and glassy material), which causes it to be highly adhesive at room temperature, which would result in the aggregation of pellets coated with pure PEtG. To develop effective fertilizer coatings with this polymer, the mechanical properties therefore need to be adjusted (i.e. by blending it with other polymers) to produce a more rigid polymer that still maintains the desired durability and degradation properties, and rapid response to the intended stimulus.

For my research, I targeted a pH-responsive end-cap with the goal that it would enable depolymerization and consequently polymer coating degradation to occur

selectively in the vicinity of plant roots, where the environment is more acidic than the surrounding soil as a result of cationic exchanges of H^+ ions (Nye 1981) (Figure 1-6). Because the physical properties of PEtG on its own are not ideal for a coating material (i.e., it is sticky), I explored the blending of PEtG with other biodegradable polymers to develop a suitable coating (at the time of development I used a uv-sensitive end-cap as the pH responsive end-cap was not developed yet).

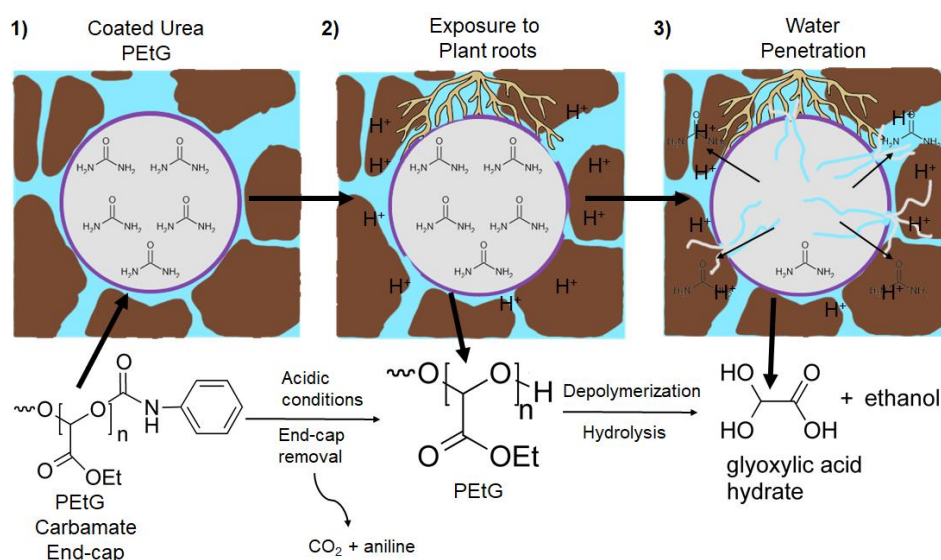


Figure 1-6 Schematic of coated PEtG pellets with a phenyl carbamate end-cap in the presence of plant roots. 1) Pellet coated with PEtG stable in wet soil 2) Plant root tips have a pH of 5 as they release hydrogen ions into the soil substrate. 3) After end-cap removal PEtG breaks down into glyoxylic acid hydrate and ethanol; once sufficient degradation has occurred water penetration occurs and urea will diffuse out through the micropores.

1.10 Specific objectives

I hypothesize that polymer blends containing PEtG could be used to produce non-aggregating and suitably rigid pellet coatings that would delay the release of fertilizer, and that end-cap sensitivity changes in pH could be triggered by plant root stimuli.

Chapter 2 of this thesis focuses on the improvement of the polymer physical properties, while Chapter 3 focuses on the characterization of the polymeric blends with the pH sensitive end-cap and the development of fertilizer coatings. My incremental objectives for developing these triggerable PEtG-coated fertilizer pellets were as follows:

Objective 1: *Improvement of polymer physical properties* – I developed blends of PEtG and polyesters to improve the properties (i.e. adequate stiffness and reduced adhesion), while still maintaining the desirable degradation properties of pure PEtG.

Objective 2: *Characterization of end-cap function* – I examined the degradation over time of polymer blends with pH sensitive end-caps when exposed to their respective chemical stimuli, and to plant roots.

Objective 3: *Optimization of coating and release*– I coated urea pellets with polymer blends and examined the timing of urea release following exposure to the respective chemical end-cap stimuli in solution.

1.11 References

- Abalos, D., S. Jeffery, A. Sanz-Cobena, G. Guardia, and A. Vallejo. 2014. Meta-analysis of the effect of urease and nitrification inhibitors on crop productivity and nitrogen use efficiency. *Agriculture Ecosystems & Environment* **189**:136-144.
- Adams, C., J. Frantz, and B. Bugbee. 2013. Macro- and micronutrient-release characteristics of three polymer-coated fertilizers: Theory and measurements. *Journal of Plant Nutrition and Soil Science* **176**:76-88.
- Akiyama, H., X. Y. Yan, and K. Yagi. 2010. Evaluation of effectiveness of enhanced-efficiency fertilizers as mitigation options for N₂O and NO emissions from agricultural soils: meta-analysis. *Global Change Biology* **16**:1837-1846.
- Amass, W., A. Amass, and B. Tighe. 1998. A review of biodegradable polymers: Uses, current developments in the synthesis and characterization of biodegradable polyesters, blends of biodegradable polymers and recent advances in biodegradation studies. *Polymer International* **47**:89-144.
- Azeem, B., K. KuShaari, Z. B. Man, A. Basit, and T. H. Thanh. 2014. Review on materials & methods to produce controlled release coated urea fertilizer. *Journal of Controlled Release* **181**:11-21.
- Bais, H. P., S. W. Park, T. L. Weir, R. M. Callaway, and J. M. Vivanco. 2004. How plants communicate using the underground information superhighway. *Trends in Plant Science* **9**:26-32.
- Bajpai, A. K., S. K. Shukla, S. Bhanu, and S. Kankane. 2008. Responsive polymers in control led drug delivery. *Progress in Polymer Science* **33**:1088-1118.
- Barber, S. A., J. M. Walker, and E. H. Vasey. 1963. Mechanisms for movement of plant nutrients from soil and fertilizer to plant root. *Journal of Agricultural and Food Chemistry* **11**:204-207.
- Belloncle, B., C. Bunel, L. Menu-Bouaouiche, O. Lesouhaitier, and F. Burel. 2012. Study of the Degradation of Poly(ethyl glyoxylate): Biodegradation, Toxicity and Ecotoxicity Assays. *Journal of Polymers and the Environment* **20**:726-731.
- Burdon, J. J., and P. H. Thrall. 2008. Pathogen evolution across the agro-ecological interface: implications for disease management. *Evolutionary Applications* **1**:57-65.
- Cameron, K. C., H. J. Di, and J. L. Moir. 2013. Nitrogen losses from the soil/plant system: a review. *Annals of Applied Biology* **162**:145-173.
- Chagas, W. F. T., D. R. Guelfi, A. L. C. Caputo, T. L. de Souza, A. B. Andrade, and V. Faquin. 2016. Ammonia volatilization from blends with stabilized and controlled-released urea in the coffee system. *Ciencia E Agrotecnologia* **40**:497-509.
- Chapin, F. S., P. M. Vitousek, and K. Vancleve. 1986. The nature of nutrient limitation in plant-communities. *American Naturalist* **127**:48-58.
- Dave, A. M., M. H. Mehta, T. M. Aminabhavi, A. R. Kulkarni, and K. S. Soppimath. 1999. A review on controlled release of nitrogen fertilizers through polymeric membrane devices. *Polymer-Plastics Technology and Engineering* **38**:675-711.
- Fan, B., and E. R. Gillies. 2002. Self-Immolative Polymers. *Encyclopedia of Polymer Science and Technology*. John Wiley & Sons, Inc.

- Fan, B., and E. R. Gillies. 2017. Poly(ethyl glyoxylate)-Poly(ethylene oxide) Nanoparticles: Stimuli-Responsive Drug Release via End-to-End Polyglyoxylate Depolymerization. *Molecular Pharmaceutics* **14**:2548-2559.
- Fan, B., J. F. Trant, and E. R. Gillies. 2016. End-Capping Strategies for Triggering End-to-End Depolymerization of Polyglyoxylates. *Macromolecules* **49**:9309-9319.
- Fan, B., J. F. Trant, G. Hemery, O. Sandre, and E. R. Gillies. 2017. Thermo-responsive self-immolative nanoassemblies: direct and indirect triggering. *Chemical Communications* **53**:12068-12071.
- Fan, B., J. F. Trant, A. D. Wong, and E. R. Gillies. 2014. Polyglyoxylates: A Versatile Class of Triggerable Self-Immolative Polymers from Readily Accessible Monomers. *Journal of the American Chemical Society* **136**:10116-10123.
- Galloway, J. N., F. J. Dentener, D. G. Capone, E. W. Boyer, R. W. Howarth, S. P. Seitzinger, G. P. Asner, C. C. Cleveland, P. A. Green, E. A. Holland, D. M. Karl, A. F. Michaels, J. H. Porter, A. R. Townsend, and C. J. Vorosmarty. 2004. Nitrogen cycles: past, present, and future. *Biogeochemistry* **70**:153-226.
- Gao, Y. F., M. L. Wei, X. Li, W. W. Xu, A. Ahiabu, J. Perdiz, Z. N. Liu, and M. J. Serpe. 2017. Stimuli-responsive polymers: Fundamental considerations and applications. *Macromolecular Research* **25**:513-527.
- Gomiero, T., D. Pimentel, and M. G. Paoletti. 2011. Environmental Impact of Different Agricultural Management Practices: Conventional vs. Organic Agriculture. *Critical Reviews in Plant Sciences* **30**:95-124.
- Gonzalez, M. E., M. Cea, J. Medina, A. Gonzalez, M. C. Diez, P. Cartes, C. Monreal, and R. Navia. 2015. Evaluation of biodegradable polymers as encapsulating agents for the development of a urea controlled-release fertilizer using biochar as support material. *Science of the Total Environment* **505**:446-453.
- Halvorson, A. D., C. S. Snyder, A. D. Blaylock, and S. J. Del Grosso. 2014. Enhanced-Efficiency Nitrogen Fertilizers: Potential Role in Nitrous Oxide Emission Mitigation. *Agronomy Journal* **106**:715-722.
- Han, X. Z., S. Chen, and X. G. Hu. 2009. Controlled-release fertilizer encapsulated by starch/polyvinyl alcohol coating. *Desalination* **240**:21-26.
- Haynes, R. J. 1990. Active ion uptake and maintenance of cation-anion balance - a critical-examination of their role in regulating rhizosphere pH. *Plant and Soil* **126**:247-264.
- Kaitz, J. A., and J. S. Moore. 2014. Copolymerization of o-Phthalaldehyde and Ethyl Glyoxylate: Cyclic Macromolecules with Alternating Sequence and Tunable Thermal Properties. *Macromolecules* **47**:5509-5513.
- Liang, R., and M. Z. Liu. 2006. Preparation and properties of a double-coated slow-release and water-retention urea fertilizer. *Journal of Agricultural and Food Chemistry* **54**:1392-1398.
- Lu, P. F., M. Zhang, Q. Li, and Y. Xu. 2013. Structure and Properties of Controlled Release Fertilizers Coated with Thermosetting Resin. *Polymer-Plastics Technology and Engineering* **52**:381-386.
- Lubkowski, K., A. Smorowska, B. Grzmił, and A. Kozłowska. 2015. Controlled-Release Fertilizer Prepared Using a Biodegradable Aliphatic Copolyester of Poly(butylene succinate) and Dimerized Fatty Acid. *Journal of Agricultural and Food Chemistry* **63**:2597-2605.

- Maathuis, F. J. M. 2009. Physiological functions of mineral macronutrients. *Current Opinion in Plant Biology* **12**:250-258.
- Majeed, Z., N. K. Ramli, N. Mansor, and Z. Man. 2015. A comprehensive review on biodegradable polymers and their blends used in controlled-release fertilizer processes. *Reviews in Chemical Engineering* **31**:69-96.
- Marschner, H., V. Romheld, and I. Cakmak. 1987. Root-induced changes of nutrient availability in the rhizosphere. *Journal of Plant Nutrition* **10**:1175-1184.
- Masclaux-Daubresse, C., F. Daniel-Vedele, J. Dechorgnat, F. Chardon, L. Gaufichon, and A. Suzuki. 2010. Nitrogen uptake, assimilation and remobilization in plants: challenges for sustainable and productive agriculture. *Annals of Botany* **105**:1141-1157.
- McBride, R. A., and E. R. Gillies. 2013. Kinetics of Self-Immolative Degradation in a Linear Polymeric System: Demonstrating the Effect of Chain Length. *Macromolecules* **46**:5157-5166.
- Morgan, K. T., K. E. Cushman, and S. Sato. 2009. Release Mechanisms for Slow- and Controlled-release Fertilizers and Strategies for Their Use in Vegetable Production. *Horttechnology* **19**:10-12.
- Morrissey, J. P., J. M. Dow, G. L. Mark, and F. O'Gara. 2004. Are microbes at the root of a solution to world food production? Rational exploitation of interactions between microbes and plants can help to transform agriculture. *Embo Reports* **5**:922-926.
- Moyle, L. C., and C. D. Muir. 2010. Reciprocal insights into adaptation from agricultural and evolutionary studies in tomato. *Evolutionary Applications* **3**:409-421.
- Nair, L. S., and C. T. Laurencin. 2007. Biodegradable polymers as biomaterials. *Progress in Polymer Science* **32**:762-798.
- Nye, P. H. 1981. Changes of pH across the rhizosphere induced by roots. *Plant and Soil* **61**:7-26.
- Paez, J. I., M. Martinelli, V. Brunetti, and M. C. Strumia. 2012. Dendronization: A Useful Synthetic Strategy to Prepare Multifunctional Materials. *Polymers* **4**:355-395.
- Paoletti, M. G., T. Gomiero, and D. Pimentel. 2011. Introduction to the Special Issue: Towards A More Sustainable Agriculture. *Critical Reviews in Plant Sciences* **30**:2-5.
- Prosser, J. I. 1989. Autotrophic nitrification in bacteria. *Advances in Microbial Physiology* **30**:125-181.
- Qiu, Y., and K. Park. 2001. Environment-sensitive hydrogels for drug delivery. *Advanced Drug Delivery Reviews* **53**:321-339.
- Raymond, J., J. L. Siefert, C. R. Staples, and R. E. Blankenship. 2004. The natural history of nitrogen fixation. *Molecular Biology and Evolution* **21**:541-554.
- Reid, R., and J. Hayes. 2003. Mechanisms and control of nutrient uptake in plants. *International Review of Cytology - a Survey of Cell Biology, Vol 229* **229**:73-114.
- Roth, M. E., O. Green, S. Gnaim, and D. Shabat. 2016. Dendritic, Oligomeric, and Polymeric Self-Immolative Molecular Amplification. *Chemical Reviews* **116**:1309-1352.
- Sagi, A., R. Weinstain, N. Karton, and D. Shabat. 2008. Self-immolative polymers. *Journal of the American Chemical Society* **130**:5434.
- Shaviv, A. 2001. Advances in controlled-release fertilizers. *Advances in Agronomy, Vol 71* **71**:1-49.

- Shaviv, A., S. Raban, and E. Zaidel. 2003. Modeling controlled nutrient release from polymer coated fertilizers: Diffusion release from single granules. *Environmental Science & Technology* **37**:2251-2256.
- Stein, R. S., and A. V. Tobolsky. 1948. An investigation of the relationship between polymer structure and mechanical properties .1. relationship between structure, mechanical properties, and birefringence. *Textile Research Journal* **18**:201-223.
- Stuart, D., R. L. Schewe, and M. McDermott. 2014. Reducing nitrogen fertilizer application as a climate change mitigation strategy: Understanding farmer decision-making and potential barriers to change in the US. *Land Use Policy* **36**:210-218.
- Stuart, M. A. C., W. T. S. Huck, J. Genzer, M. Muller, C. Ober, M. Stamm, G. B. Sukhorukov, I. Szleifer, V. V. Tsukruk, M. Urban, F. Winnik, S. Zauscher, I. Luzinov, and S. Minko. 2010. Emerging applications of stimuli-responsive polymer materials. *Nature Materials* **9**:101-113.
- Thrall, P. H., J. D. Bever, and J. J. Burdon. 2010. Evolutionary change in agriculture: the past, present and future. *Evolutionary Applications* **3**:405-408.
- Tilman, D., J. Fargione, B. Wolff, C. D'Antonio, A. Dobson, R. Howarth, D. Schindler, W. H. Schlesinger, D. Simberloff, and D. Swackhamer. 2001. Forecasting agriculturally driven global environmental change. *Science* **292**:281-284.
- Timilsena, Y. P., R. Adhikari, P. Casey, T. Muster, H. Gill, and B. Adhikari. 2015. Enhanced efficiency fertilisers: a review of formulation and nutrient release patterns. *Journal of the Science of Food and Agriculture* **95**:1131-1142.
- Tokiwa, Y., and A. Jarrerat. 2004. Biodegradation of poly(L-lactide). *Biotechnology Letters* **26**:771-777.
- Tomaszewska, M., A. Jarosiewicz, and K. Karakulski. 2002. Physical and chemical characteristics of polymer coatings in CRF formulation. *Desalination* **146**:319-323.
- van der Heijden, M. G. A., R. D. Bardgett, and N. M. van Straalen. 2008. The unseen majority: soil microbes as drivers of plant diversity and productivity in terrestrial ecosystems. *Ecology Letters* **11**:296-310.
- Van Tassel, D. L., L. R. DeHaan, and T. S. Cox. 2010. Missing domesticated plant forms: can artificial selection fill the gap? *Evolutionary Applications* **3**:434-452.
- Wei, Y., J. Li, Y. T. Li, B. Q. Zhao, L. G. Zhang, X. D. Yang, and J. Chang. 2017. Research on permeability coefficient of a polyethylene controlled-release film coating for urea and relevant nutrient release pathways. *Polymer Testing* **59**:90-98.
- Weithmann, N., J. N. Moller, M. G. J. Loder, S. Piehl, C. Laforsch, and R. Freitag. 2018. Organic fertilizer as a vehicle for the entry of microplastic into the environment. *Science Advances* **4**:7.
- White, P. J., and P. H. Brown. 2010. Plant nutrition for sustainable development and global health. *Annals of Botany* **105**:1073-1080.
- Xia, L. L., S. K. Lam, D. L. Chen, J. Y. Wang, Q. Tang, and X. Y. Yan. 2017. Can knowledge-based N management produce more staple grain with lower greenhouse gas emission and reactive nitrogen pollution? A meta-analysis. *Global Change Biology* **23**:1917-1925.
- Xu, G. H., X. R. Fan, and A. J. Miller. 2012. Plant Nitrogen Assimilation and Use Efficiency. Pages 153-182 in S. S. Merchant, editor. *Annual Review of Plant Biology*, Vol 63. Annual Reviews, Palo Alto.

- Yang, Y. C., M. Zhang, L. Zheng, D. D. Cheng, M. Liu, and Y. Q. Geng. 2011. Controlled Release Urea Improved Nitrogen Use Efficiency, Yield, and Quality of Wheat. *Agronomy Journal* **103**:479-485.
- Zhao, B., S. T. Dong, J. W. Zhang, and P. Liu. 2013. Effects of Controlled-Release Fertiliser on Nitrogen Use Efficiency in Summer Maize. *Plos One* **8**:8.
- Zhao, D. L., K. R. Reddy, V. G. Kakani, and V. R. Reddy. 2005. Nitrogen deficiency effects on plant growth, leaf photosynthesis, and hyperspectral reflectance properties of sorghum. *European Journal of Agronomy* **22**:391-403.

Chapter 2

2 Triggerable degradation of polymer coatings using polyglyoxylate-polyester blends and copolymers

2.1 Introduction

Coatings are used extensively to impart specific surface properties to objects that differ from those of the bulk material from which the object is composed. For example, fluoropolymer coatings are applied to cookware to introduce resistance to both water and oil, while poly(vinyl chloride) is applied to automobiles to prevent corrosion (Akafuah et al. 2016, McKeen 2016). In these applications, it is desirable for the coating to retain its integrity as long as possible to prolong the lifetime of the underlying surface (Li et al. 2015). However, in other applications, degradable coatings are desired. For example, coatings are applied to pharmaceutical tablets to protect them during storage, while allowing them to dissolve and release the drug after ingestion (Nampoothiri et al. 2010). In addition, coated fertilizer pellets are used to provide a slow release of fertilizer in soil over weeks to months (Chien et al. 2009).

In the case of degradable coatings, it is desirable that their erosion can be controlled to occur under specific conditions at a predetermined rate. This can be achieved with stimuli-responsive polymers, which degrade or undergo changes in their physical properties in response to a stimulus such as changes in pH (Stuart et al. 2010). For example, Eudragit® polymers have been used extensively in solid oral dosage forms of pharmaceuticals (Pignatello et al. 2002). These polymers are poly(meth)acrylates with acidic or basic groups that undergo changes in solubility as they move through the digestive

tract, thereby controlling the encapsulation and release of the underlying molecules (Lehr 1994, Langer and Peppas 2003). In addition, reduction-sensitive disulfide linkages have been used to cross-link polymer networks at the outlet of mesoporous silica, blocking the release of encapsulated drugs (Liu et al. 2008). Cleavage of the disulfides by a reducing agent triggers the release of the drugs.

One emerging class of stimuli-responsive polymers is self-immolative polymers (SIPs) (Wang and Alexander 2008, Peterson et al. 2012, Roth et al. 2016). SIPs undergo an end-to-end backbone depolymerization upon the removal of stabilizing end-caps from the polymer termini (Fan and Gillies 2002). Because the degradation of an entire polymer chain is induced by a single bond cleavage, SIPs effectively offer an amplification of the stimulus event (Chen et al. 2012, McBride and Gillies 2013). In addition, because depolymerization is controlled by the end-cap, a single SIP backbone can be engineered to respond to many different stimuli. Depolymerization stimuli that have been investigated include enzymes, heat, light, and changes in pH or redox potentials (Sagi et al. 2008b, DeWit and Gillies 2009, Fomina et al. 2010, Song et al. 2013, Okada et al. 2014, Peterson et al. 2014, Wang et al. 2014, Fan et al. 2016, Fan et al. 2017). Our group reported 6-nitroveratryl carbonate end-capped poly(ethyl glyoxylate) (PEtG, Figure 2-1 A) as a SIP with potential for a number of applications due to its breakdown to the non-toxic and environmentally friendly products glyoxylic acid hydrate and ethanol (Belloncle et al. 2012). We studied the degradation of PEtG coatings as a function of pH, film thickness, and water content, showing that PEtG offers well controlled and tunable degradation (Fan et al. 2016). However, on its own PEtG lacks suitable physical properties as a coating material due to its amorphous structure and low glass transition temperature (T_g) of -5 to -

10 °C, making it rubbery and tacky under ambient conditions (Fan et al. 2014, Kaitz and Moore 2014).

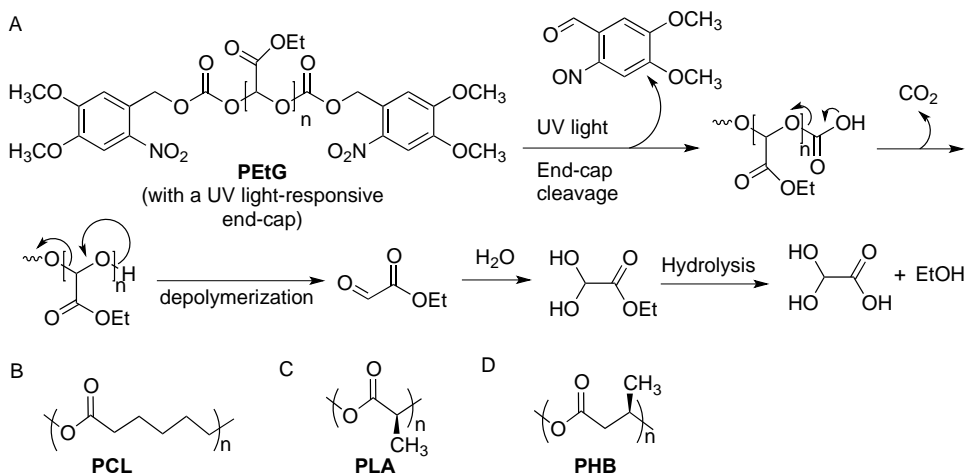


Figure 2-1 Chemical structures of A) PEtG capped with a uv-sensitive end-cap (6-nitroveratryl carbonate) and its depolymerization products; b) PCL; c) PLA; d) PHB.

A strategy to overcome the limiting physical and mechanical properties of polymers is the preparation of blends or copolymers with other polymers (Yu et al. 2006). In this approach, the resulting blend or copolymer can ideally assume the favorable properties of both components (Liu and Zhang 2011) (Yu et al. 2006). For example, in the area of SIPs, polyphthalaldehyde and ethyl glyoxylate were copolymerized with the aim of tuning the T_g and overcoming polyphthalaldehyde's brittleness (Kaitz and Moore 2014). However, to the best of our knowledge, physical blends based on SIPs have not been reported. With the aim of developing PEtG-based materials having properties suitable for coatings, we report here the preparation and study of blends of PEtG with the well-established biodegradable polymers polycaprolactone (PCL), poly(L-lactic acid) (PLA), and poly(*R*-3-hydroxybutyrate) (PHB) (Figure 1B-D) (Ramakrishna et al. 2001).

Because macroscopic phase separation is a well-known challenge for polymer blends, a block copolymer of PEtG and PCL also was synthesized, as it exhibits nanophase separation, and studied for comparison with the physical blends. The materials were characterized by thermogravimetric analysis (TGA), differential scanning calorimetry (DSC), atomic force microscopy (AFM), and tensile testing. The degradation of blend and copolymer coatings in response to end-cap cleavage also was studied, showing that it was possible to prepare materials with suitable coating properties while retaining the desirable triggered depolymerization feature of SIPs.

2.2 Experimental

2.2.1 General materials and procedures

PEtG with a 6-nitroveratryl carbonate end-cap and alkyne-PEtG were synthesized as previously reported (Fan et al. 2014). PCL ($M_n = 55$ kg/mol) was supplied by Scientific Polymer Products, poly(L-lactic acid) (PLA, $M_n = 103.5$ and purchased from 3D Solutech, and PHB ($M_n = 550$ kg/mol) was purchased from Goodfellow. CH_2Cl_2 was distilled from CaH_2 immediately before use. THF and toluene were distilled from sodium/benzophenone and degassed by three freeze-pump-thaw cycles before use. DMF was obtained from a solvent purification system using aluminum oxide columns. NMR spectra were recorded on a 600 MHz Varian INOVA 600 instrument or 400 MHz with a Bruker AvIII HD 400 instrument to confirm purity of polymer substrates. ^1H NMR spectra were referenced to residual CHCl_3 (7.27 ppm). FT-IR spectra were obtained using a PerkinElmer FT-IR Spectrum Two instrument in attenuated total reflectance mode to identify and confirm chemical composition of blends. SEC was performed in THF at 5 mg/mL of polymer using a Viscotek GPCmax VE 2001 SEC instrument equipped with an Agilent PolyPore guard column (PL1113-1500) and two sequential Agilent PolyPore to confirm polymer molecular weight and size. SEC columns packed with porous poly(styrene-*co*-divinylbenzene) particles (MW range: 200–2,000,000 g/mol; PL1113-6500) regulated at a temperature of 30 °C. Molar masses were calculated relative to polystyrene standards with a correction factor of 0.56 applied only to the PCL samples (Zhang et al. 2009).

2.2.2 Preparation of the polyester:PEtG blends

PEtG, PCL, and PLA were each dissolved in CH_2Cl_2 at a concentration of 90 mg/mL. PHB was first converted to its highly amorphous state by placing 1 g of PHB pellets within a piece of aluminum foil, then placing this in a Carver 3851 Heated Press (Carver, Wabash, IN) with both the plates set to 175 °C. Light pressure was applied until the sample melted. The aluminum foil package was then submerged in liquid nitrogen to flash freeze the PHB. The amorphous PHB along with PLA was then dissolved in CH_2Cl_2 at a concentration of 90 mg/mL in a 1:3 mixture. The stock solutions of polymer were then mixed to afford solutions containing 1:0, 75:25, 50:50, and 25:75 ratios of polyester:PEtG (Table 2-1). One third of a milliliter of solution was then drop cast into a 25 mL glass vial and the solvent was evaporated *in vacuo* until constant weight was achieved (~48 h, ~30 mg/vial). The average coating thickness of these films were around ~ 80 μm , as measured by digital calipers, after removal from the vial.

2.2.3 Synthesis of Br-PCL-low

ϵ -Caprolactone (4.0 mL, 36 mmol), 3-bromo-1-propanol (43 μL , 0.48 mmol) and dry toluene (24 mL) were combined in a flame-dried round bottom flask. Trimethylaluminum solution (2.0 M in toluene, 0.19 mL, 0.38 mmol) was then added and the solution was heated at 50 °C for 60 min. The reaction was then quickly cooled to room temperature and CH_2Cl_2 (10 mL) and methanol (3 mL) were added. The reaction mixture was precipitated into cold methanol (700 mL) and the product was isolated by filtration. The polymer was then dissolved in minimal THF, precipitated into cold methanol and dried to constant weight under reduced pressure to afford 3.67 g (92% yield) of the product. ^1H NMR (600 MHz, CDCl_3): δ 1.33 – 1.42 (m, 2H), 1.58 – 1.68 (m, 4H), 2.17 (tt, $J = 6.6, 6.1$ Hz, end

group), 2.29 (t, $J = 7.5$ Hz, 2H), 3.45 (t, $J = 6.6$ Hz, end group), 3.61-3.67 (m, end group), 4.05 (t, $J = 6.7$ Hz, 2H), 4.21 (t, $J = 6.1$ Hz, end group). IR: 2945, 2865, 1722 cm^{-1} . SEC: $M_n = 13.5$ kg/mol, $D = 1.41$.

2.2.4 Synthesis of Br-PCL-high

The same procedure as described above for the synthesis of Br-PCL-low was followed except that ϵ -caprolactone (4.65 mL, 42 mmol), 3-bromopropanol (22 μL , 0.24 mmol) and trimethylaluminum solution (100 μL , 0.19 mmol) in toluene (36 mL) were used to afford 4.41 g (95% yield) of the product. ^1H NMR (600 MHz, CDCl_3): δ 1.33 – 1.42 (m, 2H), 1.58 – 1.68 (m, 4H), 2.17 (tt, $J = 6.6, 6.1$ Hz, end group), 2.29 (t, $J = 7.5$ Hz, 2H), 3.46 (t, $J = 6.6$ Hz, end group), 3.61-3.67 (m, end group), 4.05 (t, $J = 6.7$ Hz, 2H), 4.21 (t, $J = 6.1$ Hz, end group). IR: 2945, 2865, 1722 cm^{-1} . SEC: $M_n = 29.1$ kg/mol, $D = 1.27$.

2.2.5 Synthesis of N_3 -PCL-low

Br-PCL-low (2.2 g, 0.20 mmol) was dissolved in DMF (45 mL) and heated to 50 $^\circ\text{C}$. Sodium azide (0.6 g, 8.0 mmol, 40 equiv. per Br) was then added. The reaction was stirred at 50 $^\circ\text{C}$ for 18 h, then cooled to room temperature and filtered. The filtrate was added to 150 mL of water. The mixture was extracted with CHCl_3 (4 \times 100 mL). The organic extracts were combined, washed with water (100 mL) and concentrated. The polymer was then dissolved in minimal CH_2Cl_2 and precipitated into hexanes, filtered and dried to constant weight under reduced pressure to afford 2.1 g (93% yield) of the product. ^1H NMR (600 MHz, CDCl_3): δ 1.33 – 1.42 (m, 2H), 1.58 – 1.68 (m, 4H), 1.88-1.94 (m, end

group), 2.29 (t, $J = 7.5$ Hz, 2H), 3.39 (t, $J = 6.8$ Hz, end group), 3.63-3.65 (m, end group), 4.05 (t, $J = 6.7$ Hz, 2H), 4.16 (t, $J = 6.3$ Hz, end group). IR: 2945, 2865, 2100, 1722 cm^{-1} .

2.2.6 Synthesis of N₃-PCL-high

The same procedure described above for the synthesis of N₃-PCL-low was followed except that Br-PCL-high (4.41 g, 0.18 mmol) and sodium azide (0.48 g, 7.4 mmol, 40 eq.) in DMF (75 mL) were used to afford 4.25 g (96% yield) of the product. ¹H NMR (600 MHz, CDCl₃): δ 1.33 – 1.42 (m, 2H), 1.58 – 1.68 (m, 4H), 1.88-1.93 (m, end group), 2.29 (t, $J = 7.5$ Hz, 2H), 3.39 (t, $J = 6.8$ Hz, end group), 3.62-3.67 (m, end group), 4.05 (t, $J = 6.7$ Hz, 2H), 4.16 (t, $J = 6.3$ Hz, end group). IR: 2945, 2865, 2105, 1722, 1680 cm^{-1} .

2.2.7 Synthesis triblock copolymer of PCL-*b*-PETG-*b*-PCL-low

Alkyne-PEtG ($M_n = 65$ kg/mol, 1.0 g, 1.5×10^{-2} mmol) and N₃-PCL-low (0.32 g, 2.9×10^{-2} mmol, 1.95 equiv.) were dissolved in dry DMF (15 mL). CuSO₄ (50 mg) and sodium ascorbate (50 mg) were then added. The reaction was degassed (3 \times freeze-pump-thaw cycles) and refilled with N₂. The reaction was then heated to 40 °C for 16 h, and subsequently cooled to room temperature. It was filtered twice through a 0.2 μm PTFE filter and dried under reduced pressure to constant weight to afford 1.21 g (91% yield) of the product. ¹H NMR (400 MHz, CDCl₃): δ 1.26-1.33 (m, 2.9H) 1.33 – 1.44 (m, 0.6H), 1.56 – 1.70 (m, 1.5H), 2.30 (t, $J = 7.5$ Hz, 0.6H), 4.06 (t, $J = 6.7$ Hz, 0.6H), 4.14 – 4.30 (m, 1.5H), 5.45 – 5.75 (m, 1.0H). IR: 2990, 2945, 1745, 1725 cm^{-1} . SEC: $M_n = 59.0$ kg/mol, $D = 2.0$.

2.2.8 Synthesis triblock copolymer of PCL-*b*-PEtG-*b*-PCL-high

The same procedure described above for the synthesis of PCL-*b*-PEtG-*b*-PCL-low was followed except that alkyne-PEtG ($M_n = 58$ kg/mol, 1.5 g, 2.6×10^{-2} mmol), N₃-PCL-high (1.5 g, 2.6×10^{-2} mmol), CuSO₄ (50 mg) and sodium ascorbate (50 mg) in THF (25 mL) were used to afford 2.5 g (83% yield) of the product. ¹H NMR (400 MHz, CDCl₃): δ 1.24-1.34 (m, 3.0H), 1.33 – 1.44 (m, 2.0H), 1.56 – 1.70 (m, 3.7H), 2.30 (t, $J = 6.8$ Hz, 1.8H), 4.06 (t, $J = 6.8$ Hz, 1.8H), 4.14 – 4.30 (m, 2.0H), 5.45 – 5.75 (m, 1.0H). IR: 2945, 2868, 1750, 1725 cm⁻¹. SEC: $M_n = 62.1$ kg/mol, $D = 2.1$.

2.2.9 Thermal analyses

Polymer blends were prepared by the above process. TGA was performed using a TA Instruments Q-50 TGA. Ten milligrams of polymer were placed in an aluminum Tzero pan and heated at rate of 10 °C/min between 35-500 °C under nitrogen purging. DSC was performed using a Q2000 instrument from TA instruments (New Castle, DE). The heating/cooling rate was 10 °C/min from -75 to +120 °C. The T_g and T_m values were obtained from the second heating cycle.

2.2.10 Atomic force microscopy (AFM)

Glass microscope slides were washed with acetone. Polyester:PEtG solutions were diluted to 10 mg/mL, then passed through a Promax 0.22 μ m PTFE filter 3 times. The filtered solution (20 μ L) was then dropped onto the center of a glass slide and placed in a WS-400-6NPP-LITE Spin Processor, where it was exposed to a vacuum and rotated at 3000 RPM. AFM was then performed using a Park Systems XE-100 instrument with a tip apex radius

of 10 nm. Surface topography and phase images were examined using the AFM tapping mode. The data were analyzed using XEI image processing software.

2.2.11 Tensile testing

Polyester:PEtG solutions (1:0 and 50:50, 100 mg/mL) in CHCl_3 were prepared using the same method as for the CH_2Cl_2 solutions described above. The solution was then added to a polytetrafluoroethylene mold (50 mm \times 50 mm). The samples were then left to evaporate for 18 h in a fume hood. The resulting films were cooled to -35°C , removed from the block and cut into 10 mm \times 50 mm strips (~ 0.2 mm thickness as measured by digital calipers) for tensile measurements. Tensile testing was performed using an Instron 5943 (10 N load cell) according to ASTM 882. The extension rate was 5 mm/min. At least 5 specimens were tested for each blend.

2.2.12 Coating Degradation studies

The coatings were prepared as described above (Preparation of the polyester:PEtG blends). Accurate initial masses of each coating were measured and recorded. Samples were irradiated subsequently by being placed into an ACE glass photochemistry cabinet containing a mercury light source (450 W bulb, 2.8 mW/cm² measured for UVA radiation at the sample position) for 4 h to trigger the light-sensitive end-cap. The irradiation was repeated at 10 and 20 d after initial exposure to ensure end-cap cleavage of underlying layers. Controls sample were not irradiated and were stored in the dark. All samples were submerged in 0.1 M pH 7.4 phosphate buffer solution at ambient temperature (22 °C). At

desired time points, the vials from each treatment were removed from the buffer solution, rinsed with distilled water and dried under reduced pressure for 48 h. Their masses were then recorded and compared to initial values to calculate the % initial mass remaining. Mass loss for the irradiated blends was measured over a 30-d period, while mass loss for control blends was measured over a 60-d period. Triplicate samples were measured at each time point.

2.2.13 Scanning electron microscopy

For irradiated samples, coatings from the degradation study were removed from the vials for the 0, 15, and 30 d time points. For non-irradiated control samples, coatings were removed from the vials for the 15 and 45 d time points. The samples were mounted on carbon taped aluminum stubs and sputtered with gold at a rate of 5 nm/min for 4 min (Hummer-6 sputtering system, Anatech, Union City, California). Scanning electron microscopy was performed on a Hitachi S-3400N instrument at a voltage of 3 kV and view distance of 10 (Hitachi, Toyko, Japan).

2.2.14 Data Analyses

For each response variable, a one-way analysis of variance (ANOVA) was used to assess the effects of different polymeric blends on either stress, strain, or overall Young moduli (measure of stress over strain). All statistical analyses were conducted using JMP version 14 (SAS Institute).

2.3 Results and Discussion

2.3.1 Preparation of PEtG-polyester Blends

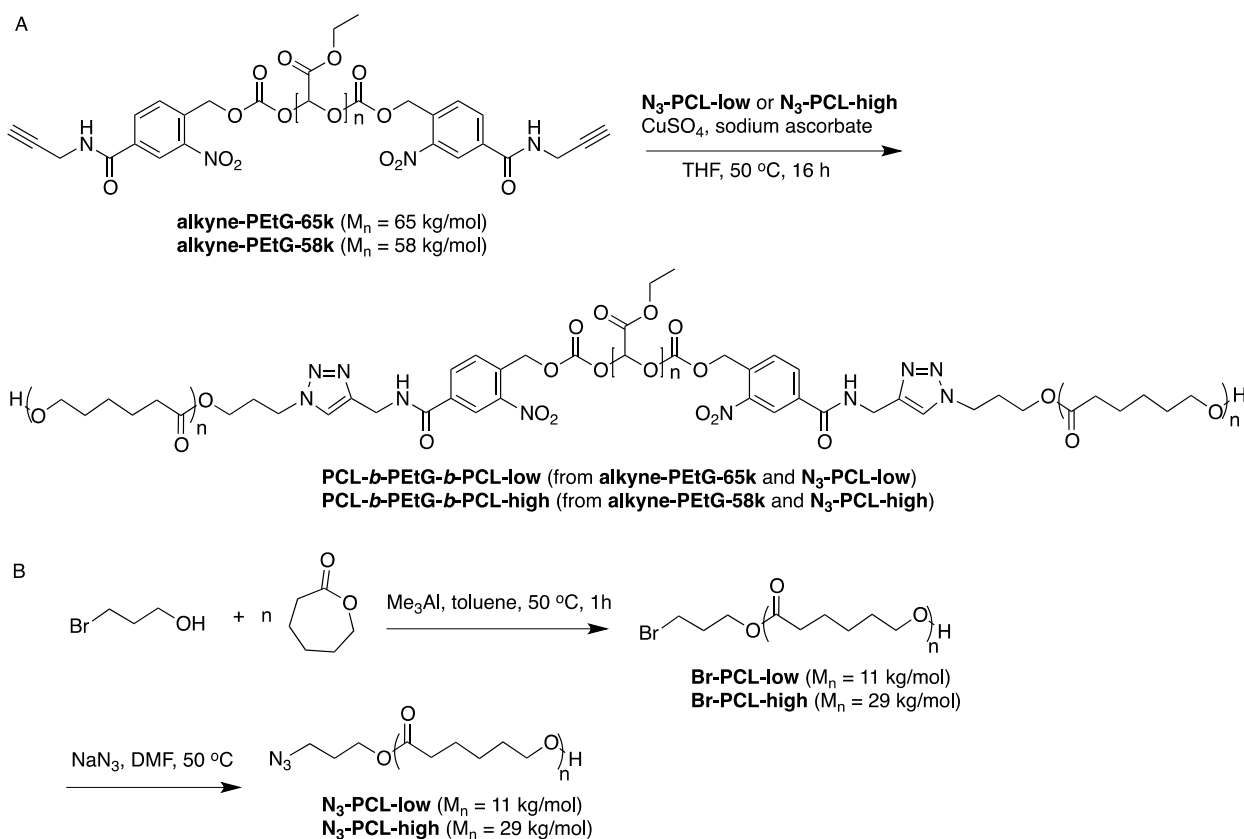
PEtG was synthesized as previously reported by a low temperature polymerization of ethyl glyoxylate and was capped using 6-nitroveratryl chloroformate to afford the corresponding carbonate end-capped polymer with an M_n of 54 kg/mol and D of 1.8 based on size exclusion chromatography (SEC) in THF relative to polystyrene standards (Belloncle et al. 2012). While various stimuli-responsive end-caps have been incorporated onto PEtG, this UV-responsive polymer serves as an ideal model system because the end-cap can be cleanly and rapidly cleaved by irradiation with UV light (360 nm), thereby triggering depolymerization (Figure 2-1 A) (Fan et al. 2016, Fan and Gillies 2017, Fan et al. 2017). The polyesters were purchased from commercial sources. PCL was selected because it is a biodegradable polyester that has been commonly blended with other polymers to improve their properties, such as processing characteristics and impact resistance. PCL has a low T_g of about $-60\text{ }^\circ\text{C}$, but is semi-crystalline with a T_m of $\sim 60\text{ }^\circ\text{C}$. PLA was selected because it is a well-established biodegradable polymer that can be obtained from renewable resources (Liu and Zhang 2011). It has a T_g of $60 - 65\text{ }^\circ\text{C}$ and a T_m of $173 - 178\text{ }^\circ\text{C}$ (Sodergard and Stolt 2002). Finally, PHB was also selected because it is a bio-derived and biodegradable plastic. Its high melting temperature ($173-180\text{ }^\circ\text{C}$) and crystallinity of $\sim 80\%$ (Abdelwahab et al. 2012) make it challenging to process, so it has commonly been combined with PLA in a PLA:PHB 3:1 ratio to improve its physical properties (Abdelwahab et al. 2012). Thus, it also was employed as a 3:1 PLA:PHB blend in this study. It was anticipated that the use of these three different blend systems (PCL, PLA, and 3:1 PLA:PHB) would enable a range

of properties to be obtained for the blends with PEtG. Blends were prepared by co-dissolving the PEtG and polyester in CH_2Cl_2 at ratios of 75:25, 50:50, and 75:25 polyester:PEtG (90 mg/mL total polymer), drop casting the solution as a coating and then evaporating the solvent *in vacuo* at ambient temperature. Due to the poor solubility of the semi-crystalline PHB, it was first heated just above the melting temperature (*ca.* 175 °C) and flash cooled in liquid N_2 to provide an amorphous state. The amorphous PHB was considerably more soluble, allowing for blend preparation, but it became semi-crystalline again upon solvent evaporation.

2.3.2 Synthesis triblock copolymer of a PEtG-PCL

While polymer blends can undergo macroscopic phase separation, the covalent linkages between blocks confine phase separation to the nanoscale for block copolymers, which can result in physical properties that are different from those of blends. These properties include the degree of tackiness, crystallinity, and elasticity. Thus, to compare the blending to the block copolymer approach, a triblock copolymer PCL-*b*-PEtG-*b*-PCL was targeted. First, UV-responsive PEtG with alkyne functionality (Scheme 1A) was prepared as previously reported (Belloncle et al. 2012). The two different batches prepared for the current work had $M_n = 65$ kg/mol and $D = 1.8$ (alkyne-PEtG-65k) and $M_n = 58$ kg/mol and $D = 1.8$ (alkyne-PEtG-58k). This alkyne moiety has previously enabled the preparation of PEG-*b*-PEtG-*b*-PEG copolymers using copper-catalyzed alkyne-azide cycloaddition (CuAAC) reactions with azide-terminated PEG (Belloncle et al. 2012). Azide-terminated PCL (N_3 -PCL) was then targeted with M_n values of 11 kg/mol (N_3 -PCL-low) and 29 kg/mol (N_3 -PCL-high) to give block copolymers with ~25 and 50 wt% PCL

after conjugation to alkyne-PEtG-65k and alkyne-PEtG-58k respectively. Initial efforts to synthesize azide-terminated PCL focused on the use of 2-azidoethanol or 3-azido-1-propanol as initiators for the ring-opening polymerization (ROP) of ϵ -caprolactone. However, the resulting polymers were unsuccessful in subsequent CuAAC reactions, likely due to the poor stability of the azide functionality during polymerization. To overcome this problem, bromine-terminated PCL (Br-PCL) was first prepared using 3-bromo-1-propanol and trimethyl aluminum as a catalyst for ROP in toluene (Scheme 1B) (Atanase et al. 2011). The M_n values determined by size exclusion chromatography were an M_n of 13.5 kg/mol and \mathcal{D} of 1.41 for Br-PCL-low, while Br-PCL-high had an M_n of 29.1 kg/mol and \mathcal{D} of 1.27 based on SEC (Figures S21-S22).



Scheme 1. A) Synthesis of PCL-PEtG triblock copolymers and B) Synthesis of azide-terminated PCL.

Next the bromide-terminated PCLs were converted to N_3 -PCL-low and N_3 -PCL-high by reaction with NaN_3 in DMF at 50 °C for 4 h. Conversion to N_3 -PCL was confirmed by ^1H NMR spectroscopy based on shifts in the peaks corresponding to the methylene groups adjacent to the bromides versus azides (Figures S6-S7). In addition, diagnostic azide peaks ($\sim 2100\text{ cm}^{-1}$) were observed in the Fourier transform infrared (FTIR) spectra of the polymers (Figures S13 and S14). The block copolymers were synthesized by CuAAC in THF at 50 °C using CuSO_4 and sodium ascorbate and with a 2:1 stoichiometric ratio of PCL:PEtG. Successful conjugation of the blocks was confirmed by SEC analysis of the mixture before and after the reaction (S23-S24). FTIR spectroscopy also confirmed

the disappearance of the peak corresponding to the azide moieties (Figures S16-S17). Analyses of the ^1H NMR spectra also were consistent with successful conjugations and confirmed that PCL-*b*-PEtG-*b*-PCL-low and PCL-*b*-PEtG-*b*-PCL-high had PCL content of ~25 and 50 wt% respectively (Figures S8-S9).

2.3.3 Thermal Properties

The thermal properties of the blends and copolymers were investigated by TGA and DSC. Based on TGA, all blends and copolymers underwent a two-phase degradation, with the PEtG degrading at ~ 180 °C and the polyesters degrading at ~ 350 °C in the case of PCL, ~ 300 °C for PLA, and ~ 275 °C for PHB (Figure 2-2 A and S25-S28). In addition, the percentage degraded at the different temperatures corresponded to the expected mass % of the respective polymers in the blends. DSC analyses confirmed that phase separation occurred for each system, because there were distinct thermal transitions for the individual polymers in the blends (Table 2-1, Figure 2-2 B and S25-S28). For example, for the PCL:PEtG blends, T_g s for the PEtG were observed at -3 to -6 °C and the T_m for the crystalline PCL phase was observed at $53 - 55$ °C. The T_g of the PEtG phase was slightly elevated with increasing PCL content relative to that of the pure polymer, while at the same time blending with PEtG lowered the PCL T_m relative to that of pure PCL, presumably due to decreasing crystal size. Similar thermal behavior was observed for the copolymers PCL-*b*-PEtG-*b*-PCL. The PCL T_g could not be detected in the blends due to the dominant transitions associated with PEtG's T_g and PCL's T_m .

In the PLA:PEtG blends, a small increase in the PEtG T_g to -6 to -7 °C also was observed. At the same time, the T_g of PLA decreased significantly, from 63 °C for the pure

polymer to 48 to 54 °C for the blends, suggesting partial mixing of the two polymers. While a T_m for PLA would be expected at 173 – 178 °C, the limited thermal stability of the PEtG prevented analysis up to these temperatures, so it could not be measured. Interestingly, the T_g of PEtG in the PLA:PHB:PEtG blends decreased to -9 to -14 °C, suggesting that blending enhances chain mobility in PEtG, perhaps due to some interpolymer mixing. T_m s were observed at 42 to 45 °C with analysis of the homopolymers, which suggested that this was due to small PHB crystalline domains that resulted from the processing method. The T_g of PLA was masked by the T_m from PHB. While preparation and thermal analysis of the 75:25 polyester:PEtG blends was of interest to elucidate trends in their thermal properties, further evaluation detailed below focused on the 50:50 and 25:75 systems as they would be more likely to exhibit the stimuli-responsive degradation properties of PEtG, whereas higher ester content would lead to dominant properties of the polyester (i.e., highly crystalline and rigid).

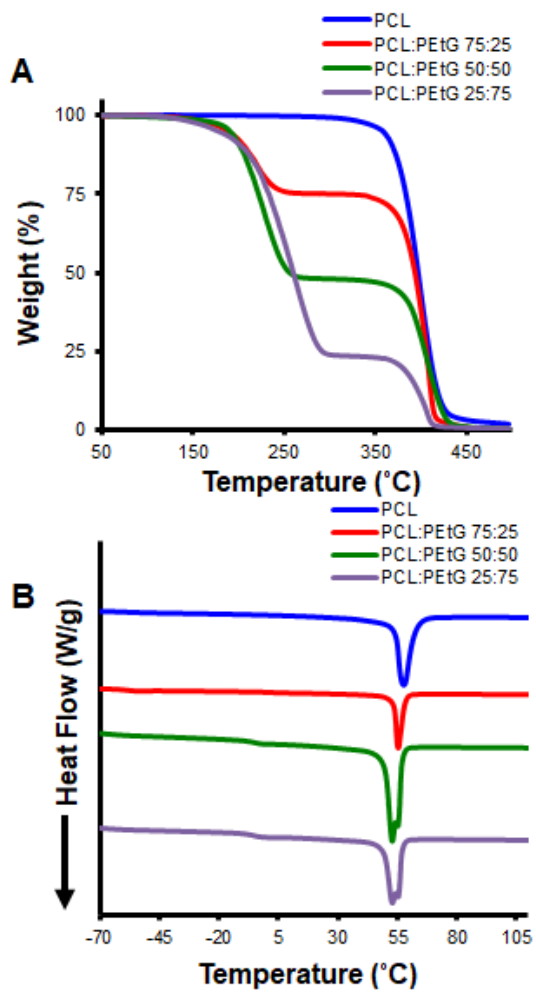


Figure 2-2 Analysis of PETG:PCL blends by A) TGA and B) DSC.

Table 2-1 . Thermal transitions from DSC for polymer blends and triblock copolymers

Sample	$T_{g,PEtG}$ (°C)	$T_{g,polyester}$ (°C)	$T_{m,polyester}$ (°C)
PEtG	-8.6	-	-
PCL	-	-60	58
PCL:PEtG 75:25	-3	ND	55
PCL:PEtG 50:50	-4	ND	53
PCL:PEtG 25:75	-6	ND	53
PCL-b-PEtG-b-PCL-low (25 wt% PCL)	-3	ND	54
PCL-b-PEtG-b-PCL-high (50 wt% PCL)	-6	ND	54
PLA	-	63	*
PLA:PEtG 75:25	-6	48	*
PLA:PEtG 50:50	-6	54	*
PLA:PEtG 25:75	-7	50	*
PLA:PHB:PEtG 75:25	-	62.4 (PLA)	45 (PHB)
PLA:PHB:PEtG 56:19:25	-9	not observed	42 (PHB)
PLA:PHB:PEtG 37.5:12.5:50	-16	not observed	45 (PHB)
PLA:PHB:PEtG 19:6:75	-14	not observed	45 (PHB)

ND = not detectable; * Not expected in the evaluated temperature range (due to limited thermal stability of PEtG).

2.3.4 Atomic force microscopy (AFM)

AFM is a powerful technique that displays visually the degree of phase separation of either the co-polymer and blends. Since the polymeric blends contain both amorphous and crystalline domains the phase contrast boundaries will be easier to identify for heterogenous polymer blends (Marquardt et al. 2001). In this case, coatings were prepared by spin coating the polymer solutions onto glass microscope slides. Phase contrast images are shown for the blend and co-polymers with PCL in Figure 2-3, while those of the PLA or PLA:PHB blends are shown in Figure 2-4, and those of the homopolymers are in Figure S29. Pure PEtG samples appeared smooth and featureless and were even difficult to detect by the tapping function of the AFM, due to its highly amorphous and tackiness (Figure S29A). Each of the PCL:PEtG blends exhibited phase separation with domains of semi-crystalline PCL having dimensions of a few to tens of micrometers, immersed in a PEtG matrix (Figures 2-3 A,B). For PCL-*b*-PEtG-*b*-PCL-low, nanophase separation was not clearly observed, but there were clearly sub-micrometer scale textures induced by the crystallinity of the PCL (Figure 2-3C). PCL-*b*-PEtG-*b*-PCL-high clearly underwent self-assembly to form lamellar structures having diameters on the order of ~10 nm (Figure 2-3 D).

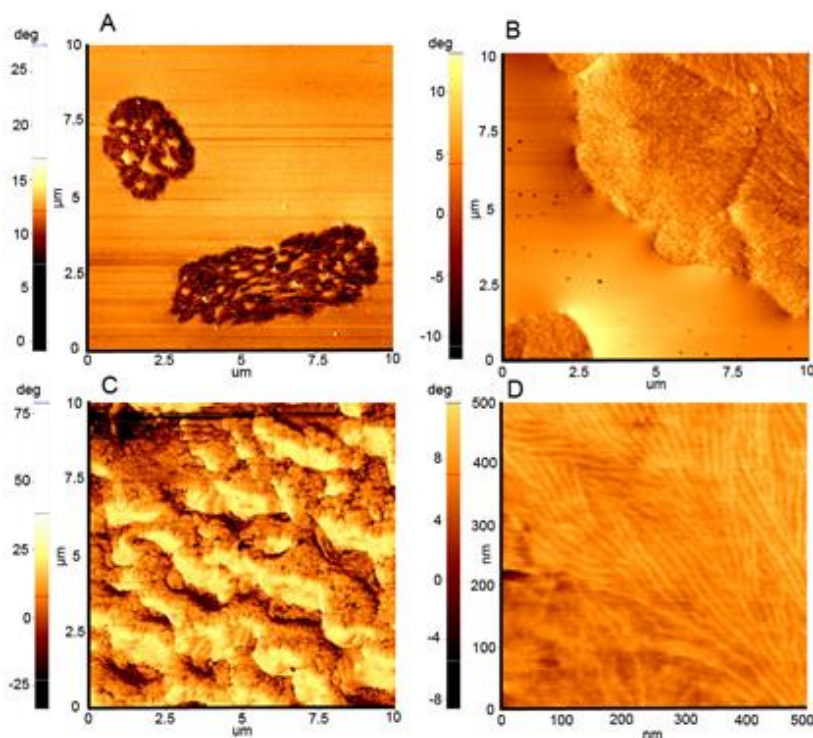


Figure 2-3 Phase contrast AFM images of PEtG blends and copolymer with PCL: A) PCL:PEtG 25:75 and B) PCL:PEtG 50:50; C) PCL-*b*-PEtG-*b*-PCL-low; D) PCL-*b*-PEtG-*b*-PCL-high. Micrometer scale phase separation was observed for the blends, whereas the copolymers exhibited sub-micrometer scale textures.

In the 25:75 PLA:PEtG blends, small ($< 2 \mu\text{m}$ diameter) domains presumed to be either glassy or semi-crystalline PLA in a matrix of PEtG were observed (Figure 2-4A). For the 50:50 blend, the AFM image suggested the presence of three phases including PEtG, glassy PLA, and crystalline PLA (Figure 2-4 B). Two phases also were observed for pure PLA, confirming its semi-crystalline structure after spin coating (Figure S29C). For the 19:6:75 PLA:PHB:PEtG blends, the AFM image suggested small ($< 2 \mu\text{m}$ diameter) crystallites of PHB immersed in a relatively homogeneous matrix of PLA and PEtG (Figure 2-4 C). On the other hand, the image of 37.5:12.5:50 PLA:PHB:PEtG was dominated by two phases, likely corresponding to PLA and PEtG (Figure 2-4 D).

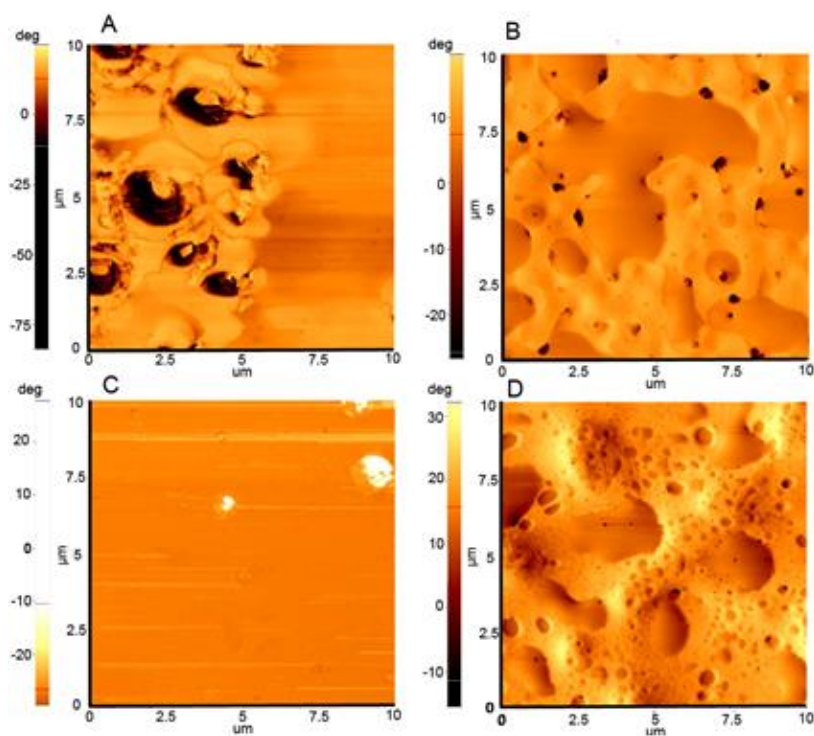


Figure 2-4 Phase contrast AFM images of PETg blends with PLA and PHB. A) PLA:PETg 25:75 with domains of PLA surrounded by PETg; B) PLA:PETg 50:50 showing domains of PETg as well as amorphous and crystalline PLA; C) PLA:PHB:PETg 19:6:75 with crystalline domains of PHB observed in an amorphous matrix; D) PLA:PHB:PETg 37.5:12.5:50 showing multiple phases corresponding to the different polymers.

2.3.5 Mechanical testing

Tensile data provides an insight in predicting structural integrity of material as well as its overall performance under straining applications. Tensile measurements will be an important factor in determining if the blend is suitable for real world applications. Tensile testing was performed to evaluate the effects of blending and copolymer synthesis on the mechanical properties of the polymers. The 25:75 polyester:PETg blends could not be evaluated due to their very poor structural integrities, so the testing focused on comparing

the pure polyesters to the 50:50 blends and to the copolymer PCL-*b*-PEtG-*b*-PCL-high. The properties of the pure polyesters were similar to those previously reported (Table 2-2, Figure S30) (Matzinos et al. 2002, Abdelwahab et al. 2012). PCL, which has a T_g well below room temperature, but a T_m above it, had a mean Young's modulus of 492 ± 25 MPa, an ultimate tensile strength of 13.4 ± 0.7 MPa, and an elongation at break of $4.1 \pm 0.3\%$ (\pm used to denote standard deviation). Both PLA and PLA:PHB 75:25 had higher Young's moduli of 1404 ± 139 and 1392 ± 133 MPa, respectively, and higher ultimate tensile strengths of 25.5 ± 1.2 and 17.7 ± 0.5 respectively. They also were very brittle, with elongation at breaks of $3.6 \pm 0.5\%$ and $2.3 \pm 0.9\%$. These properties can be attributed to PLA and PHB being in glassy, semi-crystalline states at ambient temperature.

Table 2-2 Summary of results for PEtG blends and PCL Co-polymer for mechanical property testing

Polymer Composition	Elastic modulus (MPa)	Stress at break (MPa)	Strain at break (%)
PCL	492.4 ± 25.2 C	13.4 ± 0.73 C	4.1 ± 0.30 BC
PCL:PEtG 50:50	192.0 ± 14.5 E	4.91 ± 0.46 D	4.0 ± 0.50 BC
PCL- <i>b</i> -PEtG- <i>b</i> -PCL-high	80.1 ± 19.2 F	5.44 ± 0.54 D	41.1 ± 34.1 A
PLA	1404 ± 138.6 A	25.5 ± 1.2 A	3.1 ± 0.70 C
PLA:PEtG 50:50	660 ± 70.0 B	12.0 ± 1.4 C	3.6 ± 0.50 BC
PLA:PHB 75:25	1392.0 ± 133 A	17.7 ± 0.47 B	2.3 ± 0.90 C
PLA:PHB:PEtG 37.5:12.5:50	265.6 ± 11.3 D	4.82 ± 0.16 D	6.0 ± 1.20 BC

***Letters that are different denote significant differences between samples (Tukey's tests, $p < 0.05$). Data presented are mean of five measurement per polymer and uncertainties are the standard deviations.**

The Young's moduli and ultimate tensile strength were significantly lower for all of the 50:50 blends and for the copolymers compared to the pure polyesters. In each case, the difference was a bit more than 2-fold. These differences can be attributed to decreases in the overall crystallinities of the polymers, as well as the introduction of the rubbery domains of PEtG. While PEtG has a modulus that is too low to be measured by tensile testing, it is clear that the blends and copolymer have properties intermediate between the polymers from which they are composed. Comparing the PCL:PEtG blend to the copolymer PCL-*b*-PEtG-*b*-PCL-high, it was noted that the blend had a Young's modulus of 192 ± 15 MPa, whereas the copolymer had a modulus of only 80 ± 19 MPa. The blend

and copolymer had statistically indistinguishable ultimate tensile strengths of 4.9 ± 0.5 and 5.4 ± 0.5 MPa, respectively. However, the elongation at break ($41.1.0 \pm 34.1$ %) was much larger for the copolymer compared to only 4.0 ± 0.5 % for the blend. These differences can be attributed to the different effects of micrometer-scale versus nanometer-scale phase separation and the effects of smaller versus larger crystalline PCL domains. Of the blends, the 50:50 PLA:PEtG system had the highest Young's modulus of 660 ± 70 MPa and the highest ultimate tensile strength of 12.0 ± 1.4 MPa, while retaining a similar elongation at break to the other blends. This result suggests that this blend would form the most robust coatings.

2.3.6 Coating Degradation

To determine how the degradation properties of the coatings were affected by blending and copolymer synthesis, coatings were prepared by drop casting polymer solutions (~ 80 μm thick) on the bottoms of glass vials, and then mass loss was measured following immersion in pH 7.4 buffer at ambient temperature (22 $^{\circ}\text{C}$). Triggered samples were subjected to irradiation with a mercury lamp (2.8 mW/cm^2 in the UVA range) for 240 min at $t = 0$, 10 d, and 20 d. Because the coatings were not optically transparent, the latter irradiations were designed to expose the underlying layers of PEtG to the stimulus. Untriggered control samples were stored in the dark. At each time point, irradiated and control samples ($n = 3$) were removed from the buffer, rinsed with distilled water, dried in a vacuum for 24 h, and weighed.

Mass loss began rapidly for all of the irradiated coatings containing PEtG (Figure 2-5 A, C, E). For the 25:75 polyester:PEtG blends, degradation continued over ~25 d, reaching a plateau at ~40% residual mass (Figure 2-5 A). Assuming that the polyester component would not degrade significantly over the course of the trial, the residual mass could be expected to reach 25%. However, some PEtG may remain trapped within polyester domains, preventing either its end-cap cleavage or erosion. Comparing the blends to the copolymer, the initial degradation was faster for the blends, likely due to large surface-accessible PEtG domains that could be rapidly eroded. In contrast, PCL-*b*-PEtG-*b*-PCL-low exhibited nanoscale phase separation, and the requirement for degradation products to diffuse out of the nanoscale domains may slow the process. However, over the 30 d, a lower residual mass of $29 \pm 2\%$ was achieved, compared with $35 \pm 5\%$ to $46 \pm 3\%$ for the blends, suggesting that the PEtG domains are ultimately more accessible within the copolymer coating. The 50:50 polyester:PEtG blend coatings exhibited similar trends to the 25:75 blends, except that the residual mass loss plateaued at ~60 wt%, consistent with the higher polyester content in these blends (Figure 2-5 C). The copolymer PCL-*b*-PEtG-*b*-PCL-high also underwent a slower, more linear decrease in mass loss, reaching $69 \pm 1\%$ after 30 d. Presumably the PEtG domains would have completely eroded had the experiment been conducted over a longer time frame.

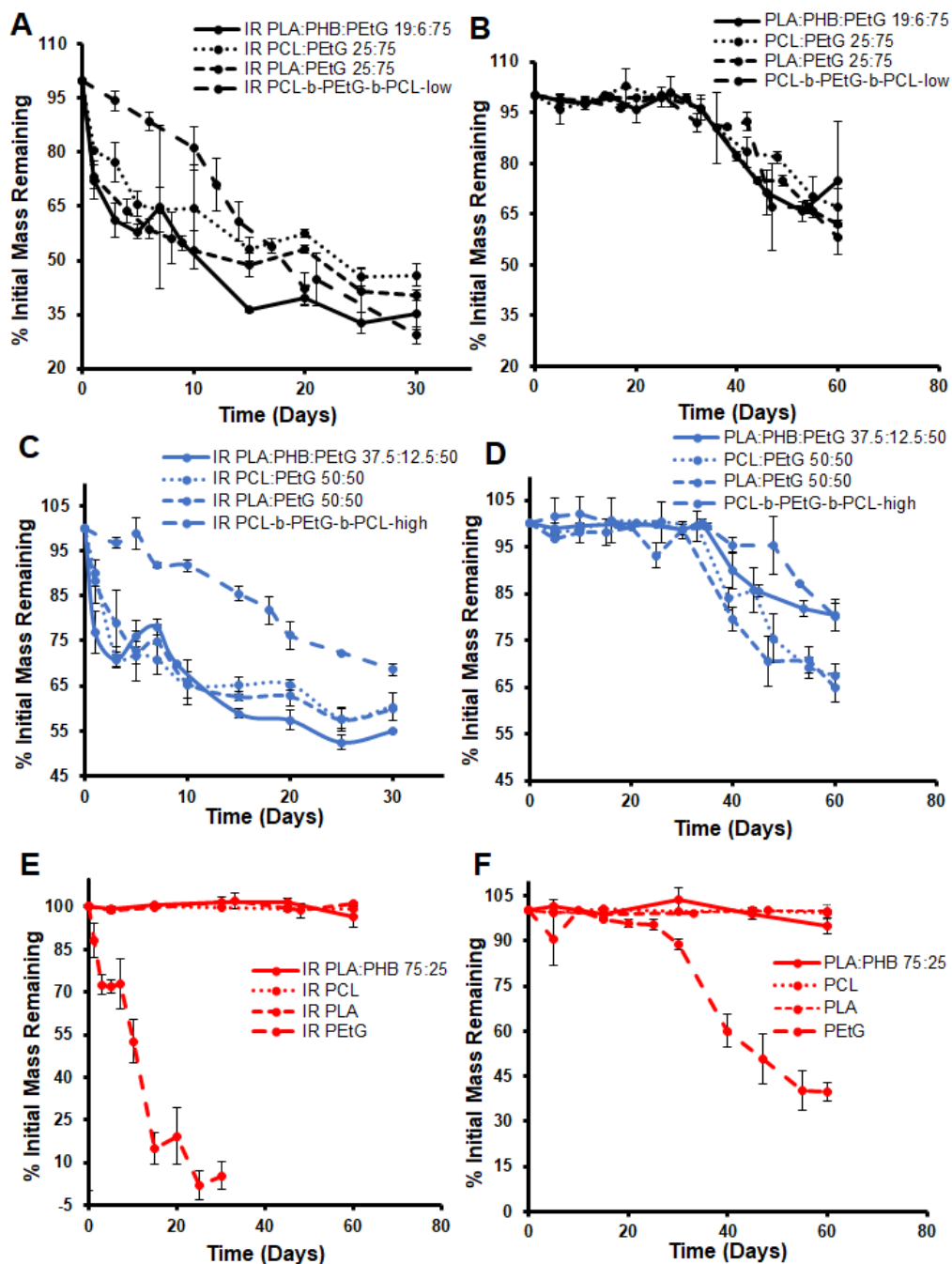


Figure 2-5 Mass loss profiles for UV light irradiated (IR; A, C, E), and non-irradiated (B, D, F) coatings immersed in 0.1 M pH 7.4 buffer at 22 °C: A-B) polyester:PEtG 25:75; C-D) polyester:PEtG 50:50; E-F) homopolymers. n=3 for each time-point with error bars denoting standard deviation.

Irradiated pure PEtG coatings eroded to $5.5 \pm 4.8\%$ residual mass in 30 d, consistent with our previous results, while pure polyesters of PCL, PLA, and 3:1 PLA:PHB underwent $< 5\%$ mass loss over 60 d (Figure 2-5 E) (Fan et al. 2016). The untriggered control coatings all remained stable for ~ 30 d, then began to rapidly erode. Water can cleave either the carbonate linkage between the polymer and the end-cap or it can hydrolyze pendant esters, resulting in carboxylic acids that can intramolecularly catalyze the cleavage of the polyacetal backbone. In either case, a single cleavage event can initiate depolymerization, explaining why erosion progresses rapidly once it begins. Nevertheless, the untriggered coatings were clearly much more stable than the triggered coatings, showing that the stimuli-responsive properties of PEtG were retained in both the blends and the copolymers.

The surface morphologies of the triggered and untriggered coatings were imaged using SEM. Representative images for the 25:75 polyester:PEtG blends and PCL-*b*-PEtG-*b*-PCL-low are shown in Figures 2-6 (triggered) and 2-7 (untriggered), while those of the 50:50 blends, PCL-*b*-PEtG-*b*-PCL-high and the pure polymers are included in the supporting information (Figures S31-S32). Prior to irradiation and immersion in the buffer, the 25:75 polyester:PEtG coatings were smooth and flat with minimal morphological differences in structures (Figures 2-6 A, D, G, J). After 15 d post-irradiation, large micrometer scale pores were revealed due to the erosion of PEtG domains from the blends (Figures 2-6 B, E, H), while the pores arising from degradation of PCL-*b*-PEtG-*b*-PCL-low were nanometer sized (Figure 2-6 I), consistent with the scales of phase separation for these different polymer systems, as observed by AFM. The coatings were even more porous at 30 d (Figures 2-6 C, F, I, L). Non-irradiated blend and copolymer coatings

remained smooth and flat at 15 d (Figures 2-7 A, C, E, G), but became porous after 45 d (Figures 2-7 B, D, F, H), consistent with the results of the mass loss studies. Similar results were observed for the 50:50 polyester:PEtG blends, PCL-*b*-PEtG-*b*-PCL-high and the pure polymers, whereas only PEtG underwent detectable degradation over 45 d (Figures S31-S33).

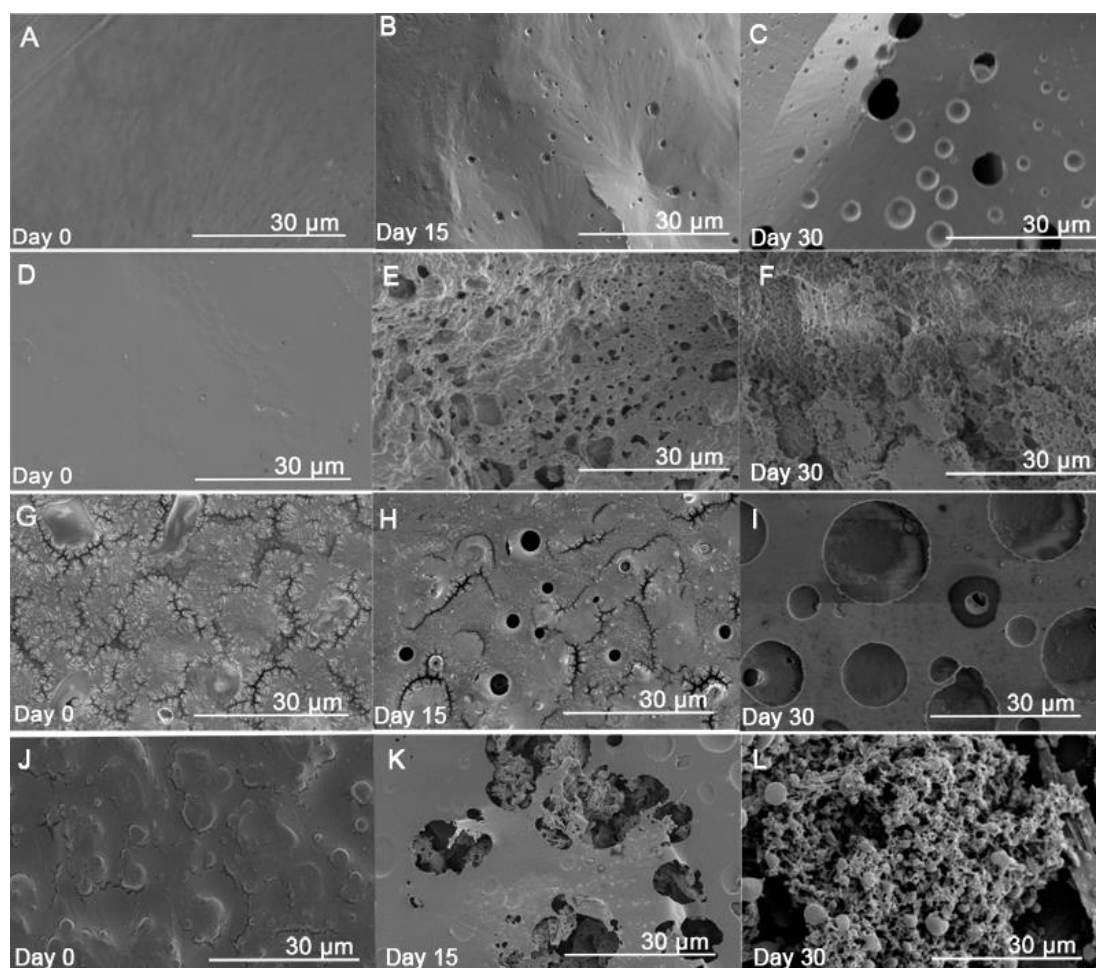


Figure 2-6 SEM images of polyester:PEtG 25:75 coatings after UV exposure and 0, 15, and 30 d of immersion in 0.1 M, pH 7.4 buffer at 22 °C. A-C): PCL:PEtG 25:75; D-F) PCL-*b*-PEtG-*b*-PCL-low; G-I) PLA:PEtG 25:75; J-M) PLA:PHB:PEtG 19:6:75.

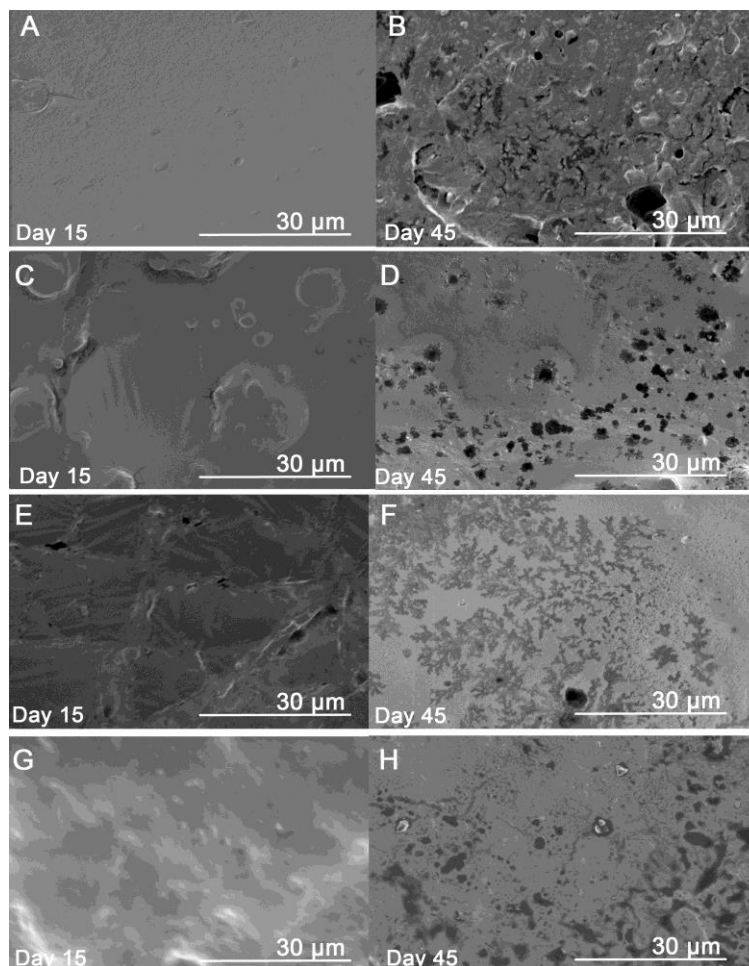


Figure 2-7 . SEM images of polyester:PEtG 25:75 coatings without UV irradiation after 15 d and 45 d of immersion in 0.1 M, pH 7.4 buffer at 22 °C. A-B) PCL:PEtG 25:75; C-D) PCL-*b*-PEtG-*b*-PCL-low; E-F) PLA:PEtG 25:75; G-H) PLA:PHB:PEtG 19:6:75.

2.4 Conclusions

This work demonstrated that it was possible to tune the properties of PEtG by blending it with PCL, PLA, or 3:1 PLA:PHB and by preparing copolymers with PCL. TGA confirmed the compositions of the blends and showed that system underwent a two-phase degradation process. DSC and AFM showed that phase separation occurred for all of the blends and copolymers, with the T_g and T_m of each component only changing to a small extent in comparison to the corresponding pure polymers. Phase separation depicts the degree of blending between polymeric domains in which PCL had the highest degree overall. However, whereas micrometer scale phase separation occurred for the blends, it was possible to achieve nanoscale phase separation for the block copolymers of PCL. While the polyester:PEtG 25:75 systems had very poor structural integrity due to their high content of PEtG, tensile testing showed that the 50:50 blends had a ~2-fold reduction in Young's modulus and ultimate tensile strength relative to those of the corresponding pure polyester systems with the elongation at break ranging from 3.6 to 6.0%. The properties of the copolymer were also significantly different than those of the blends, showing that covalent conjugation of the blocks and the consequent nanoscale phase separation can have a significant impact on the properties of the materials. Mass loss and SEM imaging studies of triggered polymers showed that PEtG retained its degradation properties when incorporated into the blends and copolymers, with the blends leading to faster initial degradation but a higher residual mass than the copolymers due to their different morphologies. Overall, these data show that it is possible to tune the properties of coatings based on the PEtG content, choice of polyester system, and choice of blend versus block copolymer while still retaining the triggered degradation of the PEtG. Future work will

explore the application of these coatings for controlled release. In this context, it will be important to investigate if and at which stage in the degradation process the release of molecules through the residual porous matrix of polyester can occur.

2.5 References

- Abdelwahab, M. A., A. Flynn, B. S. Chiou, S. Imam, W. Orts, and E. Chiellini. 2012. Thermal, mechanical and morphological characterization of plasticized PLA-PHB blends. *Polymer Degradation and Stability* **97**:1822-1828.
- Akafuah, N. K., S. Poozesh, A. Salaimh, G. Patrick, K. Lawler, and K. Saito. 2016. Evolution of the Automotive Body Coating Process-A Review. *Coatings* **6**:22.
- Atanase, L. I., O. Glaied, and G. Riess. 2011. Crystallization kinetics of PCL tagged with well-defined positional triazole defects generated by click chemistry. *Polymer* **52**:3074-3081.
- Belloncle, B., C. Bunel, L. Menu-Bouaouiche, O. Lesouhaitier, and F. Burel. 2012. Study of the Degradation of Poly(ethyl glyoxylate): Biodegradation, Toxicity and Ecotoxicity Assays. *Journal of Polymers and the Environment* **20**:726-731.
- Chen, E. K. Y., R. A. McBride, and E. R. Gillies. 2012. Self-Immolative Polymers Containing Rapidly Cyclizing Spacers: Toward Rapid Depolymerization Rates. *Macromolecules* **45**:7364-7374.
- Chien, S. H., L. I. Prochnow, and H. Cantarella. 2009. Recent developments of fertilizer production and use to improve nutrient efficiency and minimize environmental impacts. Pages 267-322 *in* D. L. Sparks, editor. *Advances in Agronomy*, Vol 102. Elsevier Academic Press Inc, San Diego.
- DeWit, M. A., and E. R. Gillies. 2009. A Cascade Biodegradable Polymer Based on Alternating Cyclization and Elimination Reactions. *Journal of the American Chemical Society* **131**:18327-18334.
- Fan, B., and E. R. Gillies. 2002. Self-Immolative Polymers. *Encyclopedia of Polymer Science and Technology*. John Wiley & Sons, Inc.
- Fan, B., and E. R. Gillies. 2017. Poly(ethyl glyoxylate)-Poly(ethylene oxide) Nanoparticles: Stimuli-Responsive Drug Release via End-to-End Polyglyoxylate Depolymerization. *Molecular Pharmaceutics* **14**:2548-2559.
- Fan, B., J. F. Trant, and E. R. Gillies. 2016. End-Capping Strategies for Triggering End-to-End Depolymerization of Polyglyoxylates. *Macromolecules* **49**:9309-9319.
- Fan, B., J. F. Trant, G. Hemery, O. Sandre, and E. R. Gillies. 2017. Thermo-responsive self-immolative nanoassemblies: direct and indirect triggering. *Chemical Communications* **53**:12068-12071.
- Fan, B., J. F. Trant, A. D. Wong, and E. R. Gillies. 2014. Polyglyoxylates: A Versatile Class of Triggerable Self-Immolative Polymers from Readily Accessible Monomers. *Journal of the American Chemical Society* **136**:10116-10123.
- Fomina, N., C. McFearin, M. Sermsakdi, O. Edigin, and A. Almutairi. 2010. UV and Near-IR Triggered Release from Polymeric Nanoparticles. *Journal of the American Chemical Society* **132**:9540-9542.
- Kaitz, J. A., and J. S. Moore. 2014. Copolymerization of o-Phthalaldehyde and Ethyl Glyoxylate: Cyclic Macromolecules with Alternating Sequence and Tunable Thermal Properties. *Macromolecules* **47**:5509-5513.
- Langer, R., and N. A. Peppas. 2003. Advances in biomaterials, drug delivery, and bionanotechnology. *Aiche Journal* **49**:2990-3006.

- Lehr, C. M. 1994. Bioadhesion technologies for the delivery of peptide and protein drugs to the gastrointestinal-tract. *Critical Reviews in Therapeutic Drug Carrier Systems* **11**:119-160.
- Li, F., Y. Liu, C. B. Qu, H. M. Xiao, Y. Hua, G. X. Sui, and S. Y. Fu. 2015. Enhanced mechanical properties of short carbon fiber reinforced polyethersulfone composites by graphene oxide coating. *Polymer* **59**:155-165.
- Liu, H. Z., and J. W. Zhang. 2011. Research Progress in Toughening Modification of Poly(lactic acid). *Journal of Polymer Science Part B-Polymer Physics* **49**:1051-1083.
- Liu, R., X. Zhao, T. Wu, and P. Y. Feng. 2008. Tunable Redox-Responsive Hybrid Nanogated Ensembles. *Journal of the American Chemical Society* **130**:14418-+.
- Marquardt, J., R. Thomann, Y. Thomann, J. Heinemann, and R. Mulhaupt. 2001. Miscibility of branched ethene homopolymers with iso- and syndiotactic polypropenes. *Macromolecules* **34**:8669-8674.
- Matzinos, P., V. Tserki, A. Kontoyiannis, and C. Panayiotou. 2002. Processing and characterization of starch/polycaprolactone products. *Polymer Degradation and Stability* **77**:17-24.
- McBride, R. A., and E. R. Gillies. 2013. Kinetics of Self-Immolative Degradation in a Linear Polymeric System: Demonstrating the Effect of Chain Length. *Macromolecules* **46**:5157-5166.
- McKeen, L. W. 2016. *Fluorinated Coatings and Finishes Handbook: The Definitive User's Guide*. 2 edition. Matthew Deans.
- Nampoothiri, K. M., N. R. Nair, and R. P. John. 2010. An overview of the recent developments in polylactide (PLA) research. *Bioresource Technology* **101**:8493-8501.
- Okada, H., K. Tanaka, W. Ohashi, and Y. Chujo. 2014. Photo-triggered molecular release based on auto-degradable polymer-containing organic-inorganic hybrids. *Bioorganic & Medicinal Chemistry* **22**:3435-3440.
- Peterson, G. I., D. C. Church, N. A. Yakelis, and A. J. Boydston. 2014. 1,2-Oxazine Linker as a Thermal Trigger for Self-Immolative Polymers. *Polymer* **55**:5980-5985.
- Peterson, G. I., M. B. Larsen, and A. J. Boydston. 2012. Controlled Depolymerization: Stimuli-Responsive Self-Immolative Polymers. *Macromolecules* **45**:7317-7328.
- Pignatello, R., C. Bucolo, P. Ferrara, A. Maltese, A. Puleo, and G. Puglisi. 2002. Eudragit RS100 (R) nanosuspensions for the ophthalmic controlled delivery of ibuprofen. *European Journal of Pharmaceutical Sciences* **16**:53-61.
- Ramakrishna, S., J. Mayer, E. Wintermantel, and K. W. Leong. 2001. Biomedical applications of polymer-composite materials: a review. *Composites Science and Technology* **61**:1189-1224.
- Roth, M. E., O. Green, S. Gnaim, and D. Shabat. 2016. Dendritic, Oligomeric, and Polymeric Self-Immolative Molecular Amplification. *Chemical Reviews* **116**:1309-1352.
- Sagi, A., R. Weinstain, N. Karton, and D. Shabat. 2008. Self-Immolative Polymers. *Journal of the American Chemical Society* **130**:5434-5435.
- Sodergard, A., and M. Stolt. 2002. Properties of lactic acid based polymers and their correlation with composition. *Progress in Polymer Science* **27**:1123-1163.

- Song, C.-C., R. Ji, F.-S. Du, and Z.-C. Li. 2013. Oxidation-Responsive Poly(amino ester)s Containing Arylboronic Ester and Self-Immolative Motif: Synthesis and Degradation Study. *Macromolecules* **46**:8416-8425.
- Stuart, M. A. C., W. T. S. Huck, J. Genzer, M. Muller, C. Ober, M. Stamm, G. B. Sukhorukov, I. Szleifer, V. V. Tsukruk, M. Urban, F. Winnik, S. Zauscher, I. Luzinov, and S. Minko. 2010. Emerging applications of stimuli-responsive polymer materials. *Nature Materials* **9**:101-113.
- Wang, W., and C. Alexander. 2008. Self-Immolative Polymers. *Angewandte Chemie International Edition* **47**:7804-7806.
- Wang, Z., J. Sun, and X. Jia. 2014. Self-immolative nanoparticles triggered by hydrogen peroxide and pH. *Journal of Polymer Science Part A: Polymer Chemistry* **52**:1962-1969.
- Yu, L., K. Dean, and L. Li. 2006. Polymer blends and composites from renewable resources. *Progress in Polymer Science* **31**:576-602.
- Zhang, G. Q., T. L. S. Clair, and C. L. Fraser. 2009. Synthesis and Fluorescent Properties of Difluoroboron Dibenzoylmethane Polycaprolactone. *Macromolecules* **42**:3092-3097.

Chapter 3

3 Plant root responsive slow-release fertilizer coatings using polyglyoxylate-polyester blends for improved nutrient delivery

3.1 Introduction

Fertilizer application typically occurs prior to peak plant nutrient demand, and fertilizer that is not taken up by plant roots in the interim can be lost readily from the soil via leaching, volatilization or trace gas losses (Costa et al. 2013, Timilsena et al. 2015). Therefore, for traditional water-soluble fertilizers, the nutrient use efficiency (NUE), defined as the amount of N contributing to overall biomass, is often low (e.g. NUE values for nitrogen range from 30-50% (Zhao et al. 2013, Abalos et al. 2014). To compensate for low NUE and to maximize crop yield, excessive amounts of fertilizer frequently are applied (Sheriff 2005, Stuart et al. 2014). Excess fertilizer can contaminate surrounding ecosystems, causing eutrophication, loss of biodiversity and increased greenhouse gas emissions (Tilman et al. 2001, Davidson and Gu 2012). Controlled release fertilizers (CRF), which involve a protective barrier against water and thereby delay nutrient release (Wilson et al. 2009), can increase NUE and minimize the release of fertilizer into the surrounding environment (Wilson et al. 2009).

Typical CRF coatings are made of polymers such as polyethylene (PE) and polyurethane (PU) (Liang and Liu 2006, Yang et al. 2011). Nutrient release from pellets constructed from these polymers is dependent on environmental conditions (primarily temperature), soil type, and coating thickness (Shaviv et al. 2003, Wei et al. 2017). Despite

improvements in NUE for current CRFs compared to conventional fertilizers, they are not directly synchronized with plant root growth. Therefore, CRFs may release nutrients in soil patches that have not yet been explored by plant roots. Moreover, CRFs are typically composed of non-biodegradable compounds and they thus contaminate fields with particles described as microplastics (Eriksen et al. 2013, Weithmann et al. 2018).

To enhance product delivery for pharmaceutical applications, stimuli-responsive biodegradable coatings have been developed, and there is potential to adapt this technology for fertilizer pellet coatings. To optimize nutrient delivery, a stimulus-responsive polymer ideally would release fertilizer directly in response to the presence of plant roots. Self-immolative polymers (SIPs) are a new class of stimuli-responsive polymers that degrade through end-to-end depolymerization after end-cap removal in response to a specific stimulus (Fan et al. 2016). Because of their controlled and reliable degradation, SIP use in fertilizer coatings could potentially increase the synchronization of fertilizer release with plant growth. In particular, the SIP poly(ethyl) glyoxylate (PEtG), has been investigated extensively and it degrades into glyoxylic acid and ethanol (Figure 3-1 A), compounds that can be metabolized in the environment and thus exhibit low ecotoxicity (Belloncle et al. 2012, Fan et al. 2014, Fan and Gillies 2017). In addition, PEtG end-caps can be designed and modified to respond to a variety of stimuli, including change in temperature or pH, as well as specific chemical species (Belloncle et al. 2012, Fan et al. 2016). There is therefore the potential to develop PEtG as a fertilizer pellet coating to improve nutrient delivery while avoiding the use of non-biodegradable polymers that accumulate as microplastics in the environment.

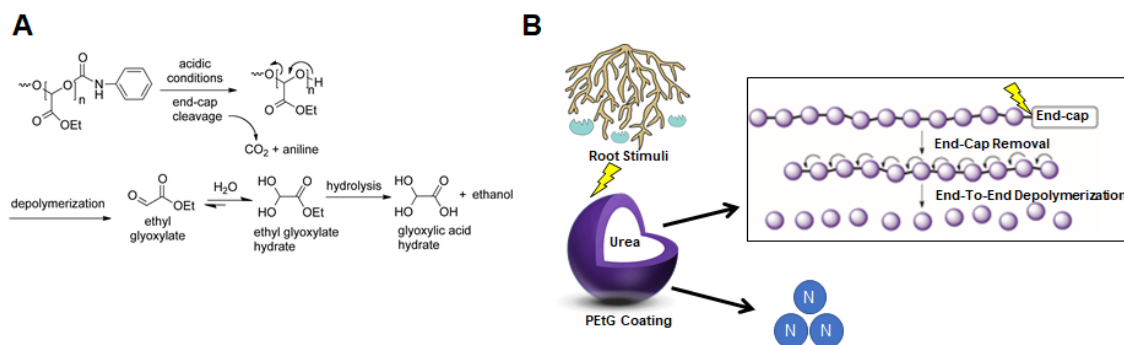


Figure 3-1 Synthesis and degradation of PETg when in the presence of acidic conditions. A) Schematic illustrating the phenyl carbamate end-cap cleavage and depolymerization of PETg initiated by acid; B) Schematic illustrating the function of a triggerable fertilizer coating.

Chemical reactions in many organisms are accompanied by decreases in pH, which makes change in pH a very attractive target stimulus for triggering degradation of a coating (Esser-Kahn et al. 2011). Plant roots release exudates into their immediate environment (the rhizosphere), and these exudates contain high levels of organic acids, sugars, amino acids, inorganic molecules and enzymes (Dakora and Phillips 2002). In addition, as plants take in cationic nutrients, they release H^+ ions into the soil to balance charges, which causes acidification of the soil around the plant root (Nye 1981, Paez-Valencia et al. 2013). To take advantage of root zone acidification as a signal for the presence of plant roots, we incorporated a phenyl carbamate end-cap for PETg that should be cleaved more rapidly at acidic than neutral pH (Figure 1) (Burel et al. 2003). However, because PETg has a very low glass transition temperature, it is highly adhesive at room temperature, and the use of pure PETg as a fertilizer coating would result in the undesirable aggregation of pellets (Fan et al. 2014, Kaitz and Moore 2014). Based on chapter 2, which explored the effects of blending on the properties of PETg, I decided to use 50 wt% of either poly(L-lactic acid)

(PLA) or polycaprolactone (PCL) to provide more mechanically robust and non-adhesive coatings. The responses of the coatings to chemical and plant root stimuli were evaluated. In addition, using creeping bentgrass (*Agrostis stolonifera*) as a model species, (grasses have a high density of roots and therefore may provide an effective stimulus for fertilizer release), the triggering of coating degradation by plant roots was studied (Jackson et al. 1997). The coatings also were used to coat urea pellets and the release properties of the coated pellets were studied. To the best of our knowledge, this paper presents the first study of an SIP for fertilizer coating applications.

3.2 Experimental section

3.2.1 General materials and procedures

All chemicals were purchased from commercial suppliers and used without further purification unless otherwise noted. PEG end-capped with a phenyl carbamate was synthesized as previously reported (Fan et al. 2014). The specific batch used for this work had a number average molar mass (M_n) of 34 kg/mol and a dispersity (D) of 1.44. PLA was purchased from 3D Solutech (PLA Filament 1 KG Natural Clear) and it is a standard PLA filament with no added plasticizers or colorants which had molar mass (M_n) of 103 kg/mol dispersity (D) of 2.56. PCL was supplied by Scientific Polymer Products and had a molar mass (M_n) of 55 kg/mol. Dichloromethane was supplied by Caledon Laboratory Chemicals. Urea was purchased from the Tractor Supply Company (London, Ontario, Canada) and consisted of commercial grade urea with a mean diameter of 4.30 mm and mass of ~ 60 mg per pellet.

3.2.2 Visualization of plant root-zone acidification

Creeping bentgrass was seeded at 2.44 g/m² into 9 cm diameter pots. After the germination stage (10 d), the plants were grown for 14 d and were fertilized weekly with 50 mL of half-strength modified Hoagland's solution (Hoagland and Arnon 1950). A pH indicator agar-film was used to visualize the acidification of the rhizosphere following the procedure described by Zhou et al. 2009 (Nye 1981, Zhou et al. 2009). For the latter, Bromocresol Purple pH-indicator was prepared at 0.1 g L⁻¹ in 9.0 g L⁻¹ of agar. The gel was autoclaved

for 20 min at 120 °C, cooled to ~ 50 °C, and poured into 51 mm diameter *petri* dishes to a depth of 0.3 cm. The agar gel was then cooled to room temperature until it solidified and it was stored in a refrigerator at 6 °C. The initial pH of the gel was 6.5 (light purple colour). Five drops of citrate buffer (pH 5) were added to an agar plate as a control to display the maximum colour change (yellow). Creeping bentgrass roots were washed in 0.2 mM CaSO₄, and rinsed with modified half-strength Hoagland's solution. The roots were then placed into the agar gel until they were embedded. To prevent algal growth the roots were covered with aluminum foil, and the plants were incubated in a greenhouse for 3 d.

3.2.3 Blend coating preparation

PEtG, PLA and PCL were separately dissolved in CH₂Cl₂ at a concentration of 90 mg/mL. Both PEtG:PLA and PEtG:PCL were combined separately in 50:50 ratios and were stirred inside glass vials at 800 rpm for 20 min. The blends were then drop-cast into glass vials/slides and the solvent was evaporated *in vacuo* for 24 h. Each film had a total mass of ~30 mg.

3.2.4 Degradation of PEtG blended films in aqueous buffer solutions

The initial masses of the films were measured and recorded. For each treatment combination, 3 replicate samples were prepared for each of the ~10 time points. The polymer films were immersed in 15 mL of 0.1 M aqueous buffer solution (citrate buffer for pH 5.0 and phosphate buffer for pH 7) at 30 °C or 22 °C. Treatments at 30 °C were

placed inside a temperature-controlled incubator, while the 22 °C samples were placed inside of a storage cabinet. All samples were stored in the dark and were capped to avoid evaporation. Periodically, 3 films for each pH and temperature treatment were removed from the buffer solution, rinsed with distilled water, dried in a lyophilizer for 24 h, then reweighed. The percent initial mass for each film was calculated as the mass at the time of sampling divided by the initial mass and multiplied by 100%. For comparing degradation among samples, the number of d needed to reach a mass loss threshold of 15% was used as the response variable.

3.2.5 Degradation of PEtG blended films in clay-loam agricultural soil

A clay-loam soil (pH 7.5, Bryanston association) was collected from an agricultural field in southern Ontario, Canada, at the Environmental Sciences Western field station (43°4'30"N, 81°20'11"W). The soil was dried at 60 °C for 72 h. Two kilograms of soil were added to 2.5 L tubs, and the pH was adjusted using either citrate buffer to pH 5 or to phosphate buffer pH 7. The resulting soil pH was assessed using an electrode pH meter immersed into a slurry formed from a 10 g subsample of soil and 100 mL of buffer, and pH was measured after 1 h following the slurry formation. The bulk soil was rehydrated to 20% moisture content with 0.1 M buffer solution. Samples were prepared similarly to the solution degradation study; however, they were drop cast onto glass slides instead of being placed into vials. The slides were placed in nylon bags and immersed in the tubs with soil (30 slides per tub). The boxes were sealed to minimize evaporation and were rehydrated occasionally to compensate for any moisture loss. Periodically, three replicate slides were

collected for each treatment and were rinsed with H₂O to remove the soil. The films were transferred to vials, dried on a lyophilizer for 24 h and weighed. Polymer mass loss was assessed as described above. For comparing degradation among samples, the number of d needed to reach a mass loss threshold of 15% was assessed.

3.2.6 Degradation of PEtG blended films exposed to plant roots

All treatments were carried out in growth chambers under the following conditions: 420 g of quartz-based gravel substrate (approximately 2 mm diameter) was placed into 120 pots (10 cm by 10 cm in size). Creeping bentgrass was seeded at 2.44 g/m² into 40 pots and was left to germinate for 10 d prior to experimentation. A citrate buffer solution (pH 5, 0.1 M) was added weekly at 50 mL per pot for the pH stimulated treatments for 40 pots. The remaining 40 pots were used as a control in which they contained polymeric blended films and gravel substrate. Two growth chambers provided 16 h of light and 8 h of darkness at a relative humidity of 70% at either 30 °C or 22 °C. The pots were fertilized once a week for a total of 50 d with 50 mL of half-strength modified Hoagland's solution that contained both macronutrients and micronutrients, but was lacking nitrogen. Urea was applied at 58 kg/Ha for all treatments and all pots were watered every other day. Films were prepared as previously described; however, they were drop cast onto half-microscope slides. Polymeric films were inserted 3 cm under the gravel substrate for all treatments. Four replicate films per treatment were removed for a total of 5 time points over 40 d and were rinsed with H₂O to remove the gravel. The films were transferred to vials, dried on a lyophilizer for 24 h, and were weighed. Mass loss determination and analyses were as described in the previous section.

3.2.7 Fourier transform infrared spectra - attenuated total reflectance (FTIR-ATR)

FTIR-ATR spectra were obtained on a PerkinElmer Spectrum Two FTIR Spectrometer using the attenuated total reflectance accessory. FTIR-ATR spectroscopy was used to study the chemical species and functional groups of the blended polyesters of PEtG, PLA and PCL. Coated pellets were frozen with liquid N₂ and were crushed with a mortar and pestle to produce a fine powder which was then inserted into the instrument.

3.2.8 Surface Morphology

Scanning electron microscopy (SEM) was performed to study the morphology of the coated polymer surfaces. It was performed on a Hitachi S-3400N instrument at a voltage of 3 kV (Hitachi, Toyko, Japan). The samples were mounted on carbon taped aluminum stubs and sputtered with gold at a rate of 5 nm/min for 4 min (Hummer-6 sputtering system, Anatech, Union City, California). The overall surface morphology was examined at a resolution of 30 μm under 3 kV.

3.2.9 Preparation of spray coated urea

Polymer blends of PEtG:PCL (50:50 mass ratio) were dissolved in CH₂Cl₂ at 10 mg/mL. Forty grams of urea pellets were added to a 15 cm diameter pan coater. Metal baffles were added to the inside of the pan coater to increase the rotation of the urea bed. Polymeric mixtures were added to a 250 mL Erlenmeyer flask with a 24/40 connection. A standard thin layer chromatography (TLC) reagent sprayer was inserted into the flask and was

attached to the house air within a fume hood. The polymeric blend mixture was sprayed from the TLC sprayer at a rate of 5 mL/min onto the rotating bed of urea at 30 rpm, which was sufficient to maintain a slumping bed. Every cycle of spraying, excess material was dissolved and reapplied in CH₂Cl₂. Urea was sprayed until there was 5 wt% of polymeric material on each urea particle. Coating thickness was approximately 80 μM, measured using digital caliper, and integrity was tested by placing pellets in water for 72 h.

3.2.10 Preparation of hand coated urea

PEtG:PCL was first dissolved in CH₂Cl₂ at 90 mg/mL in beakers overnight. Solvent was evaporated *in vacuo* for 48 h. The polymeric material was then placed inside of a water bath set at 60° C for 20 min. Once the material was melted it was scooped using a glass rod and smeared onto urea pellets (60 mg) and hand rolled to produce a spherical coating. Polymeric coatings were on average 800 μM – 1000 μM in thickness as measured by digital caliper, and coating integrity was testing by placing pellets in water for 72 h.

3.2.11 Determination of urea release rates in solution

Hand coated PEtG:PCL urea pellets were placed into vials (n = 3) with either 10 mL citrate (pH 5) or phosphate buffer (pH 7). The vials were sealed with paraffin wax and stored at 22 °C or 30 °C. Periodically, over a 21 d period, the urea samples were removed and placed into new vials with fresh buffer solution. The initial solution was then measured for nitrogen content to determine the release rate of urea resulting from polymeric coating degradation. Total nitrogen was measured by persulfate oxidation, followed by analysis for NO₃⁻ using a SmartChem 140 discrete auto analyzer (Westco Scientific Instruments

Brookfield, CT). Oxidizing reagent was prepared following the procedure of Cabrera and Beare (Cabrera and Beare 1993). 1.85 M $K_2S_2O_8$ and 3.86 M of H_3BO_4 were dissolved within 50 mL of 3.75 M of NaOH, and the flask was then topped up to 500 mL with distilled-deionized water. Urea samples were diluted by several magnitudes and pipetted into glass tubes with Teflon screw caps. Oxidizing reagent was added and the tubes were secured tightly. The tubes were then placed within an autoclave at 120 °C for 20 minutes and subsequently analyzed for NO_3^- .

3.2.12 Data analyses

For each response variable, a two-way analysis of variance (ANOVA) was used to assess the effects of temperature and pH over time on mass loss and urea release. As a response variable for comparing mass loss among samples, the number of d needed to reach a mass loss threshold of 15 wt% was assessed. All statistical analyses were conducted using JMP version 14 (SAS Institute).

3.3 Results and Discussion

3.3.1 Root zone acidification

Cationic exchanges of nutrients cause H^+ ions to build up along plant roots. Proof of sufficient rhizosphere acidification was required to support the use of the phenyl carbamate end-cap. To confirm root zone acidification, a bromocresol dye was incorporated into an agar gel on petri dishes. The ability of creeping bentgrass to acidify the agar plate was displayed visually (Figure 3-2). The indicator changed to dark purple once the roots were added at time 0 h due to the addition of Hoagland's solution, which had a pH of 7.5. Once the roots were covered and embedded themselves further into the agar over 72 h, the gel turned a vibrant yellow (~ pH 5). This colour change indicated that the creeping bentgrass roots had a very strong ability to acidify the agar substrate under photosynthetic conditions. The negative control where the prepared agar gel had no additions remained a light purple shade, which indicated around pH 6.5. A positive control using pH 5 citric acid buffer turned pale yellow (only a few drops were added, so the colour change was not as intense as the roots). Overall, the intensity of the pH change that occurred in the agar plate provided evidence that the PEtG end-cap could potentially be cleaved by plant root stimuli.

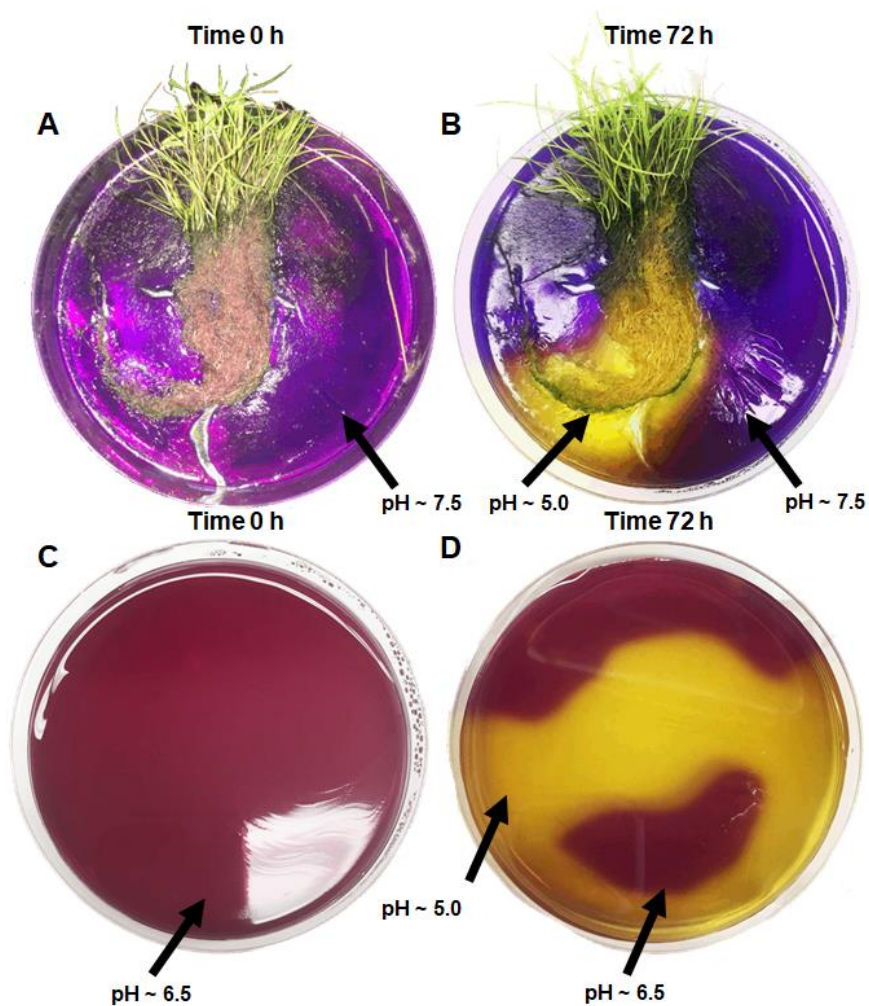


Figure 3-2 Visualization of rhizosphere acidification of creeping bentgrass roots:

A) Creeping bentgrass supplied with Hoagland's solution (pH 7.5) at time 0 h; B) Creeping bentgrass root acidification after 72 h; C) Control agar with no additives at time 0 h; D) pH control with citrate acid buffer addition after 72 h. Both plant roots and citrate acid buffer were imbedded in agar-gel with bromocresol purple pH indicator for 72 h.

3.3.2 Mass loss profiles of the coating exposed to buffer solutions

The degradation of coatings composed of pure phenyl carbamate end-capped PEtG as well as the 50:50 blends PEtG:PCL and PEtG:PLA were characterized first in buffer solutions (Figure 3-3). Films were stored at different temperatures (either 22 °C or 30 °C) and pH conditions (citrate buffer at pH 5 and phosphate buffer at pH 7). These conditions were selected to reflect the range of conditions experienced by the plant roots in the field during the early-mid growing season. Temperature dominates many physicochemical processes such as polymer degradation. Therefore, we expected backbone depolymerization and bond cleavage to increase with increasing temperature. Soil pH is commonly close to 7, because soil is composed of alkaline and silica based materials, and as demonstrated above, plant roots can decrease the rhizosphere from pH 7 to pH 5.

For pure PEtG, both high temperature ($P < 0.001$) and low pH ($P < 0.001$) decreased the numbers of d required to reach 15% mass loss (22 °C/pH 7 – 63 d, 22 °C/pH 5 – 47 d, 30 °C/pH 7 – 32 d, 30 °C/pH 5 – 17 d; Figure 3-3 A). A threshold of 15% mass loss was used, because rapid degradation generally occurred after this phase. Similarly, for PEtG:PCL, both high temperature ($P < 0.001$) and low pH ($P < 0.001$) decreased the numbers of days required to reach 15% mass loss (22 °C/pH 7 – 77 d, 22 °C/pH 5 – 54 d, 30 °C/pH 7 – 33 d, 30 °C/pH 5 – 18 d; Figure 3-3 B). For both pure PEtG and PEtG:PCL, temperature and pH also displayed a significant interaction ($P = 0.0002$), indicating that the magnitude of the pH effect was conditional on the temperature treatment level. PEtG:PLA underwent more constant degradation than pure PEtG and PEtG:PCL. Moreover, for the PEtG:PLA blend, while there was a significant temperature effect on the number of days

required to reach 15% mass loss ($P < 0.0022$; 22 °C – 53 d, 30 °C 18 d; Figure 3-3 C), there was no significant effect of pH on degradation ($P = 1.0$).

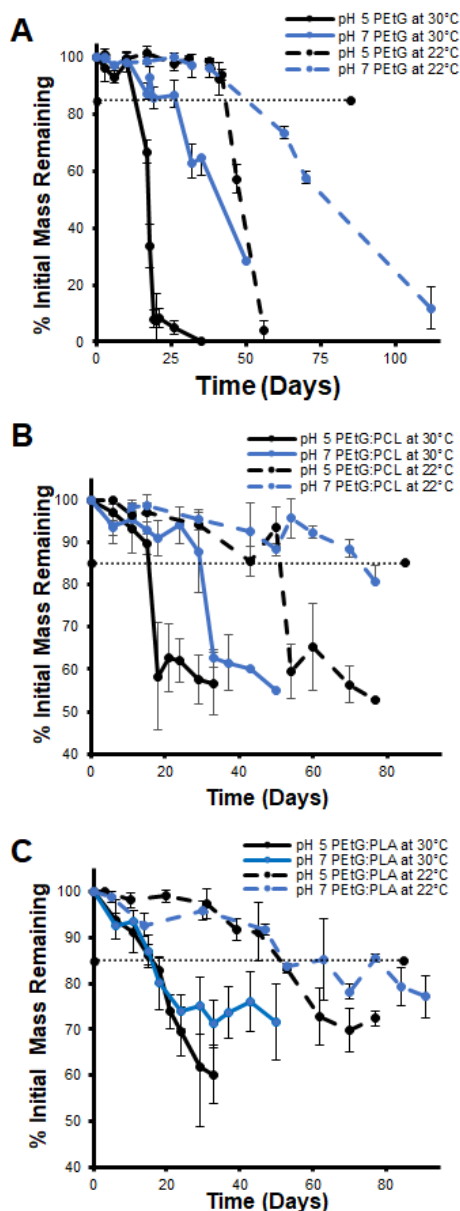


Figure 3-3 Mass loss profiles for coatings immersed in buffers at pH 5 or 7 and either 22 °C or 30 °C: Mass loss profiles for coatings immersed in buffers at pH 5 or 7 and either 22 °C or 30 °C: A) Pure phenyl carbamate end-capped PEtG; B) PEtG:PCL; C) PEtG:PLA. Dotted lines represent the threshold of 15% mass loss used for analysis. $n = 3$ for each time-point with error bars denoting standard deviation.

Most PEtG:PCL treatments exhibited a final mass loss of ~50 % at 30 °C and at low pH, which indicated that the PCL was not degrading. Though pH dependence was not statistically significant for all treatments, a trend of slower degradation was observed in the samples exposed to pH 7 at room temperature. PLA did not reach 50% mass loss in most treatments when compared on the same time scale as the PCL samples. This result suggests that blending with PLA delayed the end-cap removal from PEtG or its subsequent degradation.

Overall, PEtG degradation was temperature-dependent for all treatments, with higher mass loss observed at 30 °C than at 22 °C. However, it was only pH dependent, with increased mass loss at pH 5, for the pure PEtG and the PCL blends. Pure PEtG and PEtG:PCL blends exhibited delayed degradation until they reached a critical threshold and then underwent rapid degradation similar to that observed in a bulk degradation process. In contrast, PEtG:PLA blends exhibited more constant gradual degradation consistent with surface erosion theory (von Burkersroda et al. 2002).

3.3.3 Mass loss profiles of coatings exposed to buffered agricultural soil

Because the target application of these polymers is for coating fertilizer pellets, we investigated the degradation of the PEtG blends in locally-sourced agricultural soil. Pure PEtG was not investigated, because it is known that its properties alone are unsuitable for coating development. Background soil pH was around 7.5 and was adjusted to pH 7 and pH 5 using buffer solutions at 20 wt% moisture content. For PEtG:PCL, high temperature ($P < 0.001$) decreased the number of days required to reach 15% mass loss, pH had no

significant effect on degradation at higher temperatures, whereas there was a slight pH effect at lower temperature conditions ($P=0.0268$). (22 °C/pH 7 – 60 d, 22 °C/pH 5 – 54 d, 30 °C/pH 7 – 17 d, 30 °C/pH 5 – 15 d; Figure 3-4 A). Likewise, for the PEtG/PLA blend, there was a significant temperature effect on the number of days required to reach 15% mass loss. ($P < 0.001$); 22 °C/pH 7 – 29 d, 22 °C/pH 5 – 35 d, 30 °C/pH 7 – 18 d, 30 °C/pH 5 – 18 d; Figure 3-4 B), but no significant effect of pH on degradation ($P = 0.500$).

Overall, significant temperature dependence was observed across all treatments, which was similar to the buffer solution treatments. However, there was no apparent dependence on pH for the PCL treatments at elevated temperatures. The reasons for this result are not entirely clear, but it may have arisen from the delicate balance between rate-limiting end-cap cleavage and rate-limiting depolymerization. While cleavage of the carbamate end-cap should be faster at the more acidic pH, depolymerization exhibits a rate minimum at pH 5 (Fan et al. 2016). It also was noted that both blends exhibited a more continuous erosion than was observed in the buffer immersion study, where there was an initial plateau followed by rapid mass loss. This likely can be explained by the differences in water content between the two studies. We previously have shown that when mass loss studies were performed in water, there was a plateau in mass loss arising from trapping of ethyl glyoxylate hydrate within the eroding polymer film (Fan et al. 2016). When mass loss studies were performed under air, this plateau was not observed. Thus, due to their lower water content, the soil studies resemble more closely the erosion in the dry state.

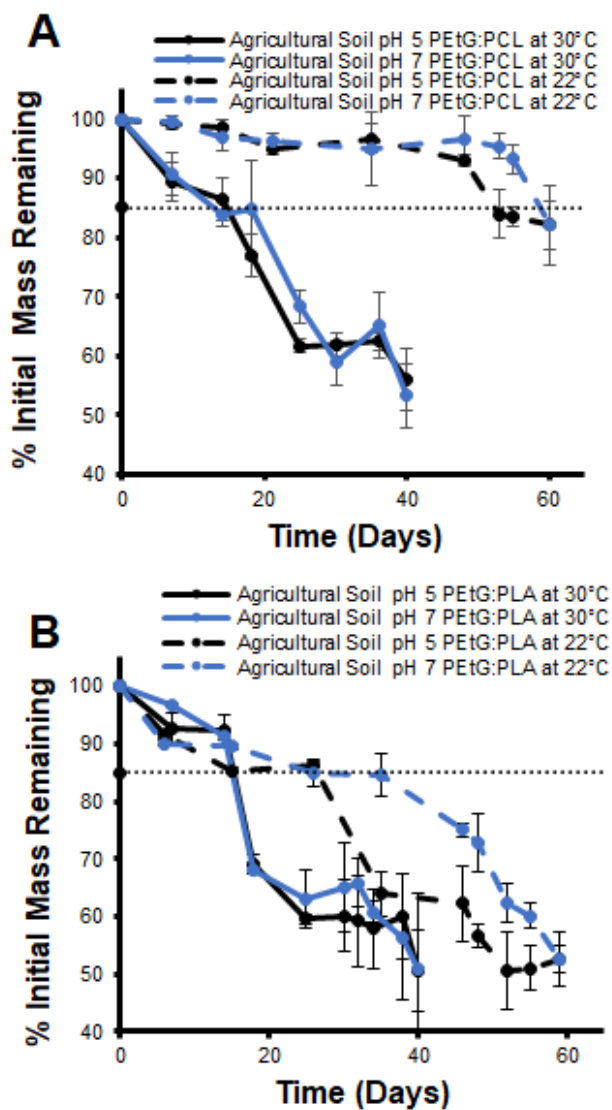


Figure 3-4 Mass loss profiles for coatings immersed in agricultural clay-loam soil with pH adjusted to either pH 5 (0.1 M citrate acid) or pH 7 (0.1 M phosphate) at 22 °C or 30 °C: A) PETg:PCL; B) PETg:PLA. Dotted lines represent the threshold of 15% mass loss used for analysis. $n=3$ for each time-point with error bars denoting standard deviation.

3.3.4 Mass loss profiles of coatings exposed to plant roots

Coatings of PEtG:PCL and PEtG:PLA were studied *in vivo* using creeping bentgrass roots in a silica-based gravel substrate (Figure 3-5C). Roots became embedded onto the polymer film after 40 d (Figure 3-5D). These trials also were carried out at temperatures of 22 °C or 30 °C. Based on the results of the root zone acidification experiment, roots were expected to acidify the soil substrate and increase the rate of coating degradation compared to the (no root) control. A positive control was established using pH 5 citrate acid buffer applied weekly to films in the gravel substrate. The films were incubated in growth chambers kept at 70% humidity, and for the 30 °C treatment, the temperature was reduced to 22 °C at night to simulate natural daily temperature fluctuations.

For the PEtG:PCL coatings, there was a significant interaction between temperature and plant roots ($P = 0.0193$), with high temperature combined with the presence of plant roots and the pH 5 buffer control decreasing the number of days required to reach 15% mass loss compared to no stimulus (22 °C/gravel control – 34.5 d, 22 °C/pH 5 – 28 d, 22 °C/plant roots – 26 d, 30 °C/gravel control – 26 d, 30 °C/pH 5 – 7 d, 22 °C/plant roots – 11 d; Figure 3-5A). For the PEtG:PLA blend, while there was a significant temperature effect on the number of days required to reach 15% mass loss ($P < 0.0001$; 22 °C – 53 d, 30 °C – 18 d; Figure 3-5B), there was no significant difference between the plant root treatment, the pH 5 buffer control, and no stimuli. Thus, these PLA blended films behaved similarly to those in the buffer solution trials as well as the soil trials, indicating that the PLA may have slowed the removal of end-cap and overall degradation, resulting in pH independence.

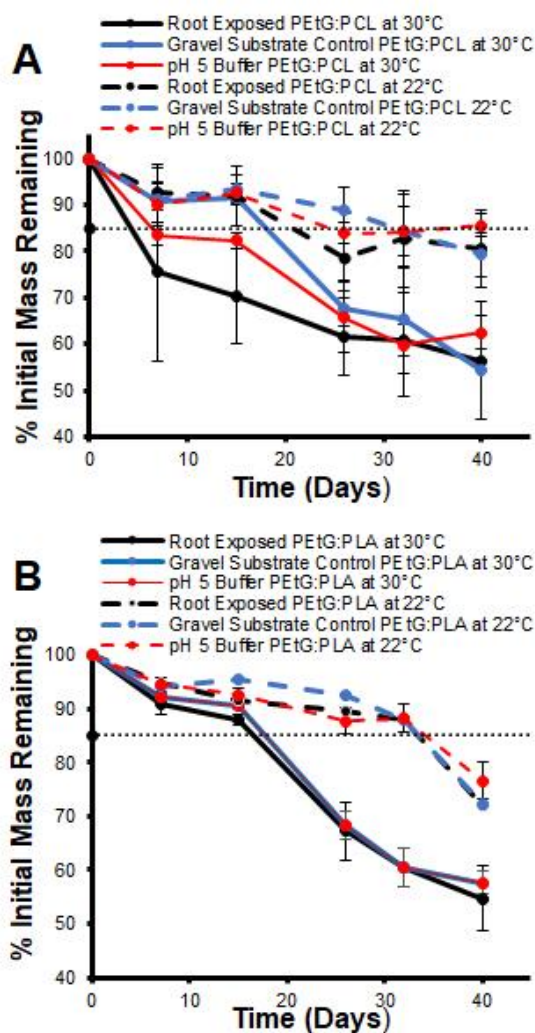


Figure 3-5 Mass loss profiles for coatings imbedded in pots with either creeping bentgrass roots, gravel substrate alone, or weekly dosages of pH 5 0.1M citrate buffer at 22 °C or 30 °C: A) PEtG:PCL; B) PEtG:PLA; C) Representative image of root bound creeping bentgrass; D) Roots imbedding into a PEtG:PCL coating. Pots were stored in growth chambers with 16 h of light, and 8 hours of darkness under 70% humidity. Dotted lines represent the threshold for degradation at 15 wt% mass loss. n = 4 for each time-point with error bars denoting standard deviation.

Moving forward, PEtG:PCL blend films appear to be best-suited for the development of fertilizer coatings given that they respond to both low pH and elevated temperatures, whereas the PLA blends were only temperature dependent. In addition, PCL tended to be stable before undergoing rapid degradation, whereas PLA samples underwent constant gradual degradation. Polymeric coatings for fertilizer pellets would likely improve plant nutrient delivery by exhibiting a stable phase after soil application, prior to triggering and degradation.

The longevity of the polymer blends in the absence of stimulus (i.e. shelf life) also was important to assess, so we prepared polymer blends in vials. These films were exposed to air under room temperature and measured periodically to assess mass loss curves. The blends were stable, with no mass loss recorded for PEtG:PLA thus far over 6 months and PEtG:PCL so far for 70 d. These initial results suggest that the polymeric blend will be stable at room temperature and will not undergo premature depolymerization during storage, prior to soil application.

3.3.5 Preparation and analysis of coated fertilizer pellets

Spray coating was applied to urea pellets by dissolving PEtG with PLA or PCL in CH_2Cl_2 at 10 mg/mL and spraying via a chemical reagent sprayer. PEtG:PCL blends were also melted together at 60 °C and manually coated onto urea pellets. The pellets were immersed in water to visualize urea leakage, which was indicated by the formation of hollow capsules that floated to the surface. In addition, SEM was used to examine the integrity of the coatings obtained by the spray coating and melt coating techniques. Images of

commercially available controlled release fertilizer also were examined for comparison (Figure S1).

For the first few batches, we observed that water penetrated the pellets quickly once they were immersed in water, resulting in rapid urea release. To attempt to reduce water penetration, we incorporated 5 wt% paraffin wax into the PEtG:PCL blend, as suggested to compensate for the defects that occurred during sample preparation of their polyurethane coated pellets (Li et al. 2012). However, the addition of paraffin worsened the integrity of our coatings, producing more holes (Figure S2A), and the pellets also started to stick together within the pan coater, causing tearing. This likely occurred due to the solvent (CH_2Cl_2) becoming trapped within the paraffin wax matrix, reducing the amount of solvent evaporation (Figure S2B). Once the wax was removed from the formulation we were able to produce coatings that were thicker and had fewer defects. The PEtG:PCL coated pellets were able to last in water for a week before water penetration began. The coatings were very smooth, but there were still small defects distributed throughout (Figure 3-6 A).

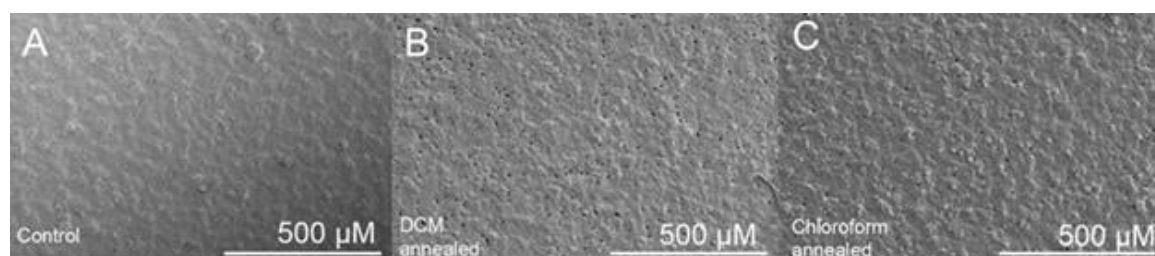


Figure 3-6 . SEM images of PEtG:PCL coatings: A) Initial coating; B) Coating after exposure to CH_2Cl_2 vapor for 24 h C) Coating after exposure to CHCl_3 vapor for 24 h

Solvent annealing as well as temperature annealing were then investigated in an attempt to reduce the holes that appeared during preparation. Through exposure to vapors of CH_2Cl_2 or CHCl_3 , it was anticipated that the polymer would soften and become sufficiently mobile to fill in the imperfections. However, based on SEM no notable improvements occurred and in some cases more defects appeared (Figure 3-6 B-C). We thus concluded that we were unable to improve the polymer properties through solvent annealing practices for the PCL blends, and indeed, these techniques caused more damage to the overall film surface structure. Similarly, heating the coatings above the T_m of PCL ($60\text{ }^\circ\text{C}$) did not result in any improvements.

While the coating process likely can still be optimized using a fluidized bed or related technologies, for the current work it was found that suitable coated pellets could be prepared from melted PEtG:PCL blends ($> 60\text{ }^\circ\text{C}$) through a manual pellet-by-pellet production process. The surface morphology achieved using this technique appeared rough, but the coatings did not have any noticeable holes, which would be critical for preventing premature urea leakage (Figure 3-7). The pellets were stable in water (at room temperature) for almost 30 d before water penetration occurred, which was a substantial improvement. The coating thickness was $\sim 1\text{ mm}$, as measured by caliper.

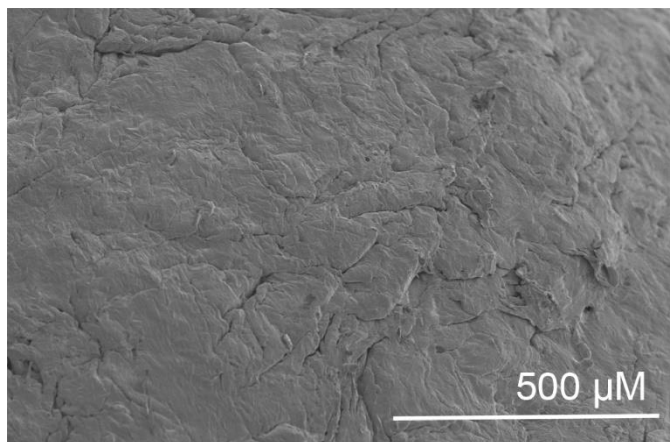


Figure 3-7 SEM image of surface morphology of PEtG:PCL manually-coated pellets from melted polymer blend.

The coated pellets also were characterized using FT-IR spectroscopy (Figure 3-8). Urea bands were confirmed by the presence of N-H stretches at $\sim 3340\text{ cm}^{-1}$ and between $1457\text{-}1696\text{ cm}^{-1}$ in both coatings. PEtG, PLA, and PCL all contained very similar vibrational bands, with their presence confirmed by peaks corresponding to C-H and C=O stretches at $2962\text{-}2934\text{ cm}^{-1}$ and $1717\text{-}1741\text{ cm}^{-1}$ respectively.

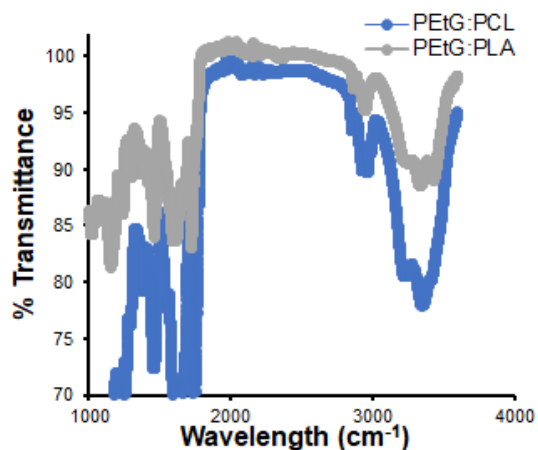


Figure 3-8 IR spectra of A) PEtG-PCL 50 wt%, and B) PEtG-PLA 50 wt%

3.3.6 Urea release study

The release of urea from the manually-coated PEtG:PCL pellets was studied. The pellets were placed into vials in either pH 5 or pH 7 buffer solution and were stored at 22 °C or 30 °C. The release of urea into the buffer solution was measured. Pellets that leaked within the first 5 d were deemed defective due to premature structural failure and thus were omitted from the results. The release rate of urea followed similar trends to the coating mass loss profiles with respect to temperature dependence, in that as the temperature increased, more urea was released, indicating coating degradation. After 21 d there was a significant temperature effect ($P < 0.001$), with almost 100% urea release for the 30 °C treatments, whereas only ~20% was released at 22 °C. However, the release rate was not pH-dependent ($P = 0.807$) (Figure 3-9). The lack of significant pH dependence may arise in part from the large sample variability. Temperature and pH showed no significant interaction ($P = 0.680$).

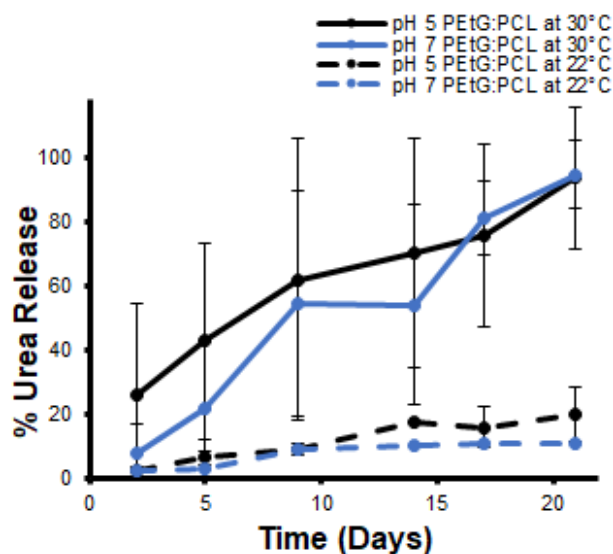


Figure 3-9 Urea release from PEtG:PCL coated pellets exposed to citrate buffer (pH 5) or phosphate buffer (pH 7) at either 22 °C or 30 °C for 21 d. n = 3 for each time-point with error bars denoting standard deviation.

Although no significant pH dependence was observed, the overall release was still sustained for more than 20 d and was responsive to temperature changes. This may have been due to the temperature response having a greater effect on depolymerization than the subtle responses achieved from pH differences. We could not quantify how much degradation of the polymeric material had to occur to enable water penetration. There may have been as little as 5% mass loss from the coating before water penetration occurred and released the urea. It should also be noted that real world applications for the coated urea pellets would not generally involve their complete immersion water (required here to maintain constant temperature and pH) and thus the observed release rates of urea measured in this experiment can be considered as upper limits. However, the results indicate that we have developed a coating that is stable at lower temperatures and releases urea slowly over time. This ultimately may increase nutrient synchronization with plant needs while reducing the accumulation of microplastics in soil substrates.

3.4 Conclusions

This work demonstrated that pH in the vicinity of the plant roots indeed decreased to ~pH 5, which was well-suited to the use a phenyl carbamate end-cap, which is sensitive to increasing acidity. For pure PEtG and PEtG:PCL blends immersed in buffer solutions, coating erosion was temperature and pH-dependent, whereas for PEtG:PLA it was only temperature-dependent. This indicated that the PEtG:PCL blends would be most suitable for the development of triggerable fertilizer coatings. However, studies in soil, in the presence of creeping bentgrass roots, and on coated urea pellets showed that while increasing the temperature provides a robust and highly reproducible response across a variety of conditions, the responsiveness to pH change was more subtle and was not always significant. A viable fertilizer coating would ideally have a predictable degradation rate, protect the granule from premature water penetration, and have polymeric byproducts that would be innocuous to the surrounding environment. PEtG:PCL blends displayed all these attributes. Further nutrient release studies are needed to optimize coating thickness and to demonstrate increased plant NUE *in situ*. However, our results provide a positive first step for the development of the first SIP fertilizer coating that can increase nutrient synchronization while also reducing microplastic accumulation in soil.

3.5 References

- Abalos, D., S. Jeffery, A. Sanz-Cobena, G. Guardia, and A. Vallejo. 2014. Meta-analysis of the effect of urease and nitrification inhibitors on crop productivity and nitrogen use efficiency. *Agriculture Ecosystems & Environment* **189**:136-144.
- Belloncle, B., C. Bunel, L. Menu-Bouaouiche, O. Lesouhaitier, and F. Burel. 2012. Study of the Degradation of Poly(ethyl glyoxylate): Biodegradation, Toxicity and Ecotoxicity Assays. *Journal of Polymers and the Environment* **20**:726-731.
- Burel, F., L. Rossignol, P. Pontvienne, J. Hartmann, N. Couesnon, and C. Bunel. 2003. Synthesis and characterization of poly(ethyl glyoxylate) - a new potentially biodegradable polymer. *E-Polymers*:12.
- Cabrera, M. L., and M. H. Beare. 1993. Alkaline persulfate oxidation for determining total nitrogen in microbial biomass extracts. *Soil Science Society of America Journal* **57**:1007-1012.
- Costa, M. M. E., E. C. M. Cabral-Albuquerque, T. L. M. Alves, J. C. Pinto, and R. L. Fialho. 2013. Use of Polyhydroxybutyrate and Ethyl Cellulose for Coating of Urea Granules. *Journal of Agricultural and Food Chemistry* **61**:9984-9991.
- Dakora, F. D., and D. A. Phillips. 2002. Root exudates as mediators of mineral acquisition in low-nutrient environments. *Plant and Soil* **245**:35-47.
- Davidson, D., and F. X. Gu. 2012. Materials for Sustained and Controlled Release of Nutrients and Molecules To Support Plant Growth. *Journal of Agricultural and Food Chemistry* **60**:870-876.
- Eriksen, M., S. Mason, S. Wilson, C. Box, A. Zellers, W. Edwards, H. Farley, and S. Amato. 2013. Microplastic pollution in the surface waters of the Laurentian Great Lakes. *Marine Pollution Bulletin* **77**:177-182.
- Esser-Kahn, A. P., S. A. Odom, N. R. Sottos, S. R. White, and J. S. Moore. 2011. Triggered Release from Polymer Capsules. *Macromolecules* **44**:5539-5553.
- Fan, B., and E. R. Gillies. 2017. Poly(ethyl glyoxylate)-Poly(ethylene oxide) Nanoparticles: Stimuli-Responsive Drug Release via End-to-End Polyglyoxylate Depolymerization. *Molecular Pharmaceutics* **14**:2548-2559.
- Fan, B., J. F. Trant, and E. R. Gillies. 2016. End-Capping Strategies for Triggering End-to-End Depolymerization of Polyglyoxylates. *Macromolecules* **49**:9309-9319.
- Fan, B., J. F. Trant, A. D. Wong, and E. R. Gillies. 2014. Polyglyoxylates: A Versatile Class of Triggerable Self-Immolative Polymers from Readily Accessible Monomers. *Journal of the American Chemical Society* **136**:10116-10123.
- Hoagland, D.R. and Arnon, D.I. (1950) The Water-Culture Method for Growing Plants without Soil. California Agricultural Experiment Station, Circular-347.
- Jackson, R. B., H. A. Mooney, and E. D. Schulze. 1997. A global budget for fine root biomass, surface area, and nutrient contents. *Proceedings of the National Academy of Sciences of the United States of America* **94**:7362-7366.
- Kaitz, J. A., and J. S. Moore. 2014. Copolymerization of o-Phthalaldehyde and Ethyl Glyoxylate: Cyclic Macromolecules with Alternating Sequence and Tunable Thermal Properties. *Macromolecules* **47**:5509-5513.
- Li, Q. S., S. Wu, T. J. Ru, L. M. Wang, G. Z. Xing, and J. M. Wang. 2012. Synthesis and Performance of Polyurethane Coated Urea as Slow/controlled Release Fertilizer.

- Journal of Wuhan University of Technology-Materials Science Edition **27**:126-129.
- Liang, R., and M. Z. Liu. 2006. Preparation and properties of a double-coated slow-release and water-retention urea fertilizer. *Journal of Agricultural and Food Chemistry* **54**:1392-1398.
- Nye, P. H. 1981. Changes of pH across the rhizosphere induced by roots. *Plant and Soil* **61**:7-26.
- Paez-Valencia, J., J. Sanchez-Lares, E. Marsh, L. T. Dorneles, M. P. Santos, D. Sanchez, A. Winter, S. Murphy, J. Cox, M. Trzaska, J. Metler, A. Kozic, A. R. Facanha, D. Schachtman, C. A. Sanchez, and R. A. Gaxiola. 2013. Enhanced Proton Translocating Pyrophosphatase Activity Improves Nitrogen Use Efficiency in Romaine Lettuce. *Plant Physiology* **161**:1557-1569.
- Shaviv, A., S. Raban, and E. Zaidel. 2003. Modeling controlled nutrient release from polymer coated fertilizers: Diffusion release from single granules. *Environmental Science & Technology* **37**:2251-2256.
- Sheriff, G. 2005. Efficient waste? Why farmers over-apply nutrients and the implications for policy design. *Review of Agricultural Economics* **27**:542-557.
- Stuart, D., R. L. Schewe, and M. McDermott. 2014. Reducing nitrogen fertilizer application as a climate change mitigation strategy: Understanding farmer decision-making and potential barriers to change in the US. *Land Use Policy* **36**:210-218.
- Tilman, D., J. Fargione, B. Wolff, C. D'Antonio, A. Dobson, R. Howarth, D. Schindler, W. H. Schlesinger, D. Simberloff, and D. Swackhamer. 2001. Forecasting agriculturally driven global environmental change. *Science* **292**:281-284.
- Timilsena, Y. P., R. Adhikari, P. Casey, T. Muster, H. Gill, and B. Adhikari. 2015. Enhanced efficiency fertilisers: a review of formulation and nutrient release patterns. *Journal of the Science of Food and Agriculture* **95**:1131-1142.
- von Burkersroda, F., L. Schedl, and A. Gopferich. 2002. Why degradable polymers undergo surface erosion or bulk erosion. *Biomaterials* **23**:4221-4231.
- Wei, Y., J. Li, Y. T. Li, B. Q. Zhao, L. G. Zhang, X. D. Yang, and J. Chang. 2017. Research on permeability coefficient of a polyethylene controlled-release film coating for urea and relevant nutrient release pathways. *Polymer Testing* **59**:90-98.
- Weithmann, N., J. N. Moller, M. G. J. Loder, S. Piehl, C. Laforsch, and R. Freitag. 2018. Organic fertilizer as a vehicle for the entry of microplastic into the environment. *Science Advances* **4**:7.
- Wilson, M. L., C. J. Rosen, and J. F. Monerief. 2009. A Comparison of Techniques for Determining Nitrogen Release from Polymer-coated Urea in the Field. *Hortscience* **44**:492-494.
- Yang, Y. C., M. Zhang, L. Zheng, D. D. Cheng, M. Liu, and Y. Q. Geng. 2011. Controlled Release Urea Improved Nitrogen Use Efficiency, Yield, and Quality of Wheat. *Agronomy Journal* **103**:479-485.
- Zhao, B., S. T. Dong, J. W. Zhang, and P. Liu. 2013. Effects of Controlled-Release Fertiliser on Nitrogen Use Efficiency in Summer Maize. *Plos One* **8**:8.
- Zhou, L. L., J. Cao, F. S. Zhang, and L. Li. 2009. Rhizosphere acidification of faba bean, soybean and maize. *Science of the Total Environment* **407**:4356-4362.

4 Summary, outlooks, and conclusions

4.1 Summary and outcomes

Since the first commercial polymer coated fertilizers were developed in the early 1970's, there has not been a high degree of change in the choice of polymeric materials used as coatings for fertilizer pellets (Majeed et al. 2015). The majority of the coatings used to encapsulate fertilizer pellets are made of plastics that are non-biodegradable and insoluble (Shaviv et al. 2003, Majeed et al. 2015). Rather than being responsive to plant stimuli, fertilizer release occurs through an interaction between environmental conditions (primarily temperature) surface defects, and water penetration occurs via osmotic exchanges with soil moisture (Adams et al. 2013). Although there has been some development of eco-friendly coatings, such as with poly (lactic acid), unlike SIPs they do not respond to plant stimuli, and bio-degradable polymers are generally not marketed because they are not as cost-effective as traditional plastics, such as polyurethane, polyethylene, or polyolefin (Majeed et al. 2015).

Ideally, a CRF coating would have the following attributes: 1) release in a controlled and delayed manner; 2) synchronized with the needs of plants; 3) inexpensive; 4) made of a non-toxic and biodegradable polymer that can be manufactured and applied on an industrial scale (Azeem et al. 2014). None of the current CRF coatings feature all of these characteristics, but my research has demonstrated that poly(ethyl glyoxylate) (PEtG) potentially could. Nevertheless, PEtG is a novel polymer, and it never has been used as a bulk material; therefore, my first objective was to characterize its structural properties. Pure PEtG does not produce a viable coating due to constraints in its thermal and

mechanical properties. Therefore, I attempted improve its these physical properties by blending PEtG with different biodegradable polyesters (PCL, PLA, PLA:PHB 3:1) commonly used for biomedical applications.

In Chapter 2, I examined what proportion of other polyesters can be blended with PEtG to improve its mechanical properties and reduce tackiness, while still maintaining the desirable degradation properties of PEtG. At the time that these blends were tested, the phenyl carbamate end-cap had not been developed, so I used a 6-nitroveratryl chloroformate (UV-responsive) end-cap to examine the degradation properties of the different polyester ratios. Higher blend ratios (75 wt%) of PEtG did not produce a viable coating. Therefore, I selected even ratios of PEtG to polyester for the next series of experiments for my second objective. Specifically, both PLA and PCL blends (50 wt%) with PEtG produced promising changes to overall stiffness and tackiness while still maintaining a desirable degradation rate.

Once suitable blends were determined for PEtG, I then tested the responsiveness of the phenyl carbamate end-cap, which had never been explored previously, for my second objective. This end-cap was designed to respond to acidic pH, which is characteristic of the plant rhizosphere relative to the pH of the surrounding soil. In Chapter 3, I demonstrated that PEtG with the phenyl carbamate end cap indeed was sensitive to acidic pH, and its activity also was temperature dependent. This is the first time a SIP has been demonstrated to respond to plant stimulus. I then demonstrated that only the PCL blend showed suitable degradation responses to pH change, in contrast to the results obtained using the UV-responsive end-cap.

Once I had characterized the coatings, I then applied them to urea pellets to assess release rates for my third objective. My initial release studies with PEtG:PCL blends had variable responses, with temperature dependence being the dominant factor. Coatings in this case were quite thick, because I had to produce each individual pellet by hand. Ideally, a coating would be thinner (e.g. less than 5 wt% of pellet mass); however, this was not achieved due to fabrication constraints. Nevertheless, most industrial applications that require coatings use a fluidized bed, which could coat fertilizer pellets more consistently.

Spray coating using chlorinated solvent was not successful for producing a coating that lacked defects and the resulting pellets were not impermeable to water. However, many current CRFs also consist of pellets with micropores and defects on the surface that allow water penetration. Therefore, even in the absence of an effective root stimulus response, the spray coated PEtG blends could delay the release of fertilizer, while degrading into by-products that are innocuous to the soil environment. The production of variable thickness coatings has the potential to further enhance the even distribution of nutrient release throughout the growing season. Granted, the chlorinated solvents used for the spray coating would not be permitted for such an application at an industrial scale, but melting and dripping the polymer mixture inside a fluidized bed could avoid the use of these solvents and possibly produce a more robust and uniform coating.

4.2 Future outlooks

A logical follow-up to my research would be a test of whether the pellets improve nitrogen use efficiency *in situ*. The effectiveness of the pellets in increasing plant N uptake and growth while minimizing N losses in comparison to uncoated urea and currently marketed CRFs could be examined. CRFs such as ESN (produced by Agrium) release fertilizer based on water penetration, thickness of coating, and temperature, whereas PEtG features a more direct plant response and less environmentally taxing substitute. By fine tuning and optimizing release rates of PEtG coated pellets, overall nutrient delivery could potential improve in comparison to current CRF benchmarks. Ideally, pellets then could be produced at a commercial scale to examine if they enhance nitrogen delivery under a range of applications (e.g. crops or turfgrass). ¹⁵N tracer could be used in the pellets to directly track the fate of the applied N, such as the proportion entering the plants and the proportion lost from the soil.

Given that soil pH can vary substantially, both within and among fields, a pH sensitive end cap may not be the optimal choice for plant-responsive coatings. As stated earlier, there are a variety of additional plant-responsive end-caps that also could be explored. Specifically, an enzyme-triggered end-cap could improve plant root-specific responsiveness, because plant roots exude enzymes in the rhizosphere, particularly in the active area surrounding the root tip (Dakora and Phillips 2002). For example, enzymes such as leucine aminopeptidases (LAPs) are released during nutrient mobilization and in plant self-defense (Fowler et al. 2009). The M1 and M17 classes of LAPs are conserved across many plant species and are used for the hydrolysis of leucine residues on amino-terminus of protein substrates (Matsui et al. 2006). They are concentrated in the

rhizosphere and could cleave a potential poly(glyoxylate) end-cap that contains a leucine residue. There are other enzymes, such as phosphatases and proteases, that plant roots utilize during nutrient mobilization, that also potentially could be targeted and exploited to develop a plant-responsive end-cap (Dakora and Phillips 2002).

4.3 Conclusions

Our society is at the apex of its commercial use of plastics that are not biodegradable. Globally, plastics are being used daily, with a large proportion of them accumulating in our ecosystems at accelerated rates. The same can be said for microplastics that are slowly accumulating within soil substrates from controlled release fertilizers. These coatings may be ending up in terrestrial ecosystems, as well making their way downstream into aquatic systems. Many current CRFs are marketed as “smart coatings,” because release is slowed, which gives the impression that release is synchronized with plant demand, indicating they are better for the environment. However, nutrient release occurs for the CRFs simply because of the presence of microscopic pores on the polymer surface. In addition to this, a majority of all CRFs are composed of plastics that do not degrade. Therefore, there is no direct release trigger, there is a low degree of control (e.g. the nutrients will be released in pockets of soil that have not yet been explored by plant roots), and microplastics do not degrade rapidly. Current innovations may be improving NUE, but they are also contaminating ecosystems with plastics.

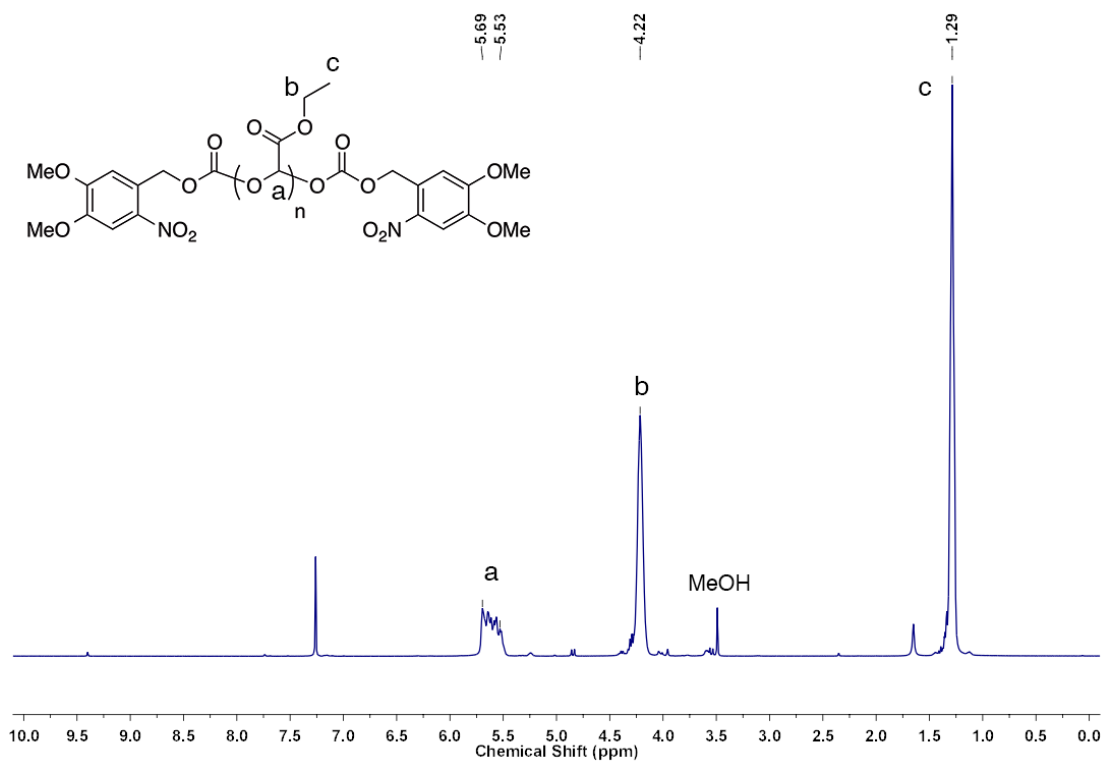
My novel research indicates that with further development, PEtG could be used to create a coating that directly responds to plant stimuli, and the by-products are innocuous. With human populations steadily increasing, fertilizer use will continue to increase along with the demand for high yielding crops. The use of stimuli-responsive biodegradable polymer coatings that react to plant-root specific stimuli offer a more targeted delivery mechanism that may enhance nutrient use efficiency and reduce the accumulation of microplastics

4.4 References

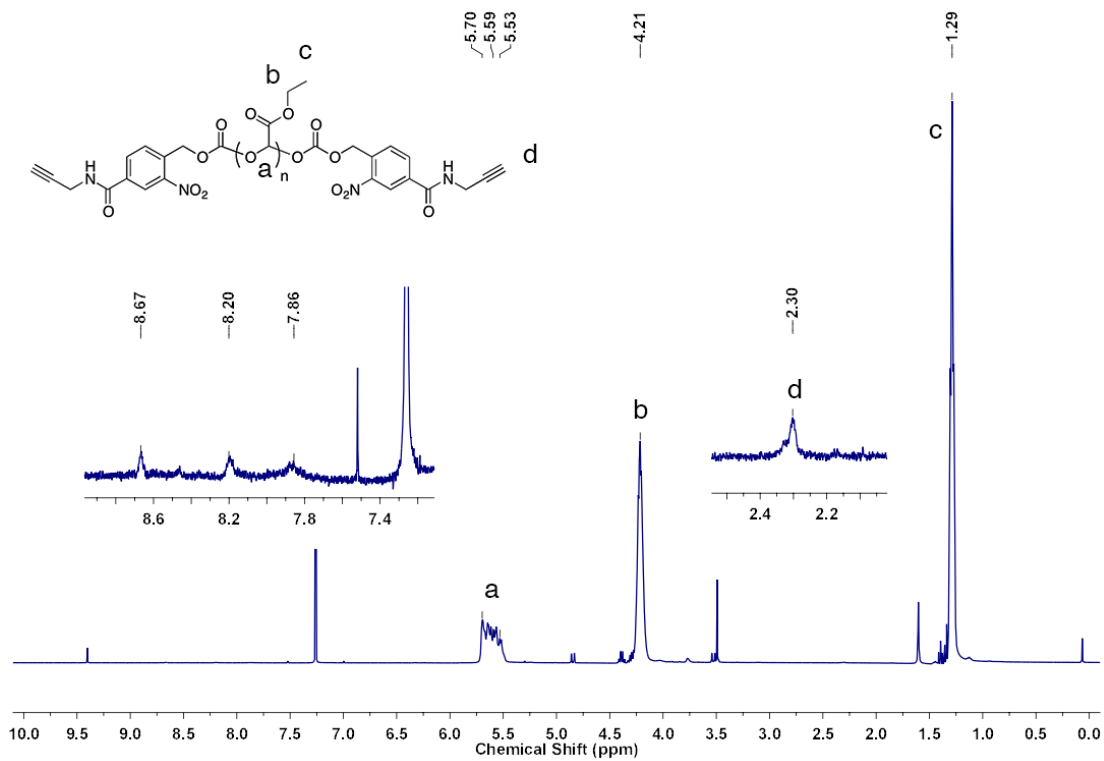
- Adams, C., J. Frantz, and B. Bugbee. 2013. Macro- and micronutrient-release characteristics of three polymer-coated fertilizers: Theory and measurements. *Journal of Plant Nutrition and Soil Science* **176**:76-88.
- Azeem, B., K. KuShaari, Z. B. Man, A. Basit, and T. H. Thanh. 2014. Review on materials & methods to produce controlled release coated urea fertilizer. *Journal of Controlled Release* **181**:11-21.
- Dakora, F. D., and D. A. Phillips. 2002. Root exudates as mediators of mineral acquisition in low-nutrient environments. *Plant and Soil* **245**:35-47.
- Fowler, J. H., J. Narvaez-Vasquez, D. N. Aromdee, V. Pautot, F. M. Holzer, and L. L. Walling. 2009. Leucine Aminopeptidase Regulates Defense and Wound Signaling in Tomato Downstream of Jasmonic Acid. *Plant Cell* **21**:1239-1251.
- Majeed, Z., N. K. Ramli, N. Mansor, and Z. Man. 2015. A comprehensive review on biodegradable polymers and their blends used in controlled-release fertilizer processes. *Reviews in Chemical Engineering* **31**:69-96.
- Matsui, M., J. H. Fowler, and L. L. Walling. 2006. Leucine aminopeptidases: diversity in structure and function. *Biological Chemistry* **387**:1535-1544.
- Shaviv, A., S. Raban, and E. Zaidel. 2003. Modeling controlled nutrient release from polymer coated fertilizers: Diffusion release from single granules. *Environmental Science & Technology* **37**:2251-2256.

Appendix

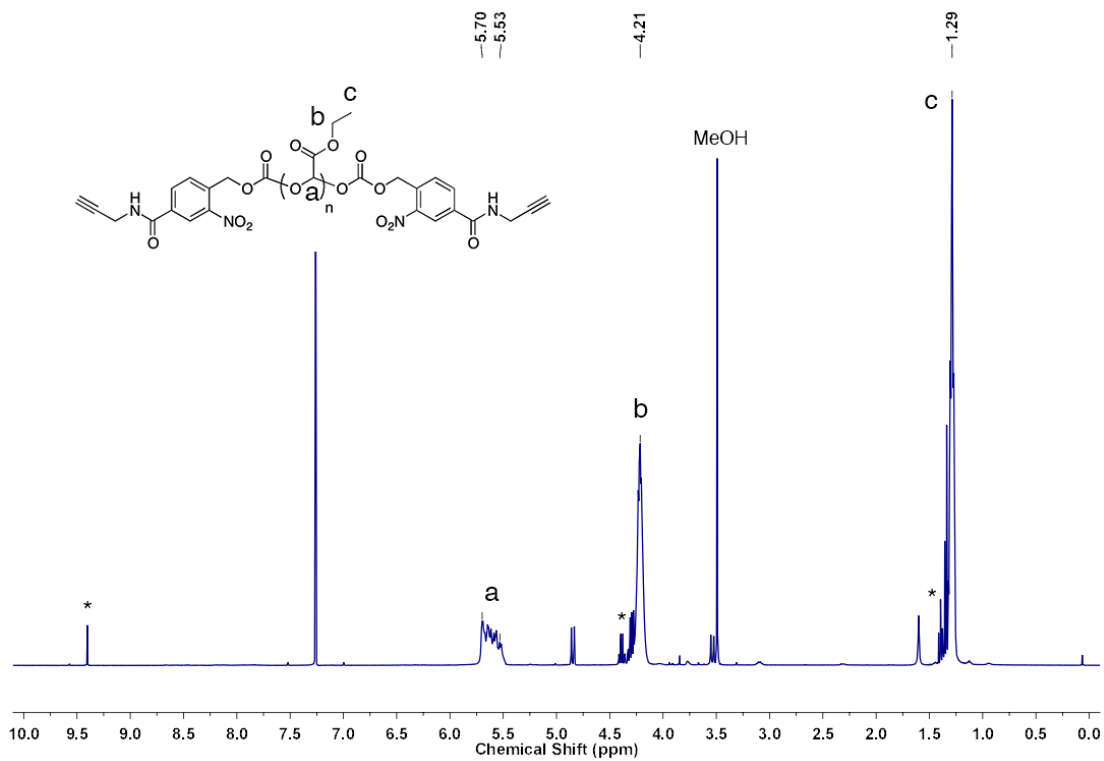
Chapter 2 Appendix A Supporting Information



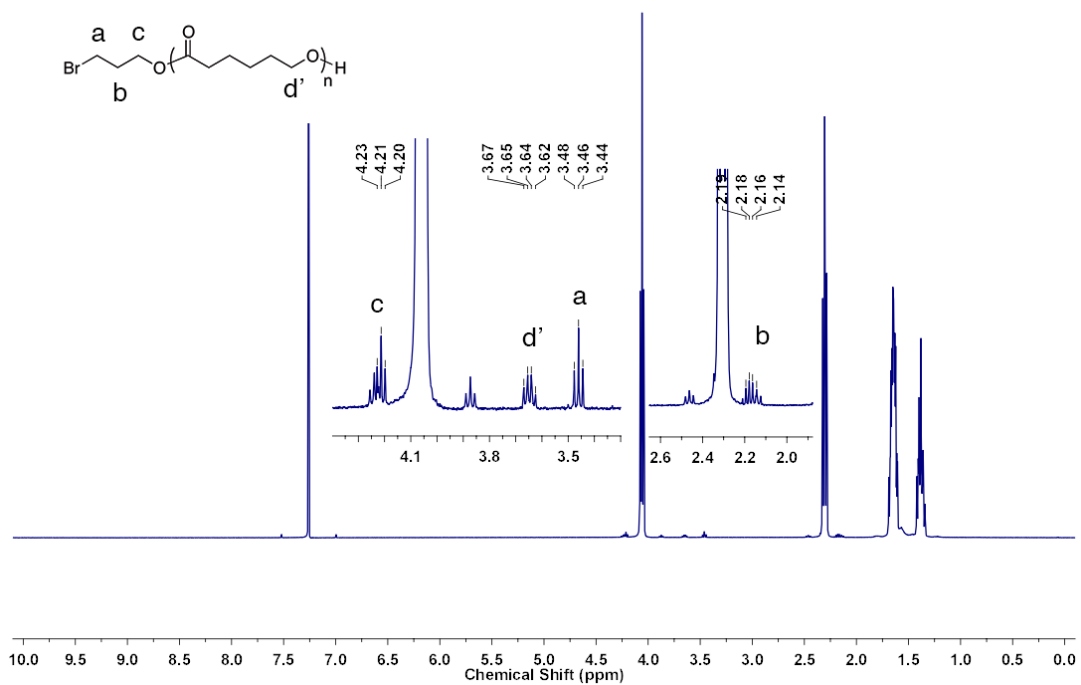
Appendix A 1. ¹H NMR spectrum of UV-responsive PEtG (600 MHz, CDCl₃).



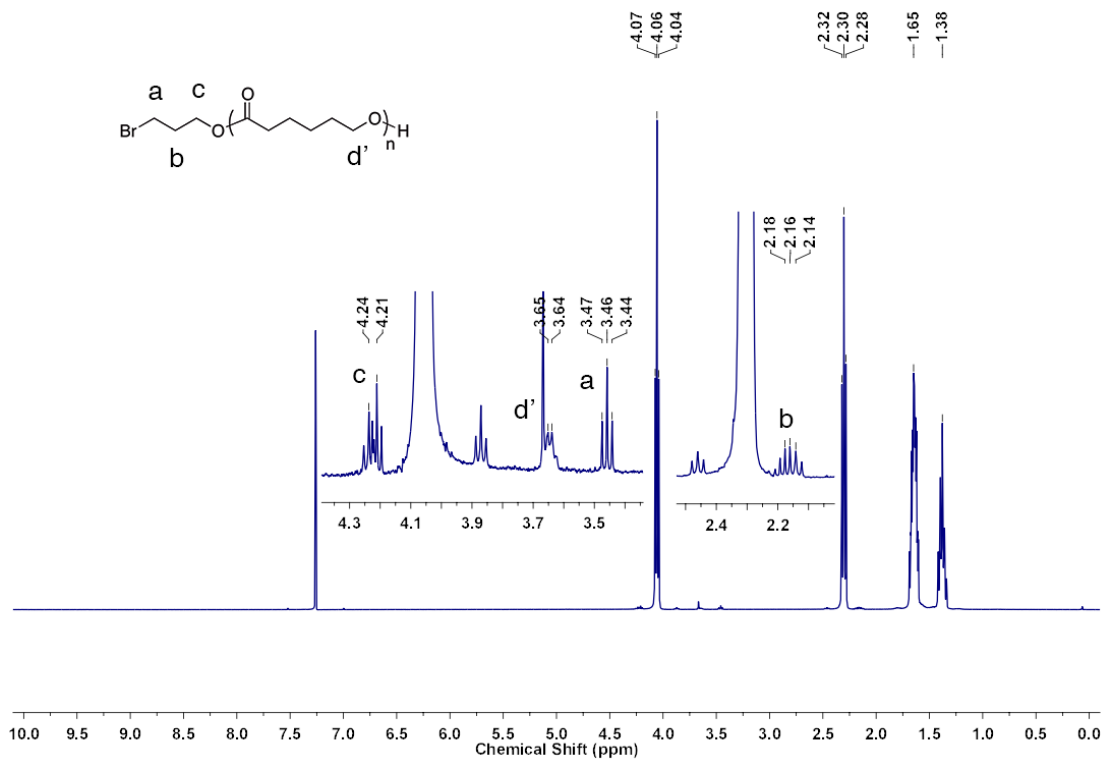
Appendix A 2. ¹H NMR spectrum of alkyne-PEtG-65k (600 MHz, CDCl₃).



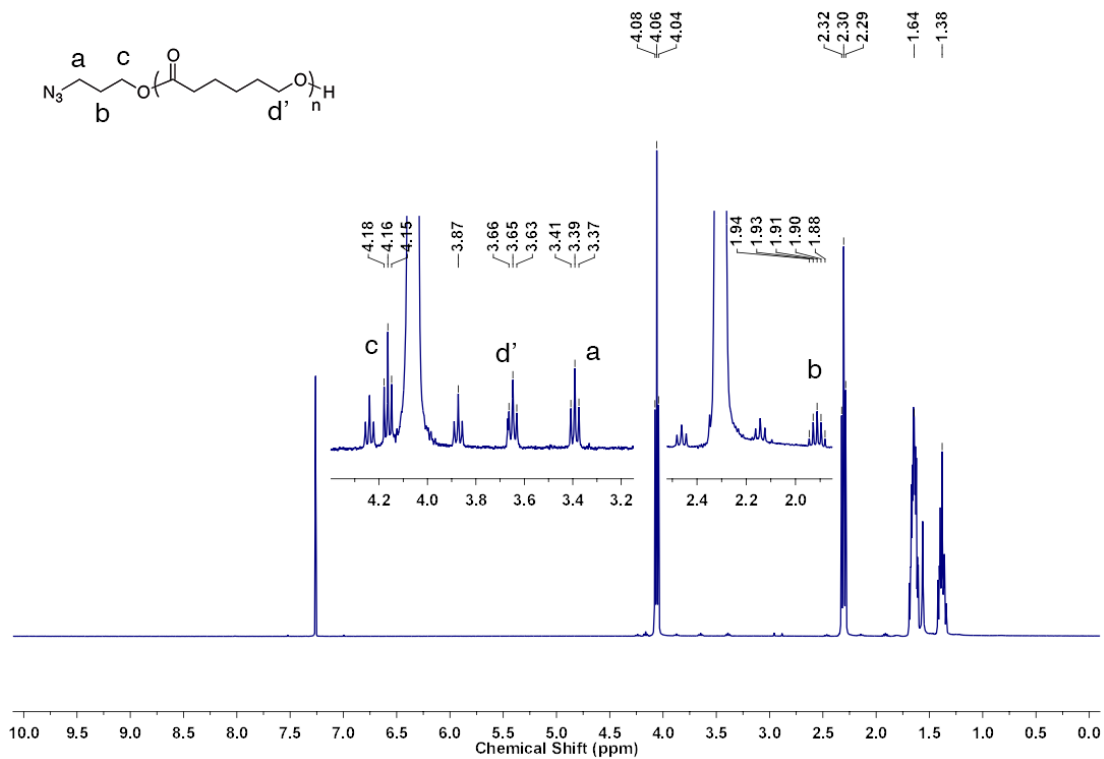
Appendix A 3. ^1H NMR spectrum of alkyne-PEtG-58k (600 MHz, CDCl_3).



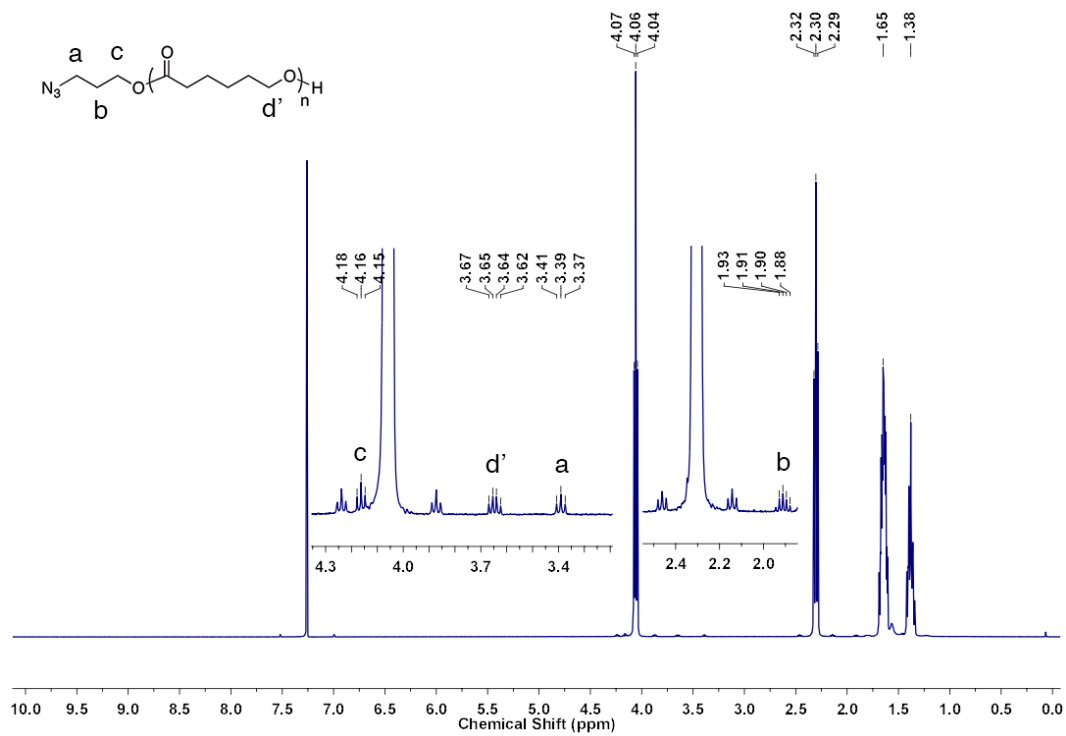
Appendix A 4. ^1H NMR spectrum of Br-PCL-low (600 MHz, CDCl_3).



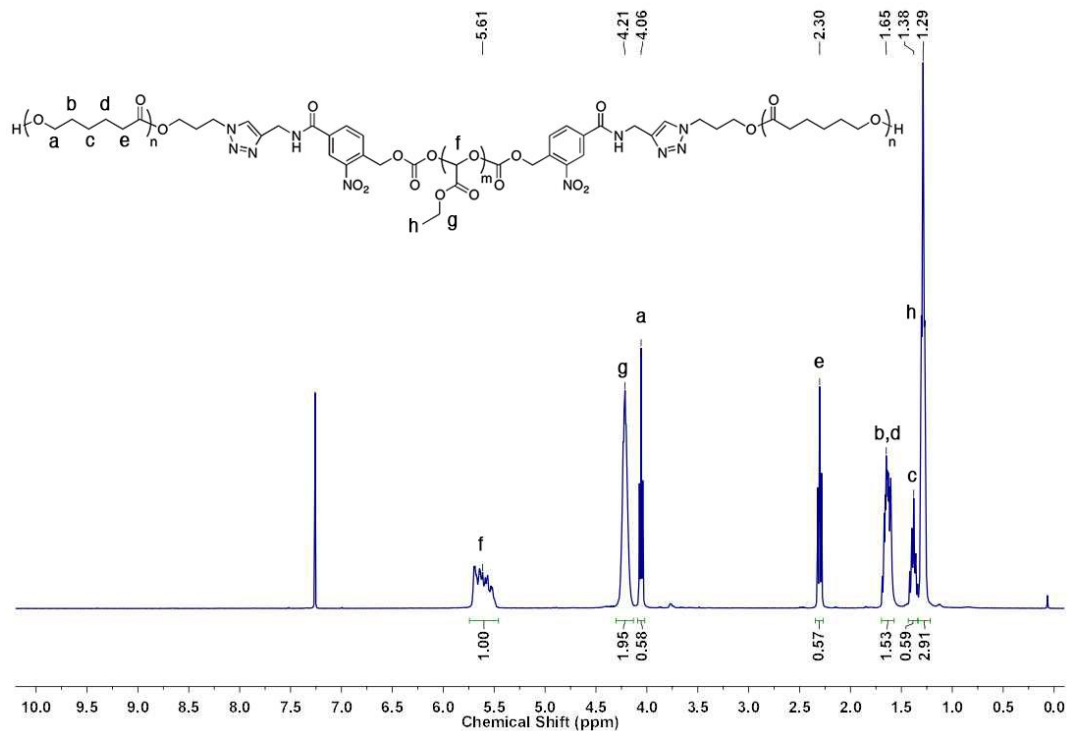
Appendix A 5. ^1H NMR spectrum of Br-PCL-high (600 MHz, CDCl_3).



Appendix A 6. ^1H NMR spectrum of N3-PCL-low (600 MHz, CDCl_3).

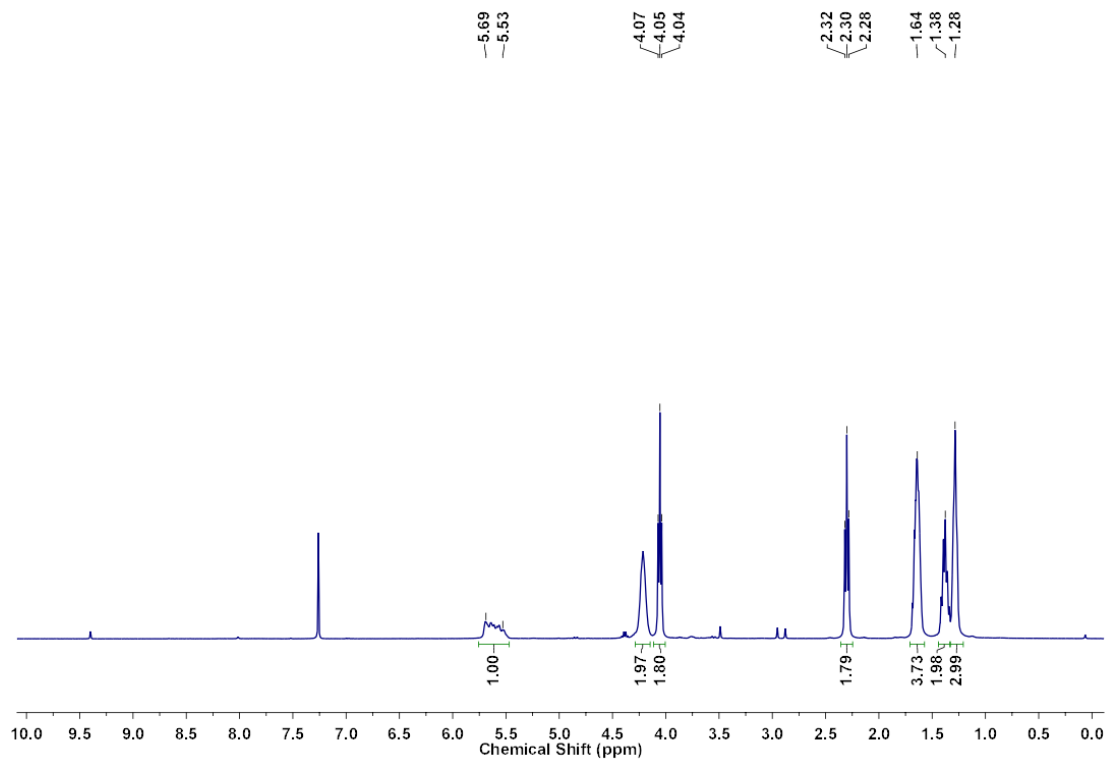


Appendix A 7. ^1H NMR spectrum of N3-PCL-high (600 MHz, CDCl_3).



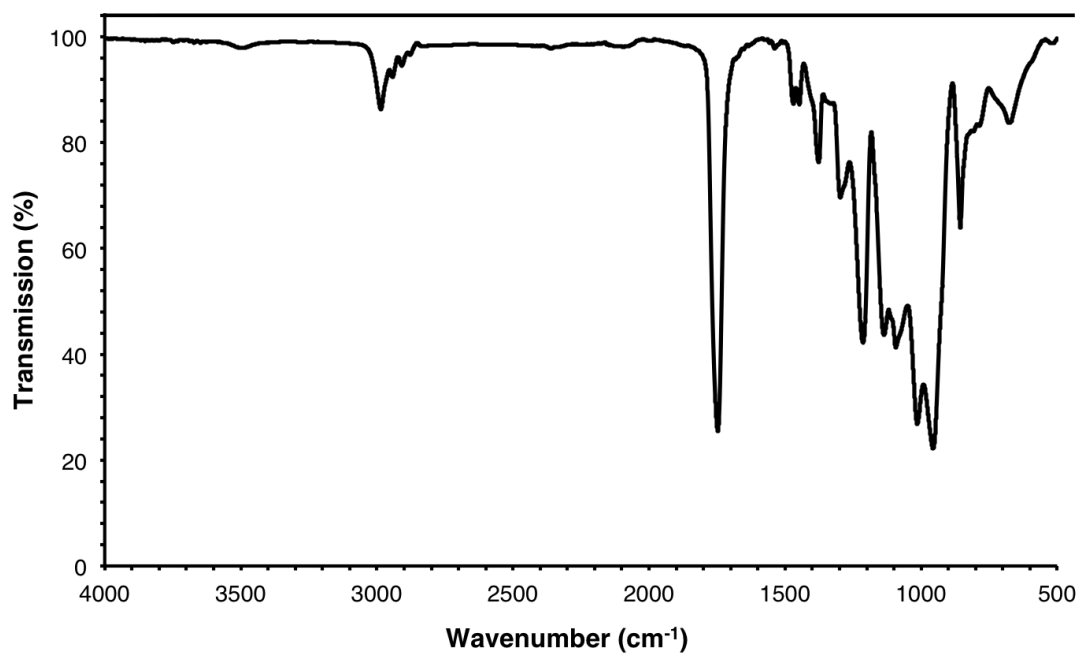
Appendix A 8. ^1H NMR spectrum of PCL-b-PEtG-b-PCL-low (400 MHz, CDCl_3).

Based on the relative integrations of the peaks corresponding to PCL versus PEtG, the mole ratio of PCL:PEtG was 0.3:1.0, corresponding to 25 wt% PCL.

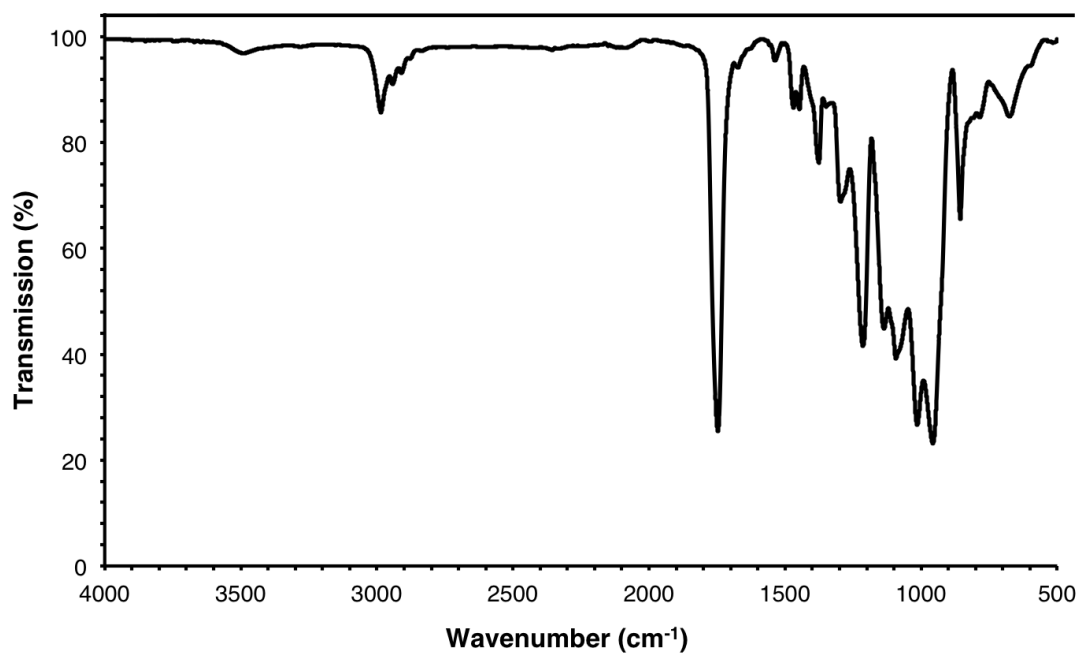


Appendix A 9. ^1H NMR spectrum of PCL-b-PEtG-b-PCL-high (400 MHz, CDCl_3).

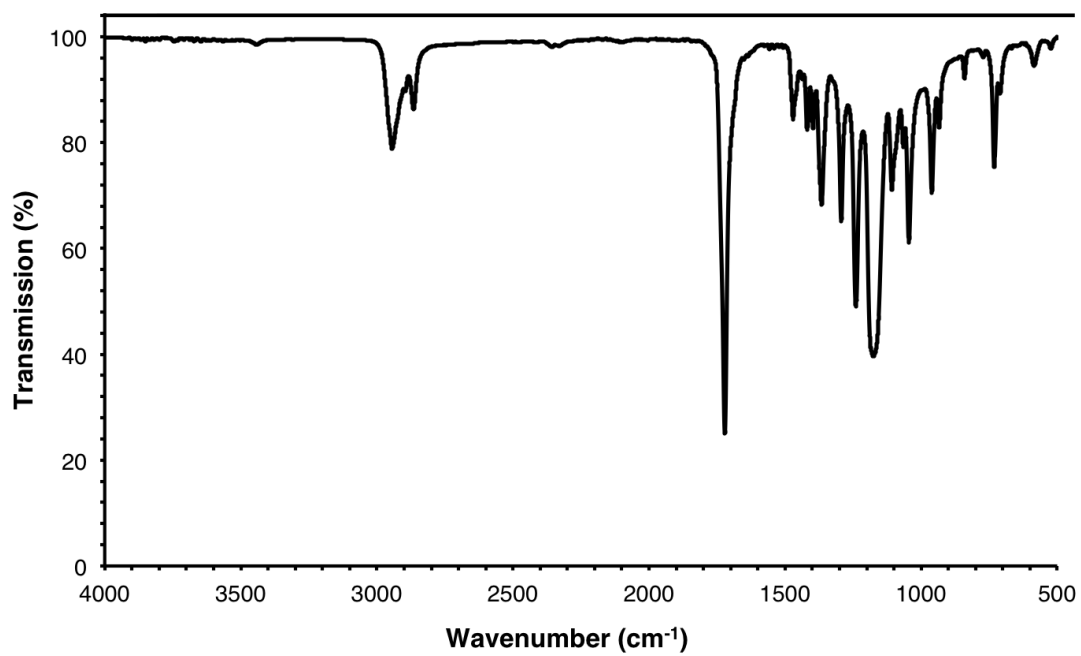
Based on the relative integrations of the peaks corresponding to PCL versus PEtG, the mole ratio of PCL:PEtG was 0.9:1.0, corresponding to 50 wt% PCL.



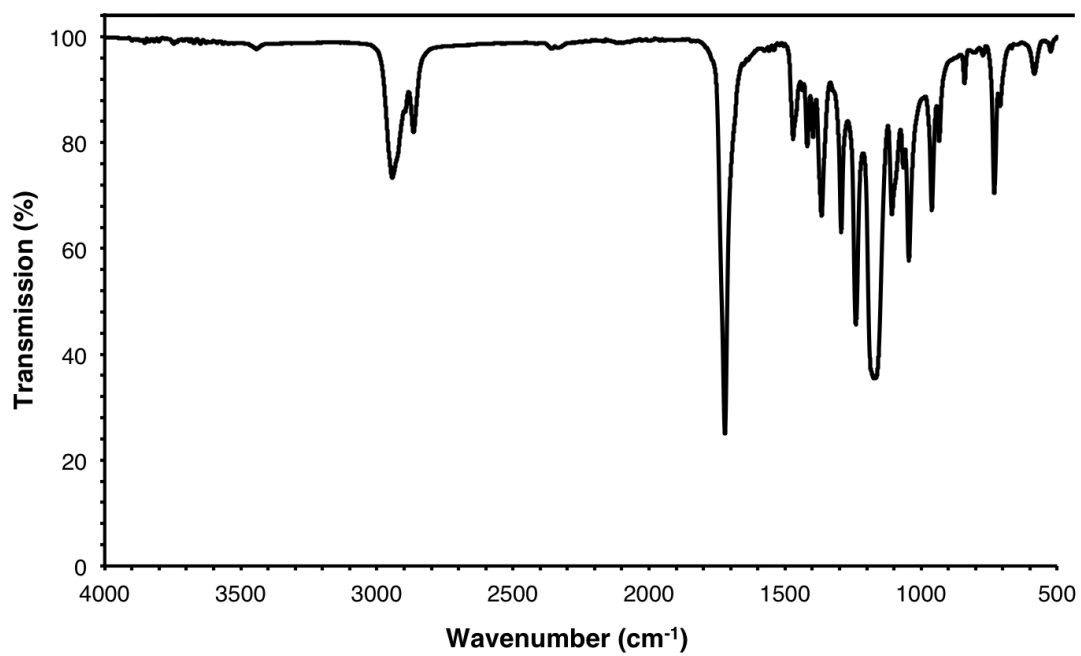
Appendix A 10. FTIR spectrum of alkyne-PEtG-65k.



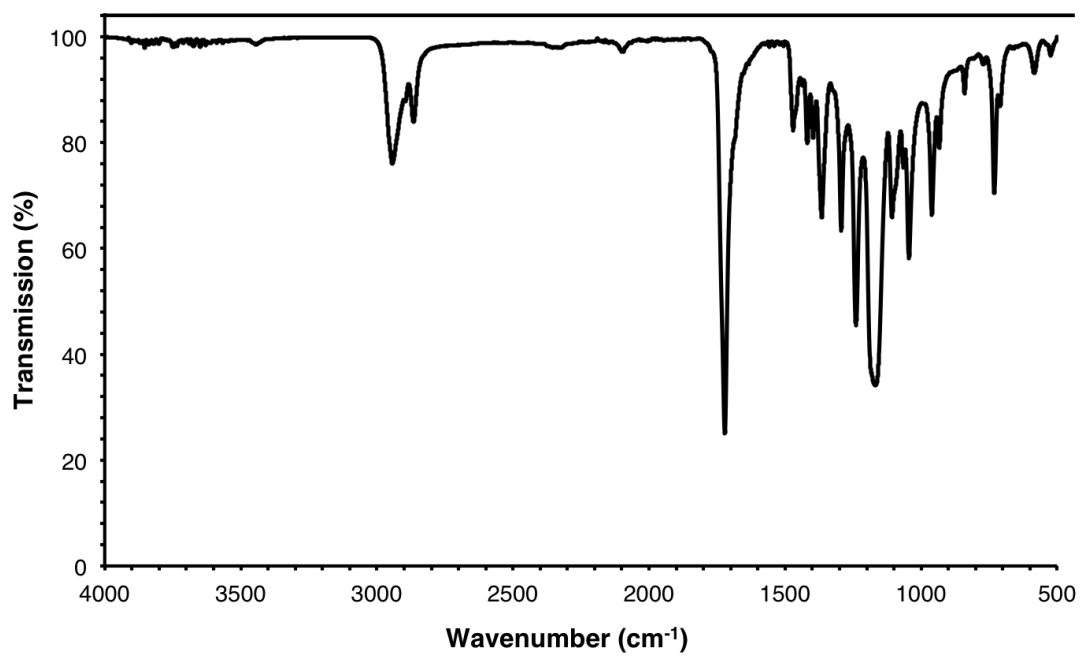
Appendix A 11. FTIR spectrum of alkyne-PEtG-58k.



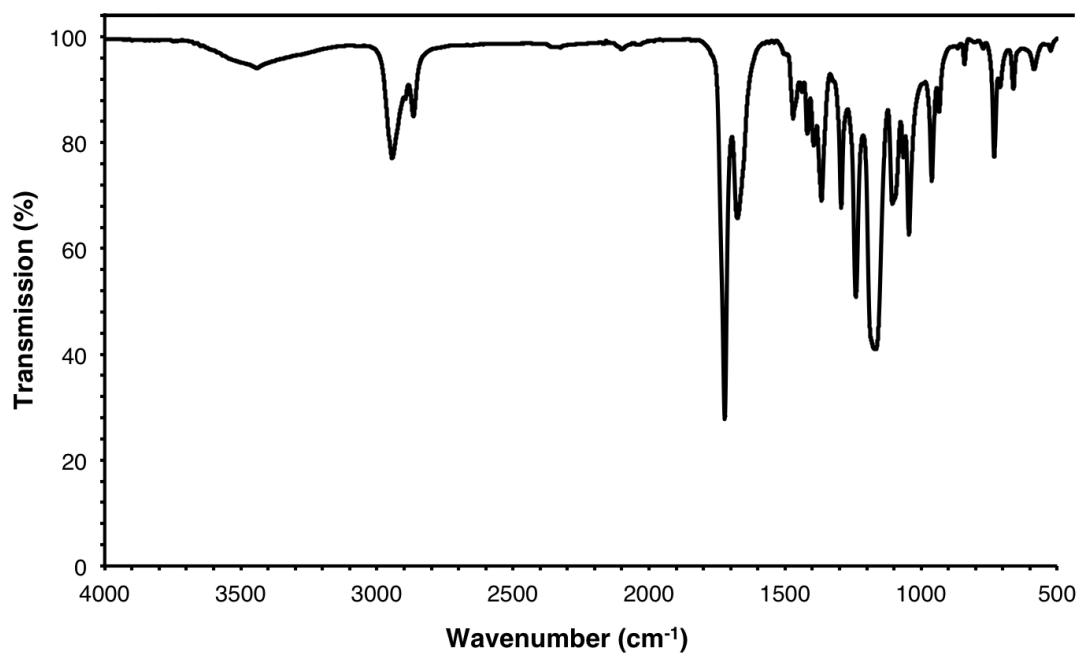
Appendix A 12. FTIR spectrum of Br-PCL-low.



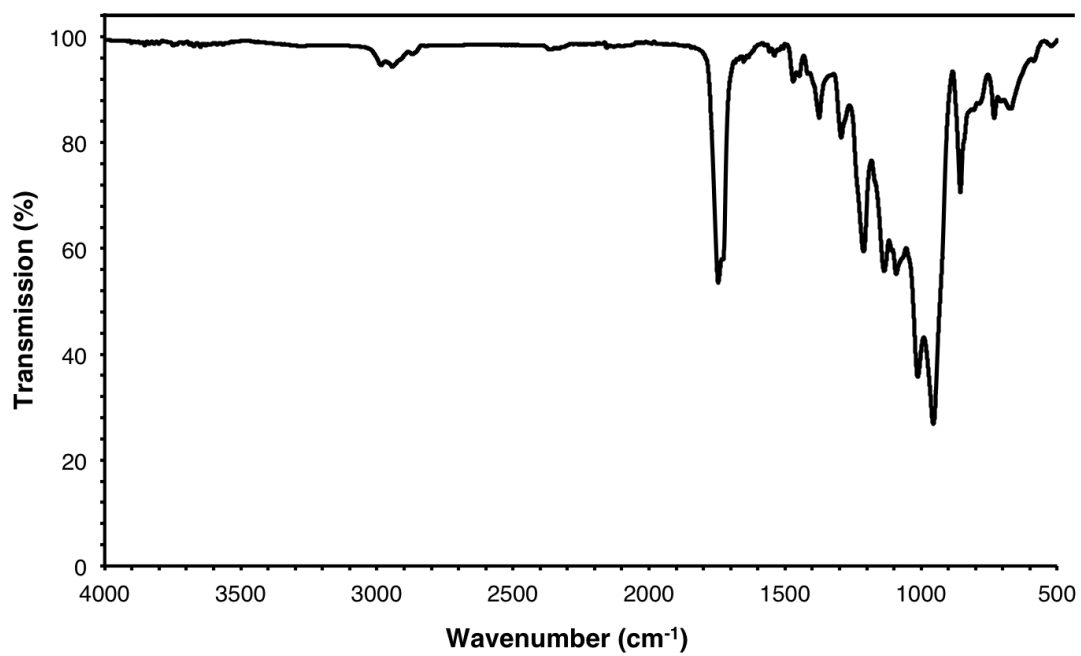
Appendix A 13. FTIR spectrum of Br-PCL-high.



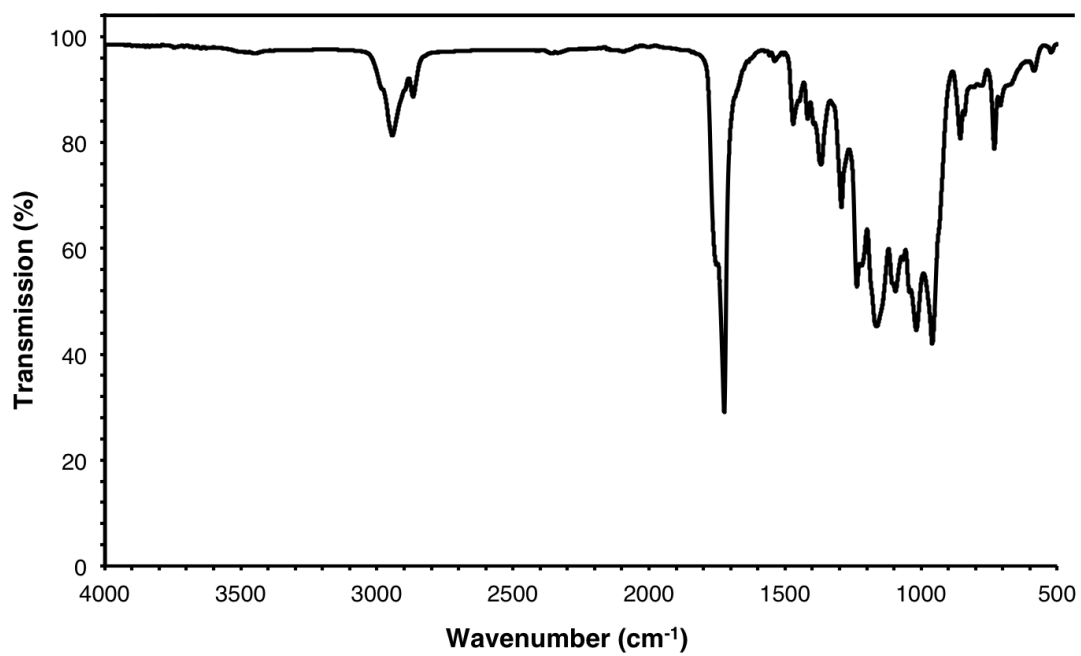
Appendix A 14. FTIR spectrum of N₃-PCL-low.



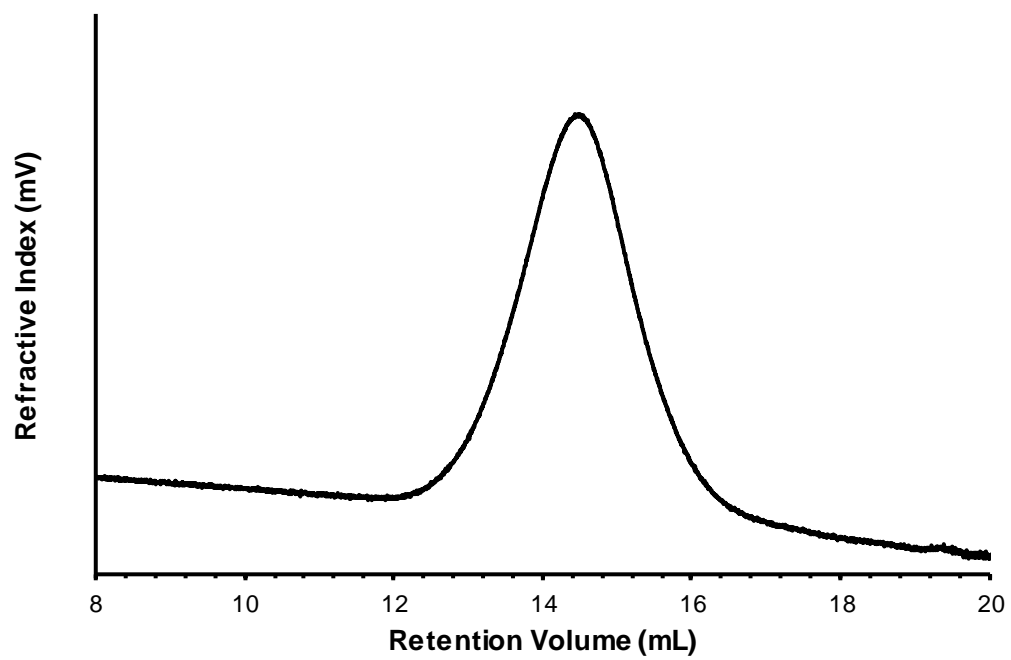
Appendix A 15. IR spectrum of N₃-PCL-high.



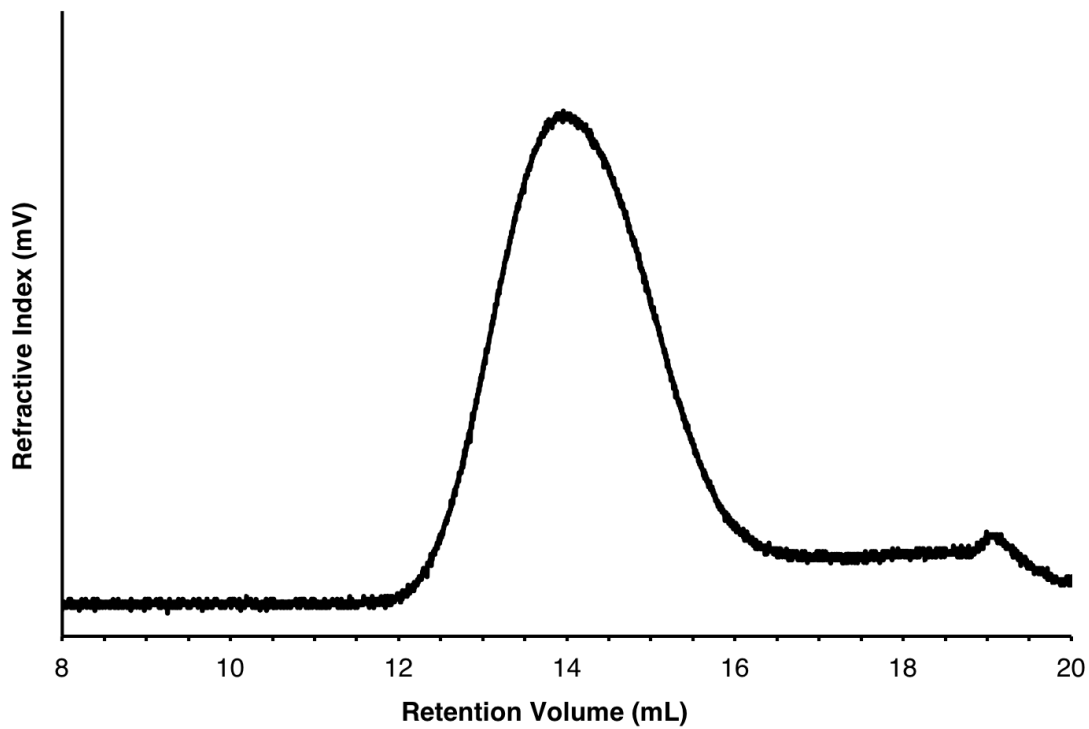
Appendix A 16. IR spectrum of PCL-*b*-PEtG-*b*-PCL-low.



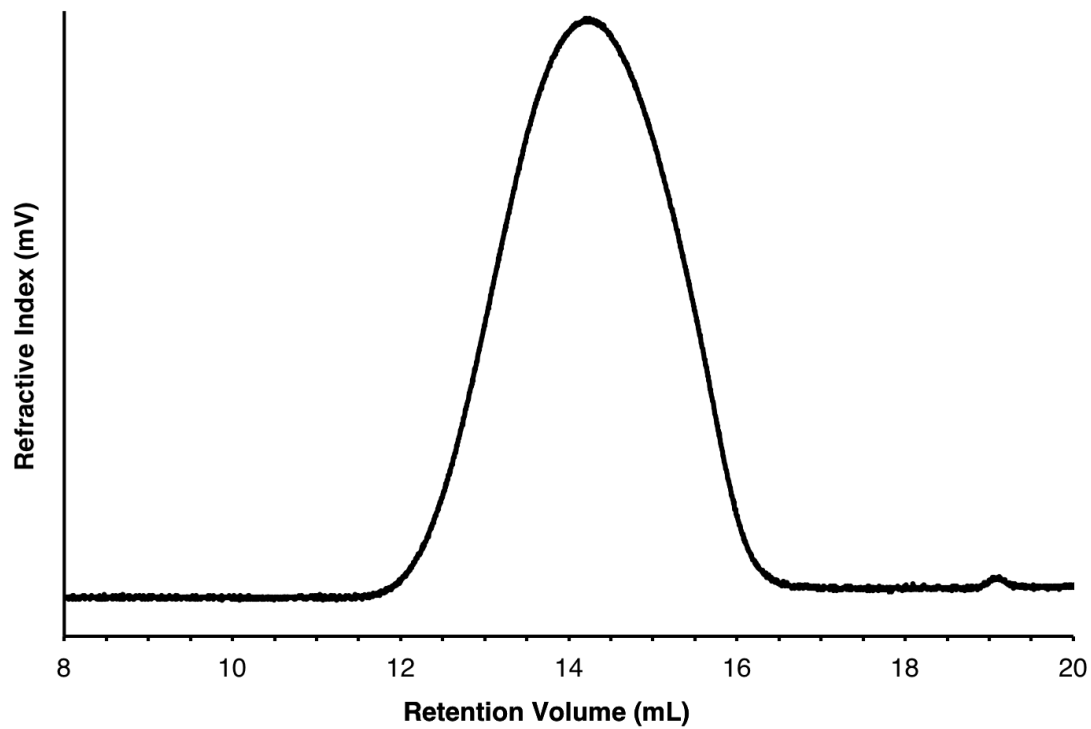
Appendix A 17. IR spectrum of PCL-*b*-PEtG-*b*-PCL-high.



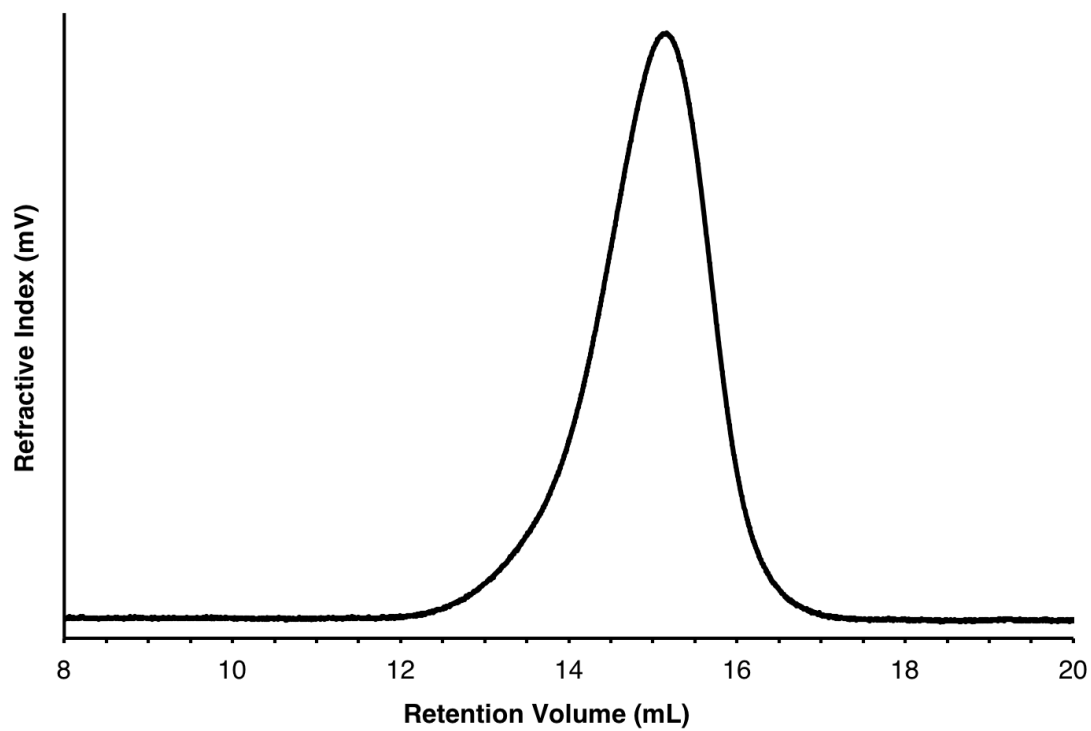
Appendix A 18. SEC trace for UV-responsive PEtG.



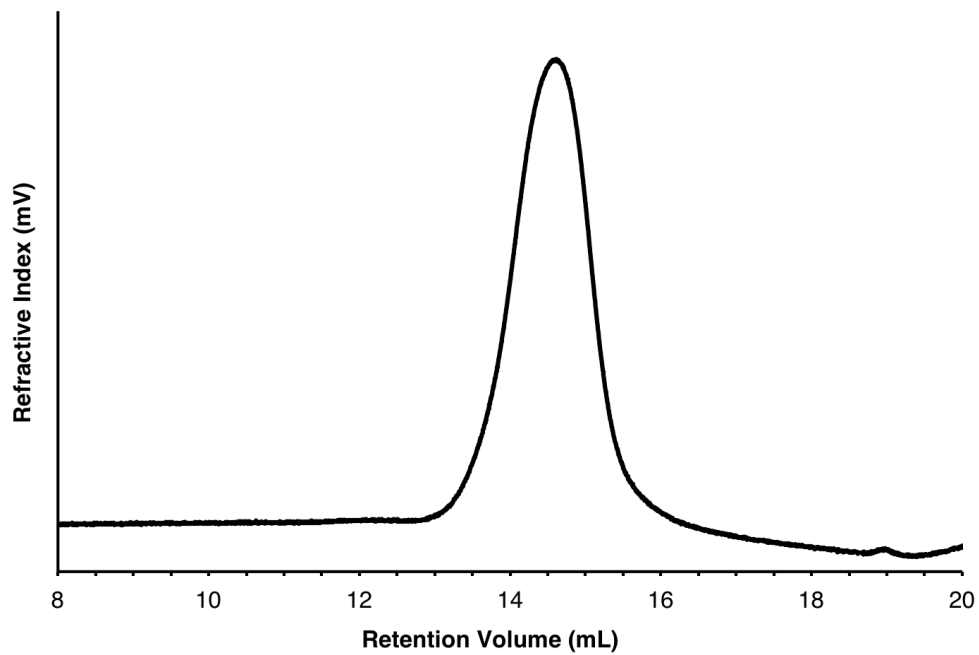
Appendix A 19. SEC trace for alkyne-PEtG-58k.



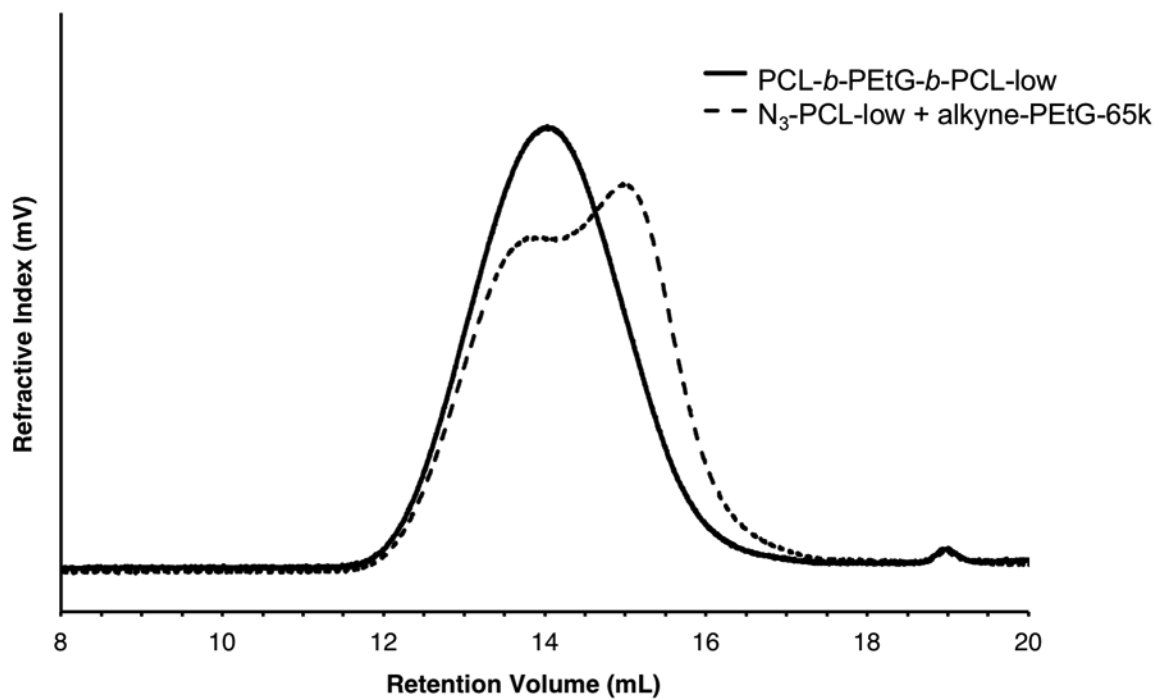
Appendix A 20. SEC trace for alkyne-PEtG-65k



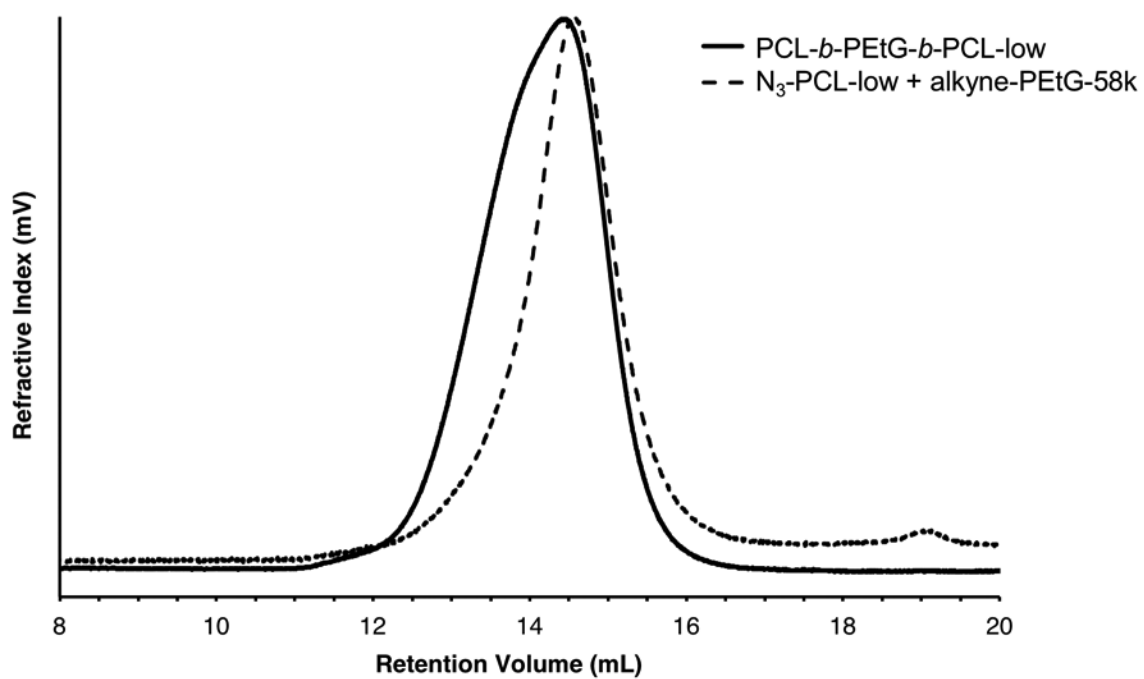
Appendix A 21. SEC trace for Br-PCL-low.



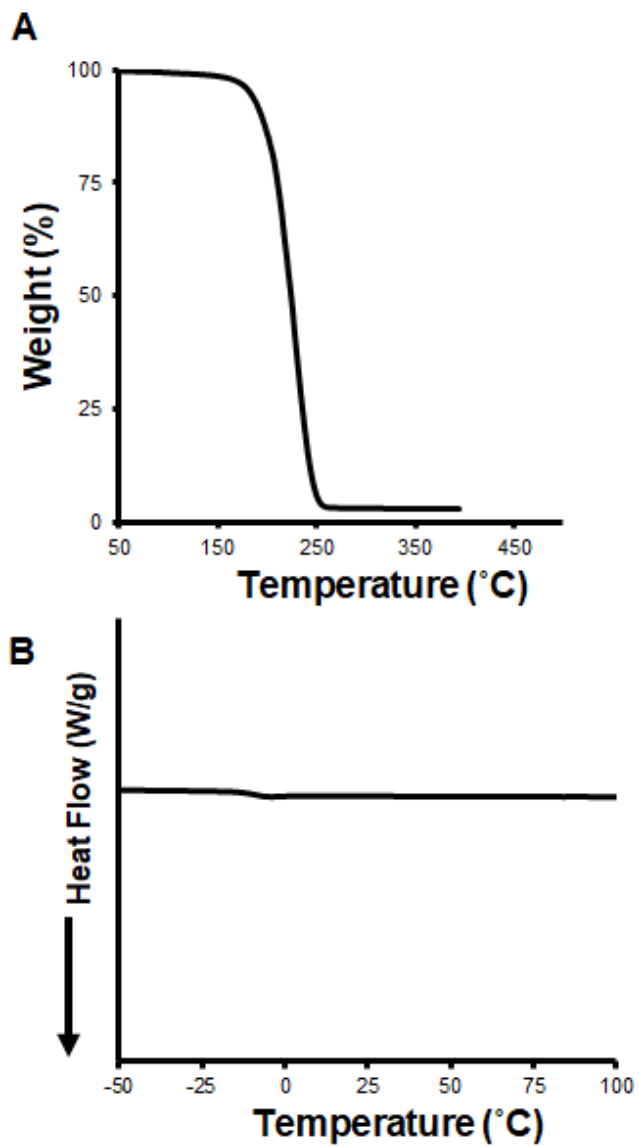
Appendix A 22. SEC trace for Br-PCL-high.



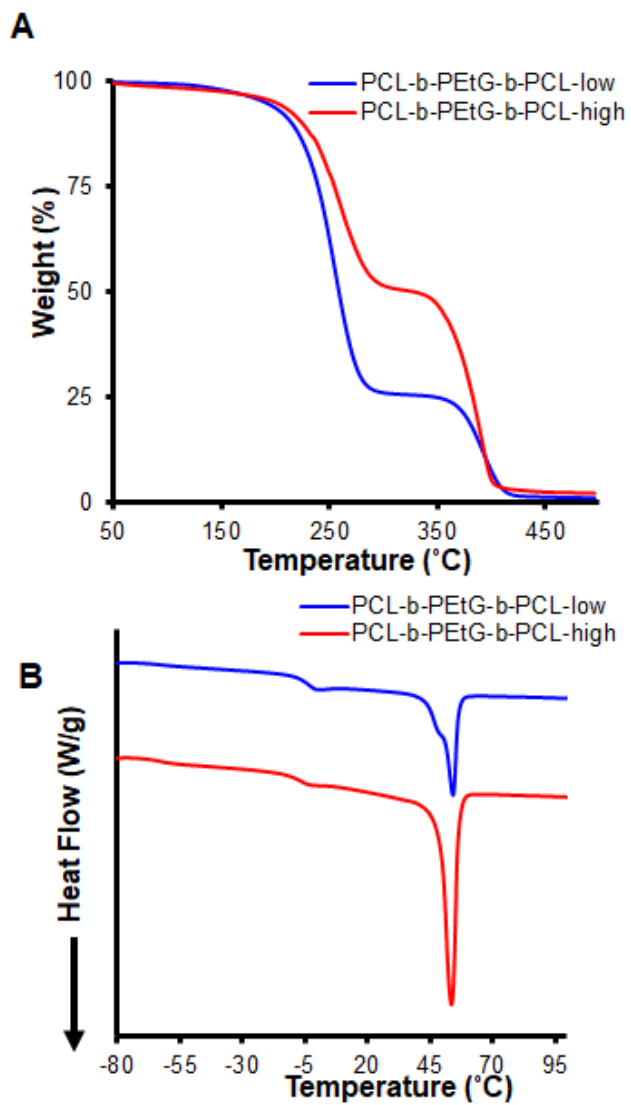
Appendix A 23. SEC traces for PCL-*b*-PEtG-*b*-PCL-low (solid line) and mixture of alkyne-PEtG-65k/N₃-PCL-low before CuAAC reaction (dashed line). Conversion of the two peaks to a single peak at lower retention volume is consistent with successful coupling.



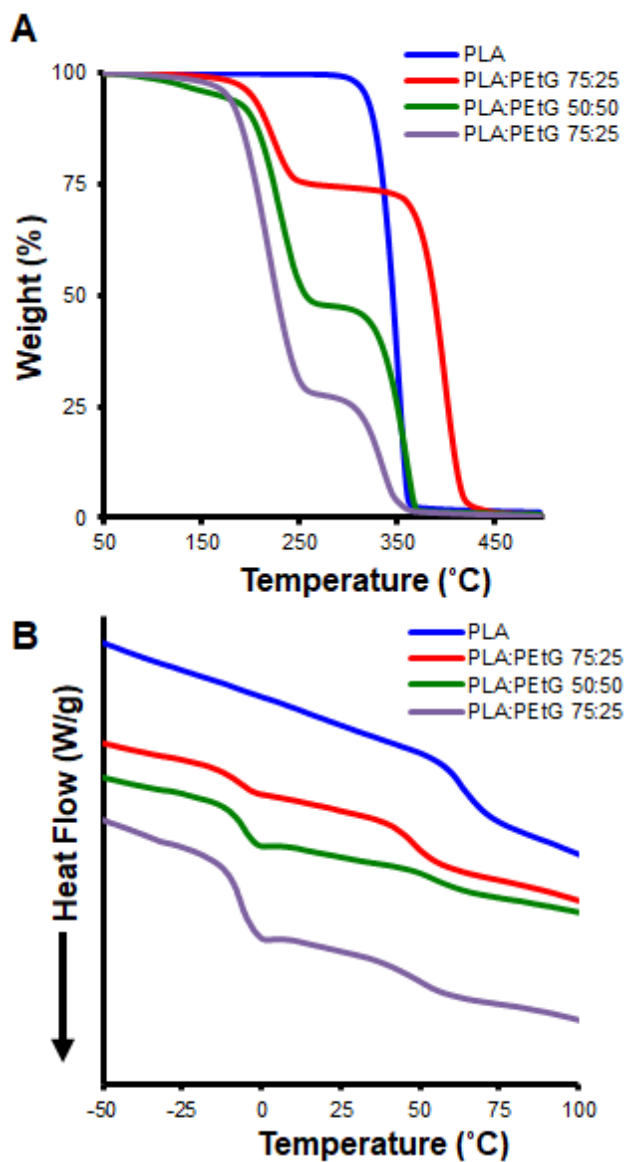
Appendix A 24. SEC traces for PCL-*b*-PEtG-*b*-PCL-high (solid line) and mixture of alkyne-PEtG-58k/N₃-PCL-high before CuAAC reaction (dashed line). In this case, the two starting polymers had overlapping traces, but conversion to a new peak at lower retention volume was consistent with successful coupling.



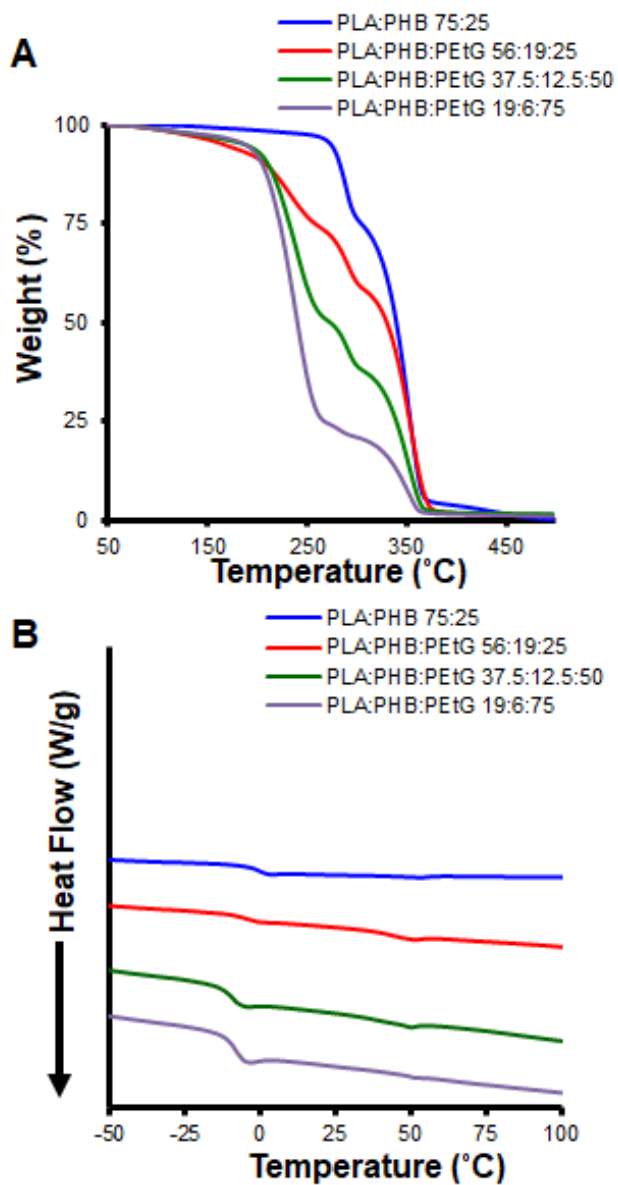
Appendix A 25. A) TGA and B) DSC thermograms for pure PETG.



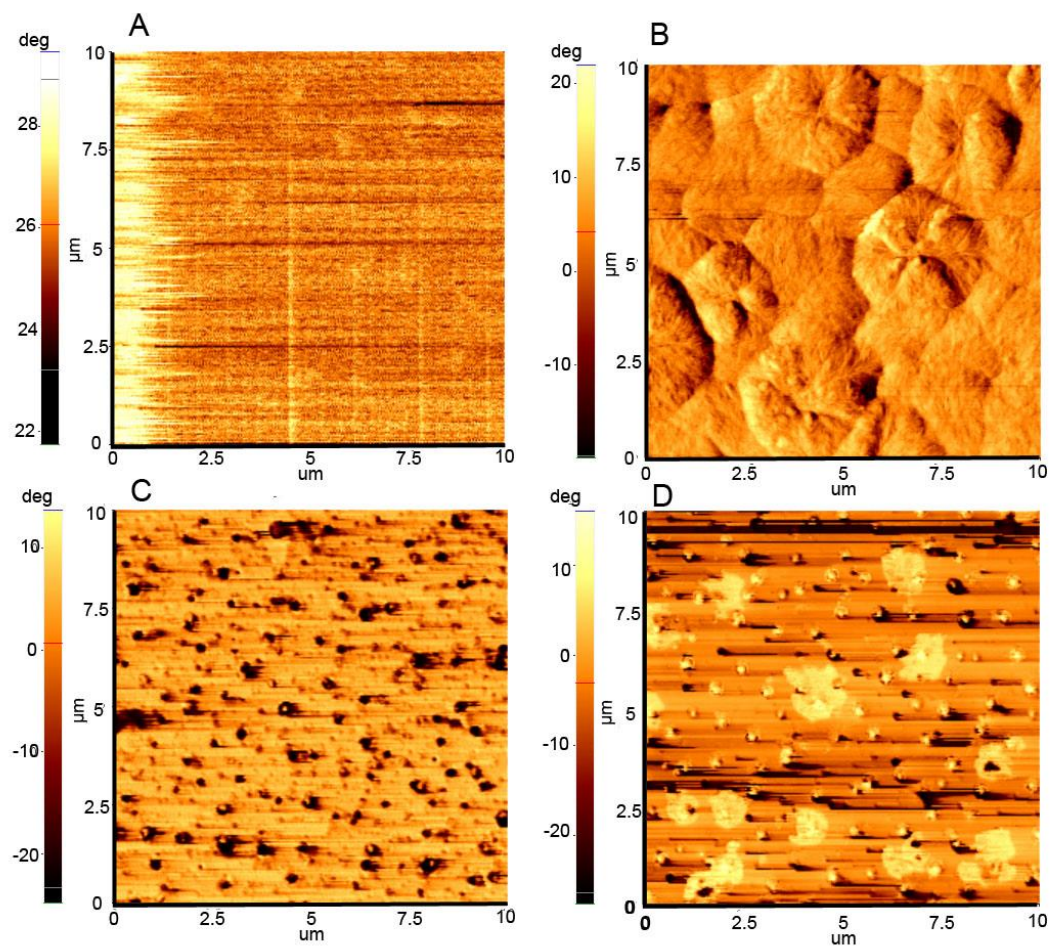
Appendix A 26. A) TGA and B) DSC thermograms for PCL-*b*-PEtG-*b*-PCL-low and PCL-*b*-PEtG-*b*-PCL-high.



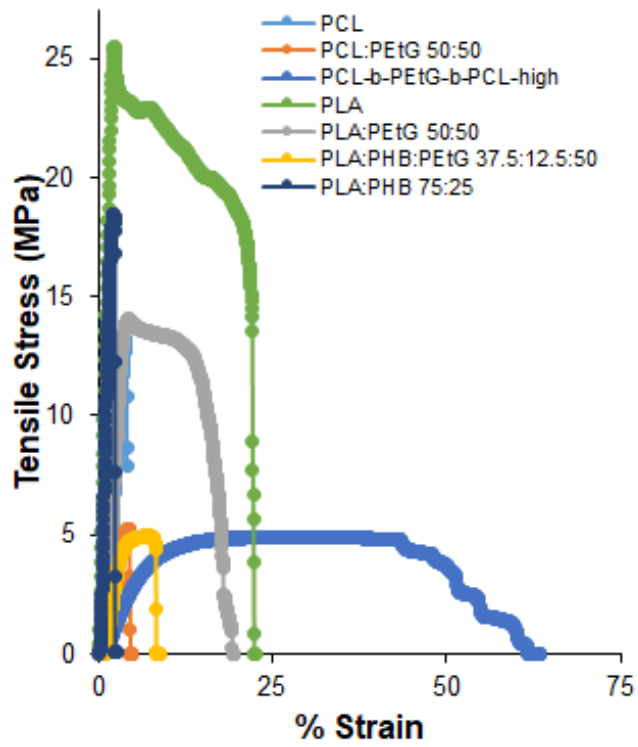
Appendix A 27. A) TGA and B) DSC thermograms of PLA:PEtG blends.



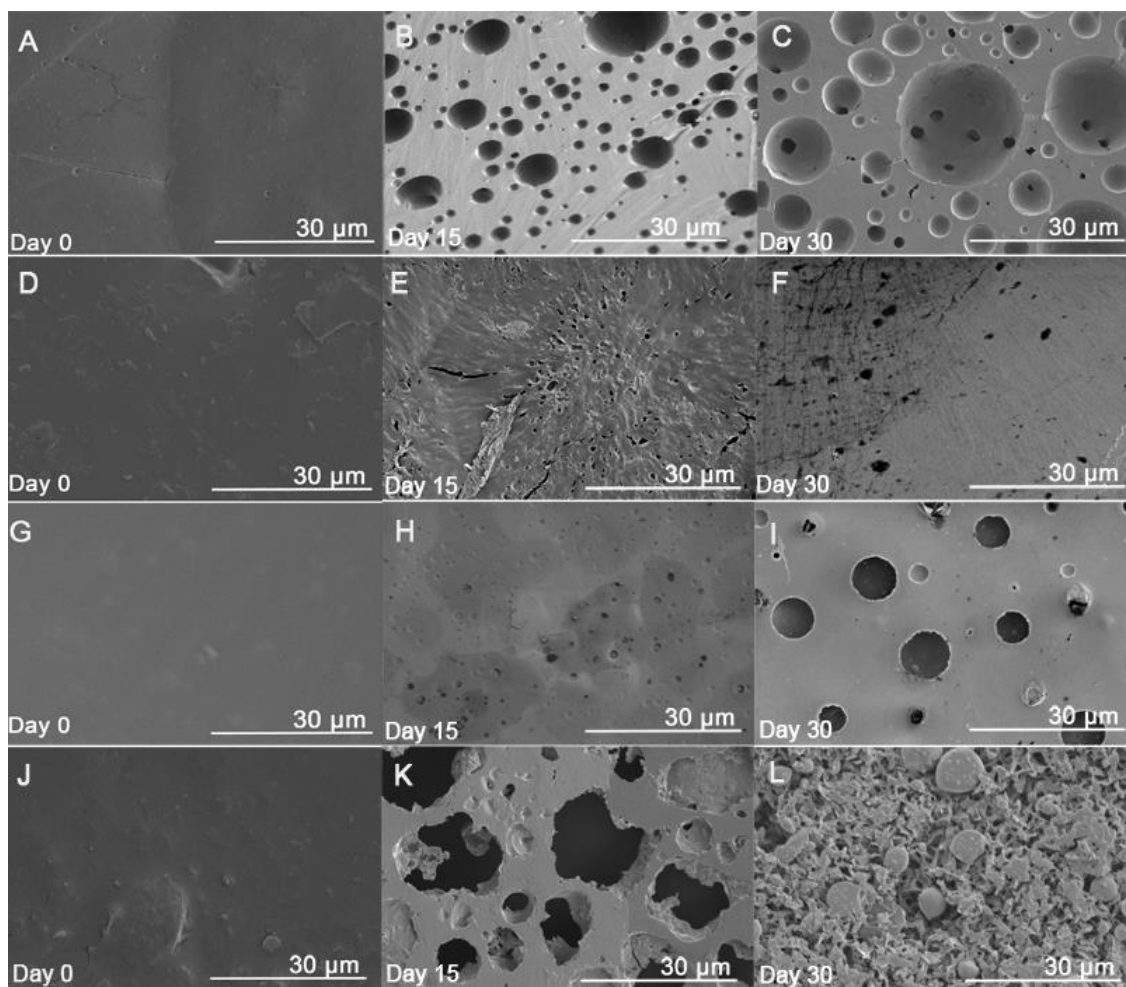
Appendix A 28. A) TGA and B) DSC thermograms for PLA:PHB:PEtG blends.



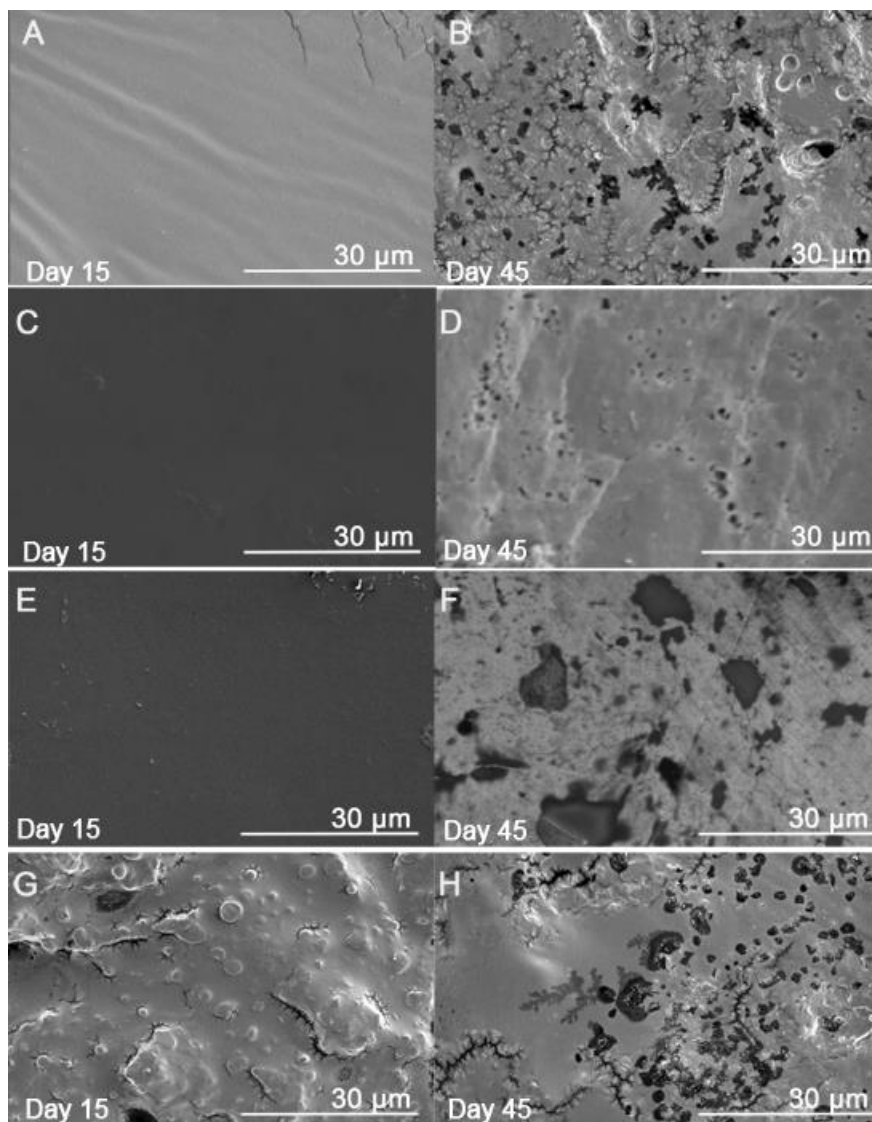
Appendix A 29. Phase contrast AFM images of the pure polymers: A) Pure PETG is generally featureless but does have grain distortion and some interference due to its tacky structure and consequent interactions with the AFM tip; B) Pure PCL, showing a high



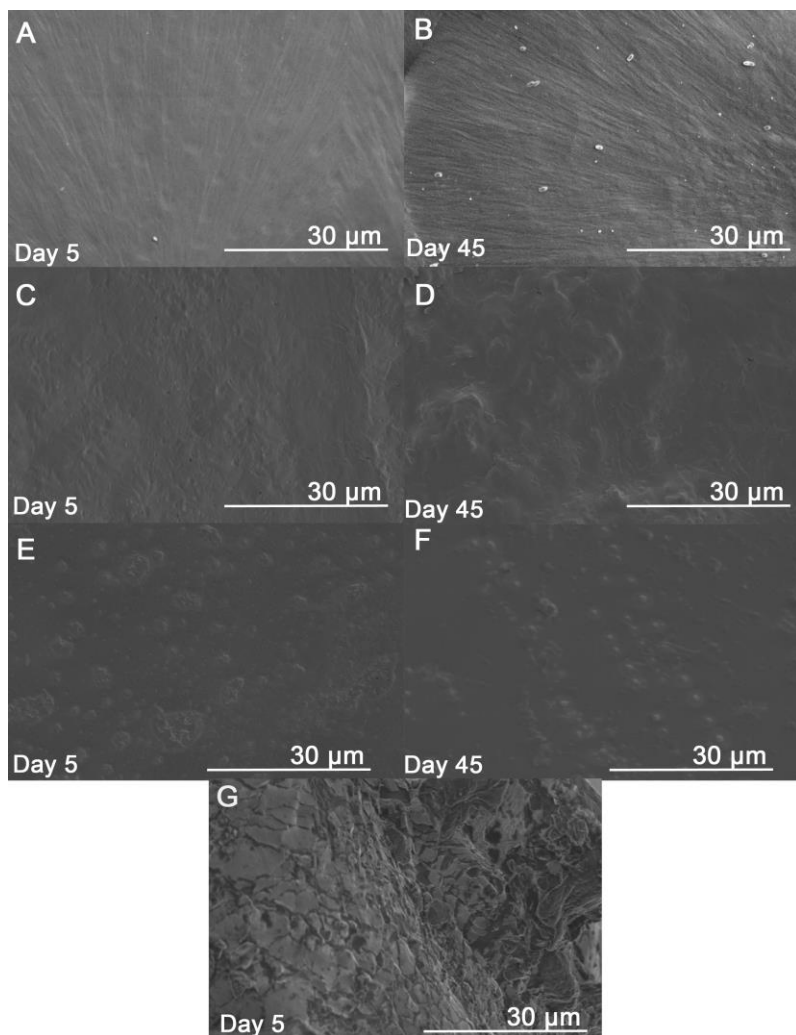
Appendix A 30. Representative stress-strain curves for the pure polymers and 50:50 polyester:PETG blends acquired by tensile testing at a strain of 5 mm/min.



Appendix A 31. SEM images of polyester:PEtG 50:50 coatings after UV exposure and 0, 15 or 30 d of immersion in 0.1 M, pH 7.4 buffer at 22 °C. A-C: PCL:PEtG 50:50; D-F) PCL-*b*-PEtG-*b*-PCL-high; G-I) PLA:PEtG 50:50; J-L) PLA:PHB:PEtG 37.5:12.5:50.

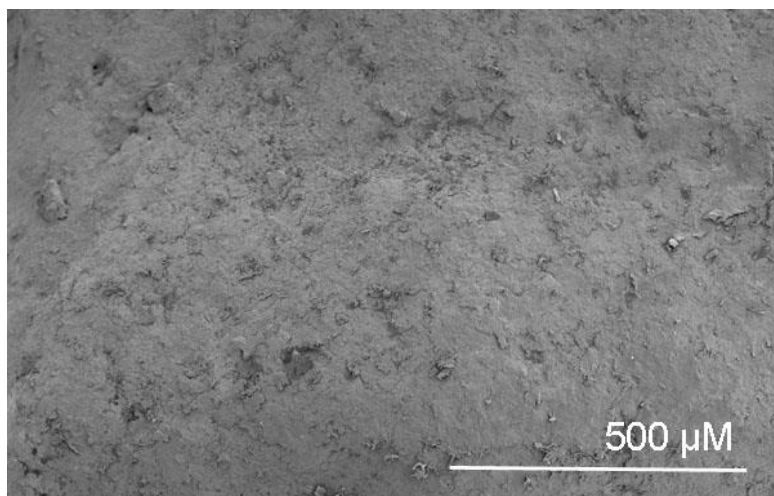


Appendix A 32. SEM images of polyester:PEtG 50:50 coatings without UV irradiation and 15 or 45 d of immersion in 0.1 M, pH 7.4 buffer at 22 °C. A-B: PCL:PEtG 50:50; C-D); PCL-*b*-PEtG-*b*-PCL-high E-F) PLA:PEtG 50:50; G-H) PLA:PHB:PEtG 37.5:12.5:50.

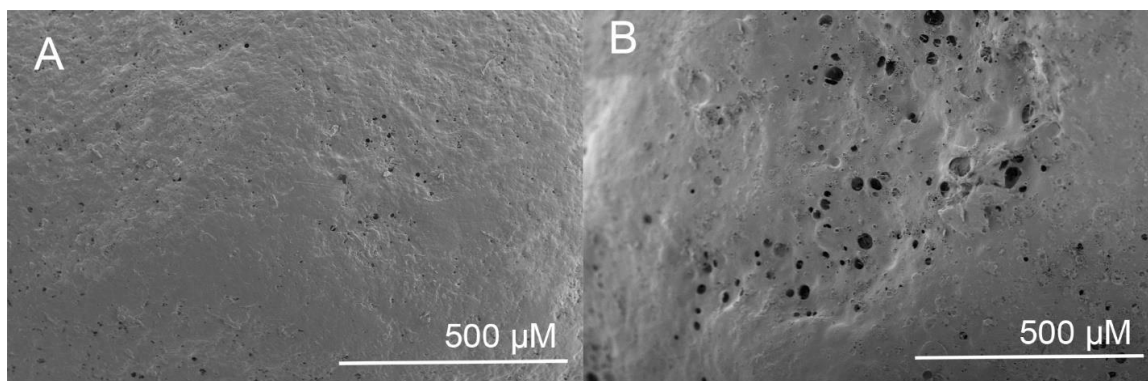


Appendix A 33. SEM images of pure polyester or PEG coatings after UV exposure and 5 or 45 d of immersion in 0.1 M, pH 7.4 buffer at 22 °C. A-B) PCL; C-D) PLA:PHB 3:1; E-F) PLA; G) pure PEG (unable to image past 5 d as no sufficient amount of polymer could be collected).

Chapter 3 Appendix B Supporting Information



Appendix B 1. SEM image of a commercially available controlled release coated urea pellet from Osmocote. Surface appears smooth with no visual structural issues at this resolution.



Appendix B 2. SEM images of PCL:PEtG spray-coated films: A) Spray coated using wax B) Continual spray coating with wax resulting in structural damages.

Curriculum Vitae

Spencer Heuchan

Education

Master of Science, Department of Biology 2016-2018 (Expected September 2018)
University of Western Ontario (UWO), London ON

Thesis: Plant stimuli-responsive biodegradable polymers for the use in timed release fertilizer coatings

Supervisors: Dr. Hugh Henry, and Dr. Elizabeth Gillies

Bachelor of Science, Department of Biology, 2012-2016
University of Western Ontario (UWO), London ON

Teaching/Research Experience

Teaching Assistant, Organismal Physiology

Biology Department, University of Western Ontario (2016-2018)

- Supervised wet labs, and taught tutorials

Teaching Assistant, Mycology

Biology Department, University of Western Ontario (2016-2018)

- Assisted with fungal identification in lab and taught tutorials

Honours

Dean's honour list (2014-2016)

Publications

Heuchan, S.M., MacDonald, J.P., Bauman, L.A., Fan, B., Henry, H.A.L., and Gillies, E.R. (2018). Triggerable degradation of polymer coatings using polyglyoxylate-polyester blends and copolymers (In progress of submitting).

Heuchan, S.M., Fan, B., Gillies E.R., and Henry, H.A.L. (2018). Plant root responsive slow-release fertilizer coatings using polyglyoxylate-polyester blends for improved nutrient delivery (In progress of submitting).

Conference Poster Presentations

Heuchan, S.M., Gillies E.R., Henry, H.A.L. (2017). Plant stimuli-responsive biodegradable polymers for the use in timed release fertilizer coatings. Ontario Ecology, Ethology, and Evolution Colloquium. Queens University, Kingston, Ontario.

Heuchan, S.M., Gillies E.R., Henry, H.A.L. (2018). Plant-responsive polymers for the use in controlled release fertilizer coatings. Fallona Family Interdisciplinary Showcase, University of Western Ontario, London, Ontario.

Heuchan, S.M., Gillies E.R., Henry, H.A.L (2018). Plant root responsive slow-release fertilizer coatings for the improvement of nutrient delivery. Ecological Society of America, New Orleans, Louisiana, USA.

Conference Oral Presentations

Heuchan, S.M., Gillies E.R., and Henry, H.A.L. (2018) Plant stimuli triggered polymers for the use in slow release fertilizer. Ontario Ecology, Ethology, and Evolution Colloquium. University of Western Ontario, London Ontario.